

TIMASSS: The IRAS16293-2422 Millimeter And Submillimeter Spectral Survey [★]

I. Observations, calibration and analysis of the line kinematics

E. Caux^{1,2}, C. Kahane³, A. Castets^{4,5,3}, A. Coutens^{1,2}, C. Ceccarelli³, A. Bacmann^{4,5,3}, S. Bisshop^{6,7}, S. Bottinelli^{1,2}, C. Comito⁸, F.P. Helmich⁹, B. Lefloch³, B. Parise⁸, P. Schilke^{8,10}, A.G.G.M. Tielens^{6,9,11}, E. van Dishoeck^{6,12}, C. Vastel^{1,2}, V. Wakelam^{4,5}, and A. Walters^{1,2}

¹ Université de Toulouse; UPS-OMP; IRAP; Toulouse, France, e-mail: caux@cesr.fr

² CNRS; IRAP; 9 Av. colonel Roche, BP 44346, F-31028 Toulouse cedex 4, France

³ Laboratoire d’Astrophysique de Grenoble, UMR 5571-CNRS, Université Joseph Fourier, Grenoble, France

⁴ Université de Bordeaux, Laboratoire d’Astrophysique de Bordeaux, 33000 Bordeaux, France

⁵ CNRS/INSU, UMR 5804, B.P. 89, 33271 Floirac cedex, France

⁶ Leiden Observatory, Leiden University, P.O. Box 9513, NL 2300 RA Leiden, The Netherlands

⁷ Center for Star and Planet Formation, University of Copenhagen, Oster Voldgade 5-7, DK-1350, Copenhagen, Denmark

⁸ Max-Planck-Institut für Radioastronomie, Auf dem Hügel 69, 53121 Bonn, Germany

⁹ SRON Netherlands Institute for Space Research, PO Box 800, 9700 AV, Groningen, The Netherlands

¹⁰ I. Physikalisches Institut, Universität zu Köln, Zülpicher Str. 77, 50937 Köln, Germany

¹¹ Kapteyn Astronomical Institute, University of Groningen, PO box 800, 9700 AV Groningen, Netherlands

¹² Max-Planck Institute für Extraterrestrische Physik, Giessenbachstr. 1, D-85748 Garching, Germany.

Received xxx, xxxx; accepted xxx, xxx

ABSTRACT

Context. Unbiased spectral surveys are powerful tools to study the chemistry and the physics of star forming regions, as they can give a complete census of the molecular content and the observed lines probe the physical structure of the source.

Aims. While unbiased surveys in the millimeter and sub-millimeter ranges observable from ground-based telescopes have previously been obtained towards several high mass protostars, very little exists on low mass protostars, believed to resemble our own Sun’s progenitor. Aiming to fill up this gap, we carried out a complete spectral survey of the bands at 3, 2, 1 and 0.8 mm towards the solar type protostar IRAS16293-2422.

Methods. The observations covered about 200 GHz and were obtained with the IRAM-30 m and JCMT-15 m telescopes during about 300 hours of observations. Particular attention was devoted to the inter-calibration of the obtained spectra with previous observations. All the lines detected with more than 3σ and free from obvious blending effects were fitted with Gaussians to estimate their basic kinematic properties.

Results. More than 4000 lines were detected (with $\sigma \geq 3$) and identified, yielding a line density of approximatively 20 lines per GHz, comparable to previous surveys in massive hot cores. The vast majority ($\sim 2/3$) of the lines are weak and due to complex organic molecules. The analysis of the profiles of more than 1000 lines belonging 70 species firmly establishes the presence of two distinct velocity components, associated with the two objects, A and B, forming the IRAS16293-2422 binary system. In the source A, the line widths of several species increase with the upper level energy of the transition, a behavior compatible with gas infalling towards a $\sim 1 M_{\odot}$ object. The source B, which does not show this effect, might have a much lower central mass of $\sim 0.1 M_{\odot}$. The difference in the rest velocities of both objects is consistent with the hypothesis that the source B rotates around the source A.

Conclusions. This spectral survey, although obtained with single-dish telescope with a low spatial resolution, allows to separate the emission from 2 different components, thanks to the large number of lines detected. The data of the survey are public and can be retrieved on the web site <http://www-laog.obs.ujf-grenoble.fr/heberges/timasss>.

Key words. Stars: protostars, Molecular data, Astrochemistry, Line: identification

1. Introduction

It is well known that the chemical composition of the gas from which the star forms influences the process of the star formation and it is, in turn, influenced by it. The first obvious example is

that the Jeans mass depends on the gas temperature which, in turn, is set by the molecular line cooling in a large range of densities and temperatures. The chemical composition of the gas is here of paramount importance, as the cooling is indeed dominated by different species as a function of the gas temperature and density and the elemental abundance (Goldsmith 2001). A second classical example is the slow contraction of the prestellar cores which is governed by ambipolar diffusion. Since only ions feel the magnetic field which counteracts the gravitational force, the chemical composition of the gas, which determines the ions

* Based on observations with the IRAM 30 m telescope (IRAM) is supported by INSU/CNRS (France), MPG (Germany) and IGN (Spain)), and with the JCMT 15 m telescope (operated by the Joint Astronomy Centre on behalf of the Particle Physics and Astronomy Research Council of the United Kingdom, the Netherlands Organisation of Scientific Research, and the National Research Council of Canada).

abundance, is crucial. In addition to this, since the gas chemical composition is largely affected by the star formation process, its study in star forming regions is a powerful diagnostic tool to track down the various processes at work. Finally, the study of the chemical composition in regions forming solar type stars is of particular importance, as it helps to understand the history of the formation of our own Solar System. For example, the comparison of the chemical composition of comets with that of solar type protostars or protoplanetary disks is used to trace back the origin of the former (Crovisier et al. 2004). The same applies to the studies of the molecular content of meteorites. In particular, the recent claim that the amino acids found in carbonaceous meteorites may have formed during the first phases of the life of the Solar System is based on the measured large deuteration in the meteoritic amino acids and in the protostellar environment (Pizzarello & Huang 2005). In this context, unbiased spectral surveys in millimeter and submillimeter wavelengths are particularly relevant as they allow to detect heavy and large molecules, and, specifically, complex organic molecules. In summary, unbiased spectral surveys in the millimeter to submillimeter wavelengths are a powerful method to characterise the molecular content of astrophysical objects, and the only way to obtain a complete census of the chemical species.

There are at least two other aspects that make unbiased spectral surveys precious tools for studying the star formation process. First, in general they provide multiple lines from the same molecule, allowing multi-frequency analysis and modelling. Since different lines from transitions with different upper level energies and Einstein coefficients are excited at different temperatures and densities, they probe different regions in the line of sight. A careful analysis can, therefore, distinguish between the various physical components in the beam. If one adds also the kinematic information provided by the line profiles, the method can be so powerful that it can identify sub-structures in the line of sight, even if the spatial resolution of the observations is inadequate. In the present article, we provide an example of this capability of unbiased spectral surveys.

Given their powerful diagnostic ability, several unbiased spectral surveys in the millimeter and sub-millimeter bands accessible from ground have been obtained in the past in the direction of star forming regions. A complete list of these surveys can be found in Herbst & van Dishoeck (2009). By far the most targeted sources are hot cores, the regions of high mass protostars formation, where the dust temperature exceeds the sublimation temperature of the water-ice grain mantles, ~ 100 K. The combined effect of the mantle sublimation and the high gas temperature triggers a singular and rich chemistry. At the same time, the relatively high densities ($\geq 10^7 \text{ cm}^{-3}$) and temperatures (≥ 100 K) are favorable for the excitation of several high lying transitions. The result is that extremely rich spectra are observed towards the hot cores. About a dozen hot cores have been targeted in different bands (Schilke et al. 1997; Helmich & van Dishoeck 1997; Hatchell et al. 1998; Schilke et al. 2001; Tercero et al. 2010). One of the most studied hot cores is the Orion-KL source. Spectral surveys covering almost all the bands accessible from the ground have been obtained, from about 80 to 900 GHz, detecting thousands of lines from hundreds of species and relative isotopologues (see for instance Schilke et al. (1997); Lee et al. (2001); Comito et al. (2005); Olofsson et al. (2007) and references therein; Demyk et al. (2007); Carvajal et al. (2009); Margulès et al. (2009); Tercero et al. (2010)). In addition, the 500–2000 GHz range is observed with the HIFI spectrometer (de Graauw et al. 2010) on board the

recently launched Herschel¹ satellite (Pilbratt et al. 2010), in the Key Program HEXOS (<http://www.submm.caltech.edu/hexos/>). Similarly, the 500–2000 GHz range is observed in other hot cores, in the Key Program CHESS (<http://www-laog.obs.ujf-grenoble.fr/heberges/chess/>). Preliminary results of the surveys performed in these two Herschel Key Programs can be found in (Bergin et al. 2010) and (Ceccarelli et al. 2010), respectively.

Although less massive and less luminous, solar type protostars also possess regions where the dust mantles sublime, yielding similar properties as those of hot cores (see Ceccarelli (2007) and references therein). These regions have been baptised hot corinos, to make it clear that they share similarities with hot cores but are not just scaled version of them (see also Bottinelli et al. 2007). The interest in observing hot corinos, whose sizes are comparable to the Solar System sizes, is amplified by the fact that they likely resemble the Solar Nebula. In other words, their study corresponds to an archeological study of our ancestor Solar System.

So far, only one (partial) spectral survey has been obtained towards a solar type protostar (Blake et al. 1994; van Dishoeck et al. 1995). The targeted source was IRAS16293-2422 (hereinafter IRAS16293), in the L1689N cloud ($d = 120$ pc, Loinard et al. 2008). This survey partially covered the two windows in the 200 GHz and 350 GHz bands accessible from ground, and has been obtained with the JCMT and CSO telescopes. The sensitivity achieved (~ 40 mK) allowed the detection of 265 lines from 24 species, namely the most abundant molecules: CO, H₂CO, CH₃OH, SO, SO₂ etc... Later, more sensitive observations have shown that the IRAS16293 line spectrum is rich in complex organic molecules (Ceccarelli et al. 2000b; Cazaux et al. 2003), and doubly (Ceccarelli et al. 1998) and triply (Parise et al. 2004) deuterated molecules. In retrospective, further support for the interest in obtaining an unbiased spectral survey towards IRAS16293 is provided by the recent Herschel/HIFI data in the 555–636 GHz range: it shows that, while IRAS16293 has much less lines than the $2 \times 10^6 L_{\odot}$ source NGC6334I, the same number of species is detected in both sources (Ceccarelli et al. 2010).

Several studies have been carried out towards IRAS16293, both with single dish telescopes and interferometers. The emerging overall picture is that IRAS16293 is a protobinary system (Wootten 1989; Mundy et al. 1992) surrounded by an envelope of about $2 M_{\odot}$ (Crimier et al. 2010). The structure of the envelope has been the target of several studies (Ceccarelli et al. 2000a; Schöier et al. 2002; Jørgensen et al. 2005). The most recent one by Crimier et al. (2010) concludes that the envelope density follows a r^{-2} power law at distances larger than about 1300 AU and $r^{-3/2}$ innerwards. The grain mantles are predicted to sublime at a distance of 75 AU, where the density is equal to $2 \times 10^8 \text{ cm}^{-3}$. The envelope extends from about 25 AU to about 6000 AU from the center. Inside the envelope, the two sources, A (South-East) and B (North-West), of the binary system are separated by about 4" (separation measured from interferometer observations at a spatial resolution of about 1"), equivalent to a linear distance of 480 AU. The source B is brighter than the source A in the millimeter continuum and in several “cold envelope” molecular lines, whereas the source A seems to be brighter in several hot corino like molecular lines (Kuan et al. 2004; Bottinelli et al. 2004; Chandler et al. 2005). Finally, Chandler et al. (2005) have claimed that source A might be a multiple sys-

¹ Herschel is an ESA space observatory with science instruments provided by European-led principal Investigator consortia and with important participation from NASA

tem and very recent observations (Pech et al. 2010) suggest that A is itself a binary system of 0.5 and $1.5 M_{\odot}$ respectively.

Despite its relatively complex structure at arcsec scales, IRAS16293 remains the brightest and best source to carry out a detailed study of the gas chemical composition in the first phases of the formation of a solar type star. As discussed above, the best way for that is to obtain unbiased spectral surveys, as sensitive as possible. In this paper, we present the results of the most sensitive unbiased spectral survey of the bands between 80 and 366 GHz observable from ground based telescopes obtained so far in direction of IRAS16293. This study is part of a more general project that plans on observing also the 500-2000 GHz frequency range with the spectrometer HIFI on board the Herschel satellite, in the context of the Herschel Key Program CHESS (*Chemical Herschel Surveys of Star forming regions*: <http://www-laog.obs.ujf-grenoble.fr/heberges/chess/>, (Ceccarelli et al. 2010).

2. Observations

The observations were obtained at the IRAM-30 m (frequency range 80-280 GHz) and JCMT-15 m (frequency range 328-366 GHz) telescopes during the period January 2004 to August 2006. Overall, the observations required a total of about 300 hours (~ 200 hr at IRAM and ~ 100 hr at JCMT) of observing time. The beam of the survey varied between 9'' and 33'', depending on the used telescope and frequency, and the spectral resolution ranged between 0.3 and 1.25 MHz, corresponding to velocity resolutions between 0.51 and 2.25 km s^{-1} . The achieved rms varied between 4 and 14 mK in 1.5 km s^{-1} bins. The observations were centered on the B (North-West) component at $\alpha(2000.0) = 16^{\text{h}} 32^{\text{m}} 22.6^{\text{s}}$, $\delta(2000.0) = -24^{\circ} 28' 33'$. A and B components, separated by 4'', are both inside the beam of our observations at all frequencies. However, at the highest frequencies observed with the IRAM 30 m telescope (i.e. the 1 mm band), the attenuation of emission from source A is not negligible as will be discussed in section 5. All observations were performed in Double-Beam-Switch observing mode, with a 90'' throw. Pointing and focus were checked every two hours on planets and on the continuum radio sources 1741-038 and 1730-130. Table 1 summarizes the observed bands and the details of the observations. More details are given below for the IRAM-30 m and JCMT-15 m telescope observations, respectively. Because of the different weather conditions during the different runs, the system temperatures varied largely. However, during the data processing, scans with too large system temperatures were removed before averaging.

2.1. IRAM Observations

The following three bands were almost fully covered by observations at the IRAM-30 m telescope: 3 mm band (80-115.5 GHz), 2 mm band (129-177.5 GHz) and 1 mm band (198-281.5 GHz).

In all IRAM-30 m observations, two frequency ranges were observed simultaneously, with two SIS receivers with orthogonal polarizations for each frequency range, in the following configuration: 3 mm receivers (A100 & B100) in parallel with 1 mm receivers (A230 & B230), and 2 mm receivers (C150 & D150) in parallel with 1 mm receivers (C270 & D270). Because of the limitation (at the time of the observations) of the IRAM-30 m backend capabilities in terms of instantaneous frequency bandwidth and spectral resolution, we privileged the largest possible spectral bandwidth to cover the IRAM-30 m bands in the smallest observing time. For simultaneous observations in the 3 mm

and 1 mm bands, the VESPA autocorrelator was split in 4 parts, 2 of them covering the whole IF band of the A&B100 receivers (0.5 GHz) with 320 kHz spectral resolution and the two others covering half of the IF band of the A&B230 receivers (1 GHz) with 1250 kHz spectral resolution. The second half of the IF band of the A&B230 receivers was covered with the 1 MHz Filter Banks (FB). For simultaneous observations in the 2 mm and upper 1 mm bands, the VESPA autocorrelator was split in 4 parts, 2 of them covering half of the IF band of the C&D150 receivers (0.5 GHz) with 320 kHz sampling two others covering half of the IF band of the C270&D270 receivers (1 GHz) with 1250 kHz sampling. The second half of the IF band of the C&D150 receivers was covered with the 1 MHz FB.

The configuration for observations in the 2 mm band resulted in different spectral resolutions for each half of the IF band of the receivers ($320 \text{ kHz} \sim 0.65 \text{ km s}^{-1}$ and $1 \text{ MHz} \sim 2 \text{ km s}^{-1}$). Therefore, we shifted the tuning frequency of the receivers by only 0.5 GHz from one tuning to the next one to cover the entire 2 mm band at the highest and at the smallest spectral resolution respectively. As a consequence, two different datasets were obtained, one at high resolution (generally used for studying brighter lines), and one at low resolution (for the faint lines).

2.2. JCMT Observations

The JCMT-15 m observations covered the 328 to 366 GHz frequency range. They were obtained with 345 GHz SIS receiver RxB3 in dual-channel single-sideband (SSB) mode. Each polarization of the receiver was connected to a unit of the ACSIS autocorrelator providing a bandwidth of 0.5 GHz for a spectral resolution of 625 kHz. At 345 GHz, this yields a velocity resolution of about 0.5 km s^{-1} .

3. Calibration

3.1. Method

At the 30 m telescope, the calibration was performed with a cold and a warm absorbers, and the atmospheric opacity was obtained using the ATM program (Cernicharo, 1985, IRAM internal report). At the JCMT, line strengths were calibrated via the chopper wheel method (Kutner & Ulich 1981).

Our spectral survey does not allow to estimate the calibration uncertainties from line observation redundancy: each spectral range has been observed only once and there is only negligible frequency overlap between adjacent spectra. From our simultaneous observations with two receivers in the 1 mm range we may estimate the receivers contribution, but to derive the total calibration uncertainties of the survey, we have performed a detailed comparison between our observations and previous observations. As our comparisons rely only on observations obtained with the same telescopes towards the same position (namely source B), there is no bias due to different sources dilution in the beams and our results are not affected by the underestimate of source A contribution at high frequency. The comparison includes virtually all the published data towards IRAS16293 obtained with the IRAM-30 m and the JCMT-15 m telescopes, as well as unpublished data obtained with the IRAM-30 m telescope. The list of the articles used for this comparison is the following: *a) IRAM-30 m bands*: Ceccarelli et al. (1998); Loinard et al. (2000); Cazaux et al. (2003); Wakelam et al. (2004); Parise et al. (2002, 2005b); *b) JCMT-15 m band*: Blake et al. (1994); van Dishoeck et al. (1995); Loinard et al. (2000); Schöier et al. (2002); Parise et al. (2004). Table 1 reports the percentage of the

Table 1. Parameters of the observations at IRAM-30 m and JCMT-15 m telescopes.

Telescope	Frequency (GHz)	Resolution (MHz)	(km.s ⁻¹)	⁽¹⁾ Backend	⁽²⁾ rms (mK)	Tsys (K)	HPBW (arcsec)	Beam efficiency	⁽³⁾ σ_{cal} (%)	⁽⁴⁾ N _{cal} lines	⁽⁵⁾ P _{cal} (%)
IRAM	80 - 115.5	0.32	0.81-1.17	VESPA	2-8	90-400	30-21	0.80-0.78	11	28	15
IRAM	129 - 177	0.32	0.53-0.72	VESPA	5-14	200-1000	19-14	0.76-0.69	17	22	12
IRAM		1.0	1.65-2.25	1 MHz FB					10 ⁽⁶⁾	84 ⁽⁶⁾	95 ⁽⁶⁾
IRAM	197 - 265	1.0	1.13-1.52	1 MHz FB	7-13	180-1200	12-9	0.65-0.51	17	36	10
IRAM		1.25	1.41-1.90	VESPA							
IRAM	265 - 280	1.25	1.34-1.41	VESPA	9-17	470-4200	9	0.51-0.47			
JCMT	328 - 366	0.625	0.51-0.57	ACIS	4-9	90-400	14	0.56-0.53	18	26	25

⁽¹⁾In the 2mm band, each frequency setting is observed twice, i.e. once at each of the two spectral resolutions (0.32 and 1 MHz), while in the 197-265 GHz band, each frequency setting is observed only one time, at a slightly different spectral resolution (1 or 1.25 MHz), ⁽²⁾rms is given in 1.5 km.s⁻¹ bins, ⁽³⁾ σ_{cal} is the calibration uncertainty, ⁽⁴⁾N_{cal} is the number of compared lines for calibration purposes, ⁽⁵⁾P_{cal} is the percentage of compared spectra for calibration purposes, ⁽⁶⁾these values refer to the "internal" comparison between VESPA and 1 MHz FB spectra simultaneously observed; the other ones refer to "external" comparisons with published or previously obtained observations.

survey spectra that could be cross-checked and calibrated against previously published data for each band. In addition, we cross-checked the calibration in the 2 mm band by comparing the data obtained with 1 MHz and 320 kHz resolution. Finally, we estimated the calibration uncertainty due to the receivers by comparing lines in the 1 mm band observed with the two receivers A230 and B230.

To quantify the differences, we obtained Gaussian fits of the considered lines and compared their characteristics (integrated intensity, peak intensity and full width at half maximum, FWHM), with the previously published values. Note that the comparison was performed in the main beam brightness scale (T_{mb}), based on the T_A^{*} /T_{mb} beam efficiency factors given in Table 1. This method provides two types of check: i) the average uncertainty over each band; and ii) possible specific calibration problems on single settings.

3.2. Calibration uncertainties

With the method described above to quantify the calibration uncertainty in the survey, we obtained the following results.

FWHM:

In all the frequency ranges, except 1mm, the agreement between the survey and the published FWHM values is within 15-20% and no systematic trend is observed. In contrast, in the 1 mm band the FWHM of the survey lines appears systematically broader by $\approx 1 \text{ km s}^{-1}$ than the published values. This is likely due to the relatively poorer spectral resolution of our survey in this range (0.8 to 1.9 km s⁻¹) compared to the linewidths (on average $\approx 4.5 \text{ km s}^{-1}$).

Integrated and peak intensity:

The comparison of the integrated and peak intensity of the lines of the survey with published values yields the same results, when the difference due to the spectral resolution described above is taken into account. Besides, since the derivation of the integrated intensities does not depend on the line shape, we choose to quantify the calibration uncertainties by comparing the integrated line intensities.

Derived uncertainties:

We can derive an estimate of the calibration uncertainty from the distribution of the integrated intensity ratios. Fig 1 shows the result for the 1mm band. If one excludes the two extremes at

≤ 0.5 and ≥ 1.5 which correspond to spectra with "anomalous intensity", the ratios distribution can be fitted by a Gaussian with a mean value R, very close to 1 and a standard deviation σ_{ratio} . With the assumption that the relative uncertainties on the published intensities, σ_{pub} , and on the survey line intensities, σ_{cal} , are independent variables, the error propagation formula leads to the following relationship:

$$\sigma_{ratio}^2 = R^2(\sigma_{cal}^2 + \sigma_{pub}^2) \quad (1)$$

Most publications report calibration uncertainties of 15% (or do not report any estimate). Except in the 3 mm frequency range, where our comparisons suggest that the calibration uncertainty is probably somewhat lower than 15%, we obtain consistent uncertainties either assuming $\sigma_{pub} = 15\%$ for all the frequency ranges or assuming that our observations are representative of average observation conditions in each frequency range, i.e. $\sigma_{pub} = \sigma_{cal}$ and thus $\sigma_{cal}^2 \approx \sigma_{ratio}^2/2$. Table 1 reports the resulting calibration uncertainties for each observed band.

It can be noticed that at 2 mm, the "external" comparisons with published spectra, which include all uncertainty factors, lead to higher values than "internal" comparisons between the VESPA and 1 MHz FB simultaneous observations, which take into account only the contribution of the backends. Similarly, at 1 mm, comparison of the line intensities observed simultaneously with the two receivers A230 and B230 shows that the receivers' contribution to the calibration uncertainties is of the order of 10%, whereas the total calibration uncertainty is 17%.

Finally, the full list of lines used for the calibration comparison is reported in the On Line Material, in Table 2 for a comparison between the survey lines and previous observations obtained with the same telescopes and in Table 3 for a comparison between the survey lines observed simultaneously with VESPA and the 1 MHz Filter Bank at the IRAM 30 m telescope.

4. Data release

The data are made publicly available on the web site <http://www-laog.obs.ujf-grenoble.fr/heberges/timasss>. The site provides the files with the IRAM-30 m and JCMT-15 m data in CLASS format (<http://www.iram.fr/IRAMFR/GILDAS>). The intensities are in T_A^{*}. Based on the discussion of the previous section, the potential user is highly recommended to verify the calibration uncertainty of the data that she/he wants to use by looking at Tables 2 and 3. We emphasize that we did not apply any "rescaling" factor to the survey data because the difference may be

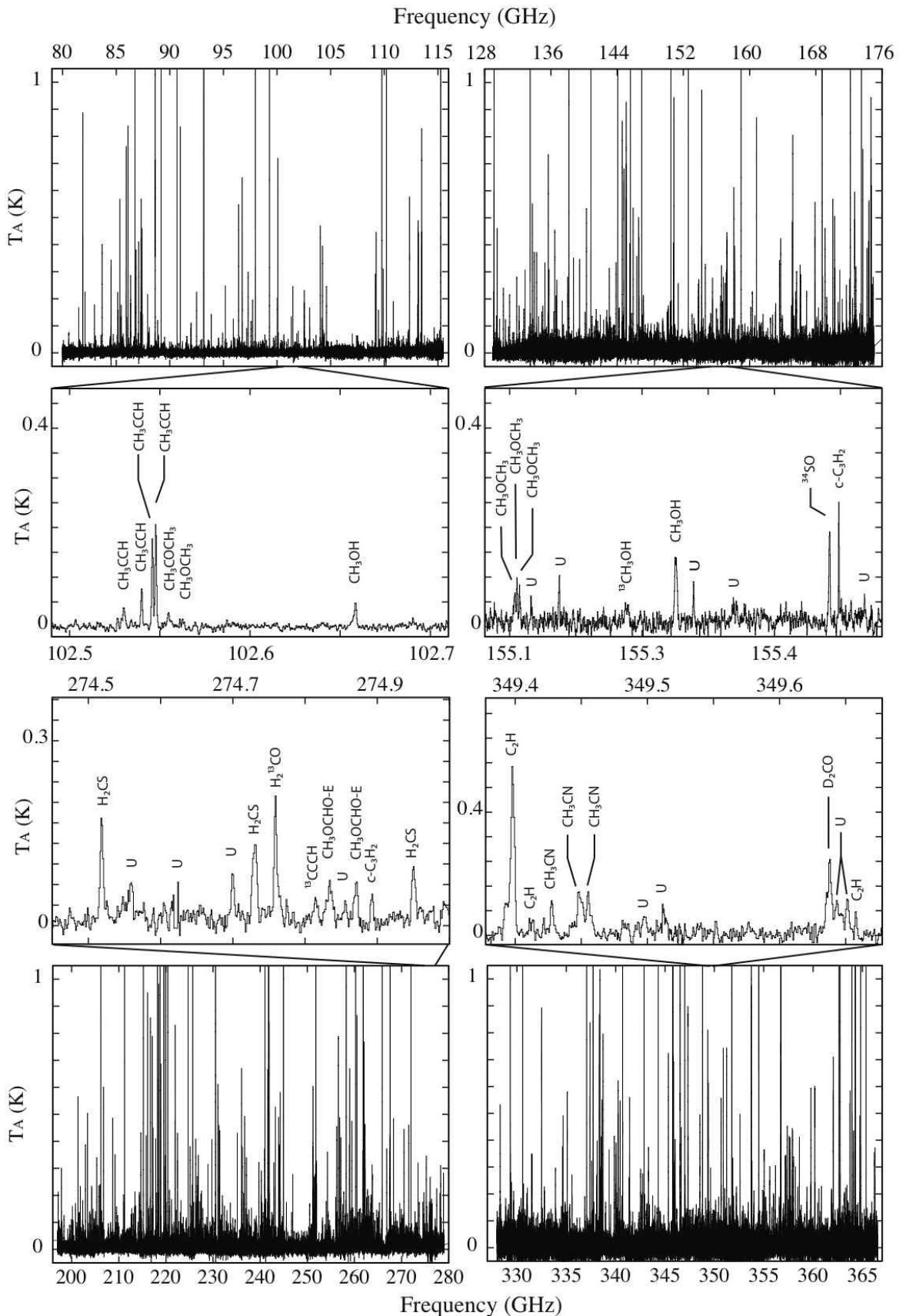


Fig. 2. The IRAS16293 spectra in the four bands of the survey. Upper panels: IRAM-30 m 3 mm and 2 mm bands. Lower panels: IRAM-30 m 1 mm and JCMT-15 m 0.8 mm bands. The middle panels are blow-ups of sample frequency ranges in the four bands respectively. These panels include lines identification based on the publicly available spectral databases (see text for details).

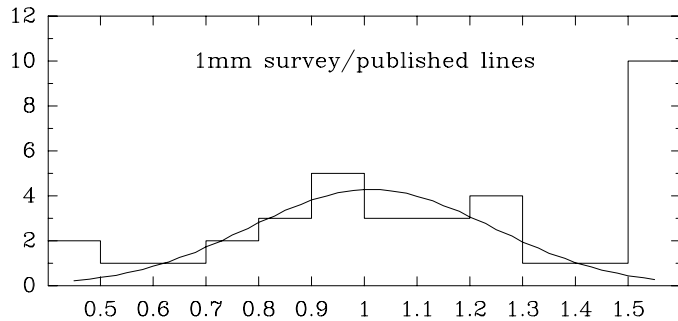


Fig. 1. Distribution of integrated intensity ratios of this survey's 1 mm lines compared to published observations obtained with the IRAM 30 m telescope. The curve is a Gaussian fit to the histogram ruling out the “anomalous” ratios (≤ 0.5 or ≥ 1.5). It can be noticed that the 12 “anomalous” ratios correspond to only 7 “anomalous spectra” among the 165 spectra observed in the 1 mm range.

caused by a wrong calibration of the published data rather than a wrong calibration of the survey data. Only a very careful scientific analysis can assess what is the best. It is, therefore, the user's responsibility to verify that the data are correctly used, based on the information provided on the web site.

5. Results

5.1. Overall survey

Figure 2 shows the full survey in the four bands and the richness of the IRAS16293 line spectrum. On average about 20 lines per GHz have been detected with a S/N larger than 3 in the 220 GHz frequency range covered by the survey. The line density seems to slightly increase with frequency: 17 lines/GHz in the 3 mm band, 19 and 23 lines/GHz in the 2 mm and 1 mm ranges respectively and up to 26 lines/GHz in the 0.9 mm range.

To quantify more rigorously the lines and species detected in the survey, we made Gaussian fits and line identification using the CASSIS package (<http://cassis.cesr.fr>²). The spectroscopic data come from the CDMS and JPL databases (Müller et al. 2001, 2005; Pickett et al. 1998 and references quoted on the databases to data producers for each species). In a few cases (ortho and para H₂CO for instance) a specific database with each form separated has been used (see <http://cassis.cesr.fr>). For the D-bearing isotopologues of methanol, only the lines reported by (Parise et al. 2002, 2004) are included in this paper.

Hereinafter we will only consider lines identified according to the following criteria: i) lines belonging to species included in the JPL and CDMS databases or to the D-bearing isotopologues of methanol, ii) lines detected with more than 3σ in the integrated line intensity, iii) unblended lines and iv) lines with upper level energies E_{up} lower than 250 K. This last condition only limits the number of methanol lines in this analysis, since such lines of other molecules are too weak in any case. When applying these criteria, we end up with ~ 1000 lines listed in Table 4 (Online Material). In the table we report the line identification together with the result of the Gaussian fit of each line (see also §5.3).

Figure 3 shows the line densities, limited to the lines satisfying the above criteria, in each of the four survey frequency ranges, for various signal to noise ratios. In the 3 mm and 2 mm

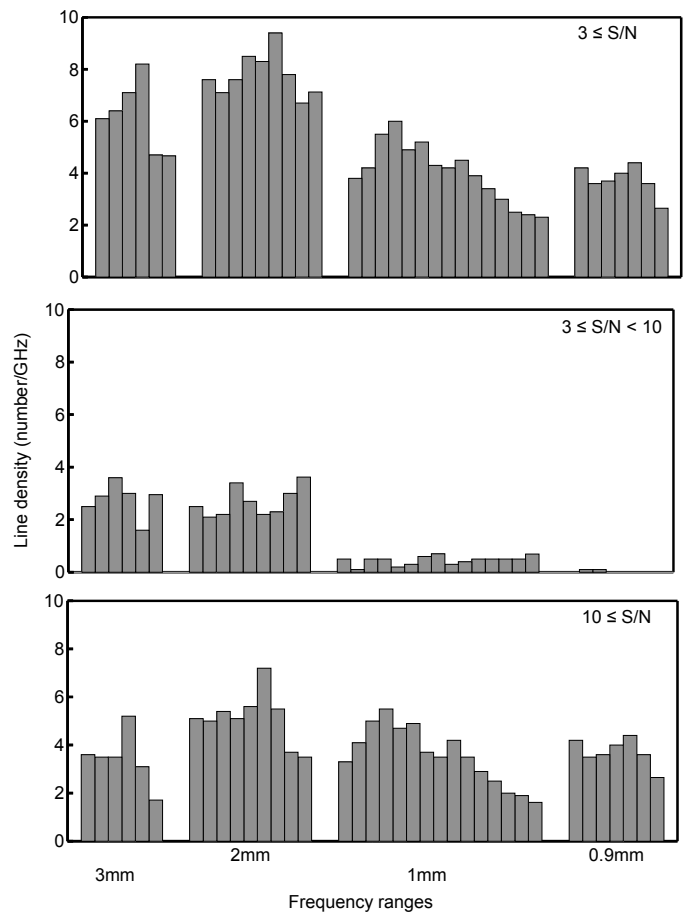


Fig. 3. Distribution of the density (averaged over 10 GHz intervals) of identified lines (see text) in each of the four frequency ranges. The upper panel corresponds to lines with $S/N \leq 3$, the central panel is restricted to lines with $3 \leq S/N < 10$ and the lower panel corresponds to lines with signal to noise ratios ≥ 10 .

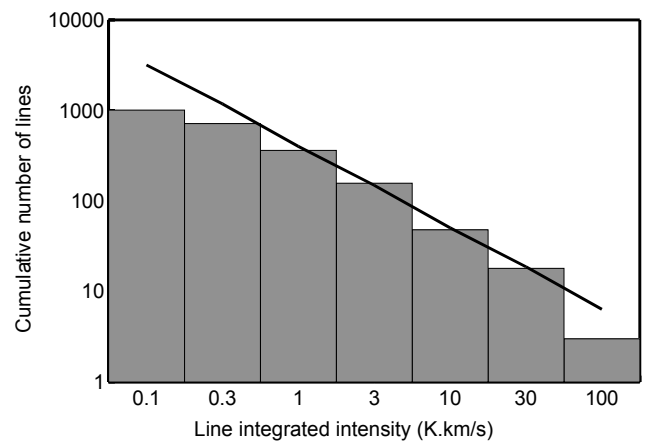


Fig. 4. Number of lines showing an integrated intensity larger than a given threshold. The solid line shows the single index power law best fit of the distribution.

ranges, these densities are a factor 2 to 3 smaller than the estimates of the total densities including blended lines. This effect is still stronger in the 1 mm and 0.9 mm ranges, where the lack of weak lines ($3 \leq S/N < 10$) is particularly striking in Fig. 3. This is a bias due to our selection criterion of non-blended

² CASSIS has been developed by CESR-UPS/CNRS

lines. In fact, these frequency ranges are rich in lines from large molecules, which emit many weak lines, so that our unblended line criterium filters out a large fraction of these moderate signal to noise ratio lines. In contrast, the 2 mm range, which benefits from a better spectral resolution compared to the 3 mm and 1 mm ranges, suffers less from this selection effect.

Overall, most of the lines retained in the 1mm and 0.9 mm ranges and a large fraction ($\approx 2/3$) of the lines retained in the 3 mm and 2 mm ranges have a high signal to noise ratio (≥ 10). The density of lines with such high S/N is relatively constant in frequency and equal to $\approx 4 - 5/\text{GHz}$.

When comparing with the line density quoted at the beginning of the section, namely about 20 lines per GHz, obtained considering lines with $S/N \geq 3$ but no other filter, clearly the introduction of the other criteria, unblended lines and, to a lesser degree, identified lines and $E_{\text{up}} \leq 250 \text{ K}$, severely underestimates the line content.

The line intensity spans more than three orders of magnitude, from 10 mK to 24 K. The **number of lines** showing an integrated intensity larger than a given threshold is given in Fig. 4. For integrated intensity ranging between 1 and 30 K.km/s, the distribution roughly follows a power law of slope -0.9. The power law breaks down in the high and low end of the distribution. This slope is identical to the those observed by Schilke et al. (2001); White et al. (2003); Comito et al. (2005) in their submillimeter surveys of Orion-KL. Similarly with what is observed in these surveys, this slope does not provide a good fit for the brightest and the weakest lines.

5.2. Detected lines and species

Table 5 lists the species detected and identified in the survey, with the number of lines, the range of upper level energy of the lines and other observational quantities (see below).

In the frame of a survey analysis restricted to the four line criteria mentioned above, 69 different molecules (including ions) have been detected. They correspond to 32 distinct chemical species and include 37 rare isotopologues. Out of the ~ 1000 lines of Table 5, about half belong to only three species: CH₃HCO, HCOOCH₃ and CH₃OH.

Most of the 4000 lines detected in our survey belong in fact to the species already identified in this source (see Table 5), among which a few molecules show extremely rich spectra, with many weak and/or blended lines, not included in the present study. Although we anticipate the presence of unidentified lines, their identification will require a careful analysis and even probably modeling of these spectra. Also, with the $E_{\text{up}} \leq 250 \text{ K}$ selection criterion used in this work, we do not identify any vibrationally excited lines. These objectives are postponed to a future article.

Table 5 also lists the sum of the line flux in each species. For species showing rich and complex spectra or with numerous lines with upper energy levels $\geq 250 \text{ K}$, this value is in fact a lower limit due to the numerous weak and blended lines not included in the present analysis.

As noted by the previous study (Blake et al. 1994; van Dishoeck et al. 1995), the millimeter and submillimeter spectrum of IRAS16293 is dominated by simple O-rich species like CO, SO, H₂CO, SO₂, and CH₃OH (the three first families alone contribute to more than 2/3 of the total flux). In the frequency range covered by our survey, the total flux emitted in the CO main and isotopic lines is about 800 K.km.s⁻¹, $\sim 30\%$ smaller than the flux emitted in the SO, H₂CO, SO₂, and CH₃OH lines

together ($\sim 1100 \text{ K.km.s}^{-1}$). Thus CO is not the major cooling agent in this frequency range. In addition, our survey shows the presence of thousands of weaker lines from heavier and more complex molecules not detected in the previous surveys. The blow-ups of Fig. 2 illustrate the situation, with several lines from CH₃CCH, CH₃CN, HCOOCH₃ etc. To have a rough estimate of the contribution of this "grass" of lines to the total cooling of the gas (in this range of frequencies), consider a line density of about 15 lines per GHz (see above) and a line integrated intensity of $\sim 0.3 \text{ K.km.s}^{-1}$. This gives approximatively an integrated line intensity of 900 K.km.s⁻¹, namely comparable to the contribution of CO and its isotopologues.

5.3. Line parameters

A Gaussian fit has been performed for each of the lines of Table 4. The parameters of the fit (integrated intensity, line width FWHM and rest velocity v_{LSR}) are reported in the same table. The uncertainties on the integrated line intensity take into account the spectra noise and the calibration uncertainties reported in Table 1. Note that we have verified that even when the line profile differs from a simple Gaussian (for example in self-absorbed lines, or lines with broad wings) the Gaussian fit area is very close to the true integrated line intensity and, therefore, reliable. The uncertainties on the line width FWHM and rest velocity v_{LSR} take into account the statistical errors (from the fit) and the uncertainty due to the limited spectral resolution, which indeed dominates the error. The cases when the line profiles are clearly not Gaussian are marked in Table 4. The average $\langle \text{FWHM} \rangle$ and $\langle v_{\text{LSR}} \rangle$ for each species and isotopologues are reported in Table 5, except for those which show severe blending due to unresolved or partially resolved hyperfine structure (CH₃CN, HNCO, NH₂D, NS).

In the following, we analyze the information derived from the Gaussian FWHM and v_{LSR} of the lines.

Figure 5 shows the FWHM versus v_{LSR} for each species. In the plots, we have regrouped the isotopologues of the same species and, in a few cases, species with a small number of lines. Note that in these cases we verified that the species have similar FWHM and v_{LSR} to avoid introducing artificial trends in the plot. Figure 5 shows a remarkable and unexpected behavior: *the FWHM and v_{LSR} distributions are not the same but, on the contrary, they depend on the species*.

Based on the different FWHM and v_{LSR} distributions, it is possible to identify four types of "kinematical behaviors":

1. Type I (first row of Fig. 5): $\langle v_{\text{LSR}} \rangle \sim 4.0 \text{ km.s}^{-1}$ and $\langle \text{FWHM} \rangle \sim 2.5 \text{ km.s}^{-1}$. The lines show very little dispersion both in terms of rest velocities and in term of line widths. Small carbon chains and rings, and "small molecules" belong to this group.
2. Type II (second row): $\langle v_{\text{LSR}} \rangle \sim 3.7 \text{ km.s}^{-1}$ with a very little dispersion, FWHM from $\sim 2 \text{ km.s}^{-1}$ to $\sim 8 \text{ km.s}^{-1}$. All species in this group are S- or N- bearing molecules. It can be noticed that HCO⁺ and C₃H₂ (in the first row) show a behavior intermediate between Type I and Type II.
3. Type III (third row): $\langle v_{\text{LSR}} \rangle \sim 2.5 - 3.0 \text{ km.s}^{-1}$, $\langle \text{FWHM} \rangle \leq 4.0 \text{ km.s}^{-1}$. Four complex organic molecules show this behavior.
4. Type IV (fourth row): v_{LSR} and FWHM showing a mixed behavior, with characteristics belonging to the two last groups. CH₃OH lines have v_{LSR} and FWHM ranging from 2 to 9 km.s⁻¹; H₂CO and CH₃CCH lines have moderate FWHM (4–5 km.s⁻¹) and v_{LSR} ranging from 2.5 to 4 km.s⁻¹; lines

Table 5. Detected species ordered by decreasing fluxes of the main isotopologue.

TAG (1)	Species (3)	Nb ⁽²⁾ lines	E _{up} (K) min-max	<V _{LSR} > (km.s ⁻¹)	<FWHM> (K.km.s ⁻¹)	$\int T_{mb} dv$	TAG (1)	Species (3)	Nb ⁽²⁾ lines	E _{up} (K) min-max	<V _{LSR} > (km.s ⁻¹)	<FWHM> (K.km.s ⁻¹)	$\int T_{mb} dv$
28503	^(aa) CO	3	5.5–33.2	5.93±0.71	9.47±1.77	605.8	41001	^(bb) CH ₃ CN	>30	20.4–21.2			58.6
29501	^(ab) ¹³ CO	3	5.3–31.7	3.94±0.36	4.13±1.16	116.0	46509	^(bc) H ₂ CS	26	9.9–143.4	3.61±0.35	4.53±1.34	51.2
30502	^(ac) C ¹⁸ O	3	5.3–31.6	3.72±0.18	2.90±0.61	67.6	47505	^(bd) H ₂ ¹³ CS	4	22.5–97.1	4.09±0.79	4.61±2.29	2.9
29006	^(ad) C ¹⁷ O	3	5.4–32.4	3.84±0.35	3.75±0.66	25.5	47504	^(be) HDCS	5	8.9–30.9	3.77±0.12	2.81±0.88	0.8
48501	^(ae) SO	20	9.2–87.5	3.98±0.20	4.18±0.55	339.5	60503	^(bf) OCS	12	16.3–134.8	3.13±0.33	5.12±0.77	38.6
50501	^(af) ³⁴ SO	13	15.6–86.1	3.81±0.27	4.87±0.84	28.0	62505	^(bg) OC ³⁴ S	9	15.9–157.2	2.51±0.26	3.98±0.65	7.8
30591	^(ag) o-H ₂ CO	10	6.8–143.3	3.45±0.58	4.09±0.58	163.3	61502	^(bg) O ¹³ CS	10	20.9–147.2	2.58±0.51	4.49±1.25	5.6
30581	^(ag) p-H ₂ CO	7	10.5–99.7	3.67±0.12	3.92±0.65	93.6	60003	^(bh) HCOOCH ₃	182	17.9–145.0	2.52±0.32	2.71±0.77	51.6
31501	^(ah) HDCO	10	17.6–102.6	3.39±0.58	3.99±1.06	26.7	44505	^(bi) SiO	6	6.2–75.0	4.40±0.46	5.57±0.78	49.7
31503	^(ai) H ₂ ¹³ CO	12	10.2–157.5	2.96±0.38	2.86±1.29	12.7	27002	^(bj) HNC	3	4.3–43.5	3.80±0.56	2.81±1.08	32.1
32592	^(aj) o-D ₂ CO	6	16.8–81.2	3.51±0.61	3.80±0.84	11.7	28508	^(bk) DNC	2	11.0–22.0	4.31±0.02	2.47±1.19	4.9
32582	^(aj) p-D ₂ CO	8	5.3–99.5	3.38±0.72	2.76±1.24	5.5	28005	^(as) HN ¹³ C	4	4.2–41.8	3.74±0.61	3.44±1.76	4.8
32503	^(ak) H ₂ C ¹⁸ O	4	20.0–63.4	2.71±0.16	2.67±1.21	1.9	51501	^(bl) HC ₃ N	17	19.6–203.0	3.53±0.44	4.67±1.97	35.4
64502	^(al) SO ₂	82	7.7–248.5	3.74±0.32	5.30±1.22	238.3	52005	^(bm) DC ₃ N	6	22.3–77.0	4.29±0.23	2.61±0.41	1.0
66002	^(am) ³⁴ SO ₂	5	7.6–69.7	3.33±0.72	4.20±1.71	1.6	34502	^(bn) H ₂ S	2	27.9–84.0	3.55±0.52	4.90±0.08	25.2
32504	^(an) CH ₃ OH	99	7.0–233.6	3.42±0.42	5.91±1.35	217.6	35001	^(bo) HDS	2	11.7–34.7	3.05±0.55	2.41±2.09	0.7
33502	^(ao) ¹³ CH ₃ OH	9	6.8–94.6	2.93±0.47	3.92±1.63	2.8	38082	^(bp) o-C ₃ H ₂	14	4.1–48.3	4.10±0.27	2.73±0.70	14.5
	^(ap) CH ₂ DOH	12	4.5–40.8	2.74±0.64	5.89±0.91	6.4	38092	^(bp) p-C ₃ H ₂	9	6.4–47.5	4.27±0.26	2.57±1.29	4.5
	^(ap) CHD ₂ OH	7	4.2–53.5	3.70±0.88	4.76±1.58	2.6	39003	^(bu) c-C ₃ HD	5	17.4–25.34	4.44±0.31	1.91±0.88	1.5
	^(ap) CH ₃ OD	4	6.0–26.8	2.55±0.84	3.96±1.29	2.3	46008	^(br) CH ₃ OCH ₃	82	11.1–169.8	2.53±0.29	2.27±0.69	18.8
	^(aq) CD ₃ OH	3	12.2–42.0	2.43±0.21	2.03±0.49	0.5	40502	^(bs) CH ₃ CCH	26	12.3–176.6	3.62±0.32	3.03±0.58	17.4
29507	^(ar) HCO ⁺	3	4.3–42.8	3.29±0.16	2.87±1.39	144.2	41502	^(bt) CH ₂ DCCH	4	16.3–38.1	4.34±0.31	1.93±0.40	0.2
30504	^(ar) H ¹³ CO ⁺	4	4.2–41.6	3.94±0.46	2.43±0.44	31.5	25501	^(bu) CCH	13	4.2–25.1	3.83±0.09	2.08±0.20	14.7
30510	^(as) DCO ⁺	3	10.4–51.9	4.19±0.29	2.34±0.83	14.3	26501	^(bv) CCD	4	10.4–10.3	4.32±0.52	2.54±0.86	0.8
31506	^(at) HC ¹⁸ O ⁺	3	4.1–24.5	4.04±0.37	2.15±0.51	1.6	43002	^(bw) HNCO	>8	10.5–143.5			13.8
31508	^(ar) D ¹³ CO ⁺	2	10.2–20.4	4.52±0.16	2.34±1.36	0.6	26504	^(bx) CN	7	5.4–5.4	4.45±0.10	1.82±0.16	8.5
30505	^(aw) HC ¹⁷ O ⁺	1	12.5–12.5	3.94±0.22	4.03±0.71	0.4	45506	^(by) HCS ⁺	5	6.1–73.7	3.72±0.20	3.32±0.70	5.1
44501	^(av) CS	4	7.0–65.8	3.70±0.12	3.56±0.43	126.5	42501	^(bz) H ₂ CCO	13	9.7–66.9	3.00±0.26	2.58±0.44	4.8
46501	^(av) C ³⁴ S	4	6.9–64.8	3.63±0.16	3.60±0.68	21.1	18501	^(ca) NH ₂ D	>3	16.6–182.8			4.7
45501	^(av) ¹³ CS	4	6.7–46.6	3.69±0.22	4.06±0.96	9.0	30008	^(cb) NO	7	7.2–36.1	4.02±0.12	2.25±1.42	3.7
45502	^(av) C ³³ S	4	7.0–65.3	3.68±0.66	5.05±1.67	7.2	56007	^(cc) C ₂ S	12	15.4–53.8	4.10±0.17	2.12±0.62	2.6
27501	^(aw) HCN	3	4.2–42.5	3.57±0.78	7.06±2.12	97.5	45013	^(cd) PN	>3	13.5–63.1			2.1
28002	^(ax) H ¹³ CN	5	4.1–41.4	3.77±0.26	4.05±1.85	17.1	19002	^(ce) HDO	1	95.2–95.2	2.87±0.21	6.13±0.58	2.1
28509	^(ay) DCN	3	10.4–52.1	3.63±0.46	4.09±0.55	11.3	46010	^(cf) NS	>6	9.9–17.8			1.3
28003	^(az) HC ¹⁵ N	4	4.1–41.3	3.60±0.33	5.52±1.47	6.4	49503	^(cg) C ₄ H	6	20.5–30.2	4.00±0.08	1.58±0.28	0.7
44003	^(ba) CH ₃ CHO	192	13.8–194.5	2.79±0.39	2.68±1.00	70.0	37003	^(ch) c-C ₃ H	3	4.39–10.8	4.42±0.22	1.79±0.10	0.3

(1) In the CDMS as in the JPL catalog, the species are associated to a five digit number, called TAG; the first two digits correspond to their molecular weight in atomic mass units, and the third digit is a 5 in the CDMS catalog, and a 0 in the JPL catalog. Our identification of the ortho and para forms of H₂CO, D₂CO and c-C₃H₂ relies on the VASTEL Spectroscopic database (<http://www.astro.caltech.edu/~vastel/CHIPPENDALES>) so that these species are associated with specific TAG. The deuterated isotopologues of methanol, not yet included in the CDMS and JPL databases, do not have a TAG. Our identification of their lines is based on the data given in Parise et al. (2002) and Parise et al. (2004) and references therein.

(2) For most N-bearing species, due to unresolved hyperfine structure, this number is a lower limit corresponding to groups of blended lines.

(3) For each species, the spectroscopic references given here are the most recent cited in the CDMS and JPL databases. All of them should be read as reference and references therein: ^{aa}Winnewisser et al. (1997); ^{ab}Cazzoli et al. (2004); ^{ac}Klapper et al. (2001); ^{ad}Klapper et al. (2003); ^{ae}Bogey et al. (1997); ^{af}Klaus et al. (1996); ^{ag}Müller et al. (2000d); ^{ah}Bocquet et al. (1999); ^{ai}Müller et al. (2000c); ^{aj}Lohilah & Hornerman (2004); ^{ak}Müller et al. (2000b); ^{al}Müller et al. (2000a); ^{am}Belov et al. (1998); ^{an}Müller et al. (2004); ^{ao}Xu & Lovas (1997); ^{ap}Parise et al. (2002); ^{ar}Parise et al. (2004); ^{at}Lattanzi et al. (2007); ^{as}van der Tak et al. (2009); ^{au}Schmid-Burgk et al. (2004); ^{av}Dore et al. (2001); ^{av}Kim & Yamamoto (2003); ^{aw}Thorwirth et al. (2003); ^{ax}Cazzoli & Puzzarini (2005); ^{ay}Brünken et al. (2004); ^{az}Cazzoli et al. (2005); ^{ba}Kleiner et al. (1996); ^{bb}Müller et al. (2009); ^{bc}Clouthier et al. (1994); ^{bd}Brown et al. (1987); ^{be}Minowa et al. (1997); ^{bf}Golubiatnikov et al. (2005); ^{bg}Lovas & Suenram (1987); ^{bh}Maeda et al. (2008); ^{bi}Cho & Saito (1998); ^{bj}Thorwirth et al. (2000a); ^{bk}Brünken et al. (2006); ^{bl}Thorwirth et al. (2000b); ^{bm}Spahn et al. (2008); ^{bn}Belov (1995); ^{bo}Camy-Peyret et al. (1985); ^{bp}Mollaaghatababa et al. (1993); ^{bq}Bogey et al. (1987); ^{br}Neustock et al. (1990); ^{bs}Cazzoli & Puzzarini (2008); ^{bt}Leguennec et al. (1993); ^{bu}Padovani et al. (2009); ^{bv}Bogey et al. (1985); ^{bw}Lapinov et al. (2007); ^{bx}Klisch et al. (1995); ^{by}Margulès et al. (2003); ^{bz}Guarnieri & Huckauf (2003); ^{ca}Fusina et al. (1988); ^{cb}Meerts & Dymanus (1972); ^{cc}Lovas et al. (1992); ^{cd}Cazzoli et al. (2006); ^{ce}Johns (1985); ^{cf}Lovas & Suenram (1982); ^{cg}Chen et al. (1995); ^{ch}Yamamoto & Saito (1994);

from the rare isotopes of OCS have $v_{LSR} \sim 2.5 \text{ km.s}^{-1}$ and $\text{FWHM} \leq 4 \text{ km.s}^{-1}$.

It can be noted that the FWHM averaged over each of the four frequency bands of the survey is similar, between 2 and 5 km.s^{-1} , with a slight increase in the 1 mm band due to a poorer

spectral resolution. We have verified that none of the four kinematical behaviors is an artifact due to this instrumental effect. Table 6 summarizes the situation. In order to better understand the physical meaning of the plots in Fig. 5 (and of the four identified Types) we have plotted in Fig. 6 the values of the FWHM as function of the upper level energy E_{up} of the transition. The

species have been grouped as in Fig. 5; it is striking that the distinction between the four Types defined by the (FWHM, v_{LSR}) distribution is visible also in this plot.

Table 6. Distribution of the detected species in four kinematical types.

Type (Source)	v_{LSR} (km s^{-1})	FWHM	E_{up} (K)	FWHM behavior	Species
Type I (Envelope)	~ 4	≤ 2.5	0–50	constant	CN, NO, C ₂ S, C ₂ H, C ₃ H, C ₄ H, HCO ⁺ , C ₃ H ₂
Type II (Source A)	~ 3.7	2–8	0–250	increases	HCN, HC ₃ N, HNC, SO, SO ₂ , CS, HCS ⁺ , H ₂ CS
Type III (Source B)	2.5–3	≤ 4	0–200	constant	CH ₃ CHO, HCOOCH ₃ , CH ₃ OCH ₃ , H ₂ CCO
Type IV (mixed)	2.5–4	2–8	0–250	increases	CH ₃ OH, H ₂ CO, CH ₃ CCH, OCS

First column reports the associated component (see §6), second, third and fourth columns report the typical velocities, FWHM and upper level energy E_{up} ranges of the detected lines. Fifth column describes the behavior of FWHM with increasing E_{up} and last column lists the species belonging to each type.

Type I species have lines with E_{up} lower than 50 K. It should be noted that this is not an observational bias: excepted in a few cases of very light molecules, such as C₂H, the species associated to Type I present high energy transitions in the survey frequency range, but the line intensities decrease abruptly when E_{up} becomes larger than 50 K. In contrast, Type II, III and IV species present lines with E_{up} up to 200 K but show different behaviors. For Type II species, the FWHM increases with E_{up} , whereas for Type III and IV the FWHM is constant and does not depend on E_{up} . In contrast, analogous plots of v_{LSR} vs E_{up} show that the lines' velocity does not depend on E_{up} in any species. A related effect has already been observed by Schöier et al. (2002), who noted a correlation between the linewidths and the excitation temperatures derived by Blake et al. (1994) and van Dishoeck et al. (1995). These properties will be used to give a physical meaning to the four Types in §6. Finally, it can be noticed that when detected, the deuterated species show the same behaviour as the main isotopomers, except the D-isotopomers of Type III species that anyway present too weak lines to be detected in our survey.

6. Discussion

6.1. Comparison with previous surveys

When compared to the previous survey toward IRAS16293 (Blake et al. 1994; van Dishoeck et al. 1995), the present one not only enlarges the covered frequency range (~ 200 GHz versus ~ 40 GHz) but also the number of detected species, thanks

to the higher sensitivity (~ 10 mK versus ~ 40 mK). The average line density of the previous unbiased survey of IRAS16293 was 7 lines per GHz to compare with 20 lines per GHz for the present one. Several species detected in our survey were not detected in the previous one: complex organic molecules (HCOOCH₃, HCOOCH₃ and CH₃OCH₃), carbon chains and rings (C₂S, C₄H, c-C₃H), N-bearing species (NO, PN, NS) and several D-bearing molecules.

Towards hot cores, numerous surveys have been performed. They cover the whole range of frequencies reachable from the ground, from the 3 mm range observed with IRAM, SEST, NRAO or JCMT to the submillimeter windows observable with the CSO and JCMT (MacDonald et al. 1996; Schilke et al. 1997; Helmich & van Dishoeck 1997; Nummelin et al. 1998; Thompson & MacDonald 1999; Kim et al. 2000; Nummelin et al. 2000; Lee et al. 2001; Schilke et al. 2001; White et al. 2003; Comito et al. 2005; Kim et al. 2006; Belloche et al. 2007; Olofsson et al. 2007; Tercero et al. 2010). The line densities usually range from 10 to 20 lines per GHz, i.e. comparable to the present survey. SgrB2 appears as a noticeable exception, with significantly higher line densities, as high as 100 lines per GHz in the 3 mm range observed with IRAM (Belloche et al. 2007) or 40 lines per GHz in the 1 mm range observed with SEST (Nummelin et al. 1998, 2000). Interestingly, the slope of -0.9 that we observe for the cumulative number of lines versus flux threshold is identical to the slopes observed by Schilke et al. (2001); White et al. (2003); Comito et al. (2005) in their submillimeter surveys of Orion-KL.

In conclusion, in terms of molecular content, our survey reveals a richness comparable to that of hot cores and confirms that the high abundance of deuterated isotopologues, which are easily detected for a number of species, is a distinctive characteristic of low mass protostars.

6.2. Kinematical types and associated components

As mentioned in the Introduction, IRAS16293 is formed by a proto-binary system surrounded by an infalling envelope. In addition, multiple outflows originate from the system (e.g. Castets et al. 2001). Before attempting to interpret the observations of §5.3 and, specifically, the meaning of the four kinematical types of Table 6, based on the line rest velocities and widths, we review what is known so far about the envelope and the proto-binary system.

a) Envelope

The envelope extends for 6000–7000 AU in radius, equivalent to about 100'' in diameter, and it is relatively massive ($\sim 2 M_{\odot}$) (Crimier et al. 2010). At the border of the envelope the dust temperature is ~ 13 K and the density is $\sim 10^5 \text{ cm}^{-3}$. The dust temperature reaches 100 K at a radius 75–86 AU, where the density is $(2\text{--}3)\times 10^8 \text{ cm}^{-3}$, creating the region called hot corino. The rest velocity of the cold envelope has been measured in several studies and it is $\sim 3.9 \text{ km.s}^{-1}$ (Mizuno et al. 1990; Bottinelli et al. 2004; Takakuwa et al. 2007). Molecules probing the cold envelope have $\sim 2 \text{ km.s}^{-1}$ line widths.

b) Proto-binary system

Several interferometric studies have been carried out in the past to better characterize the nature of the two sources, A (South-East) and B (North-West), forming the binary system (Kuan et al. (2004); Bottinelli et al. (2004); Chandler et al. (2005); Bisschop et al. (2008); see also references in Table 7). Some

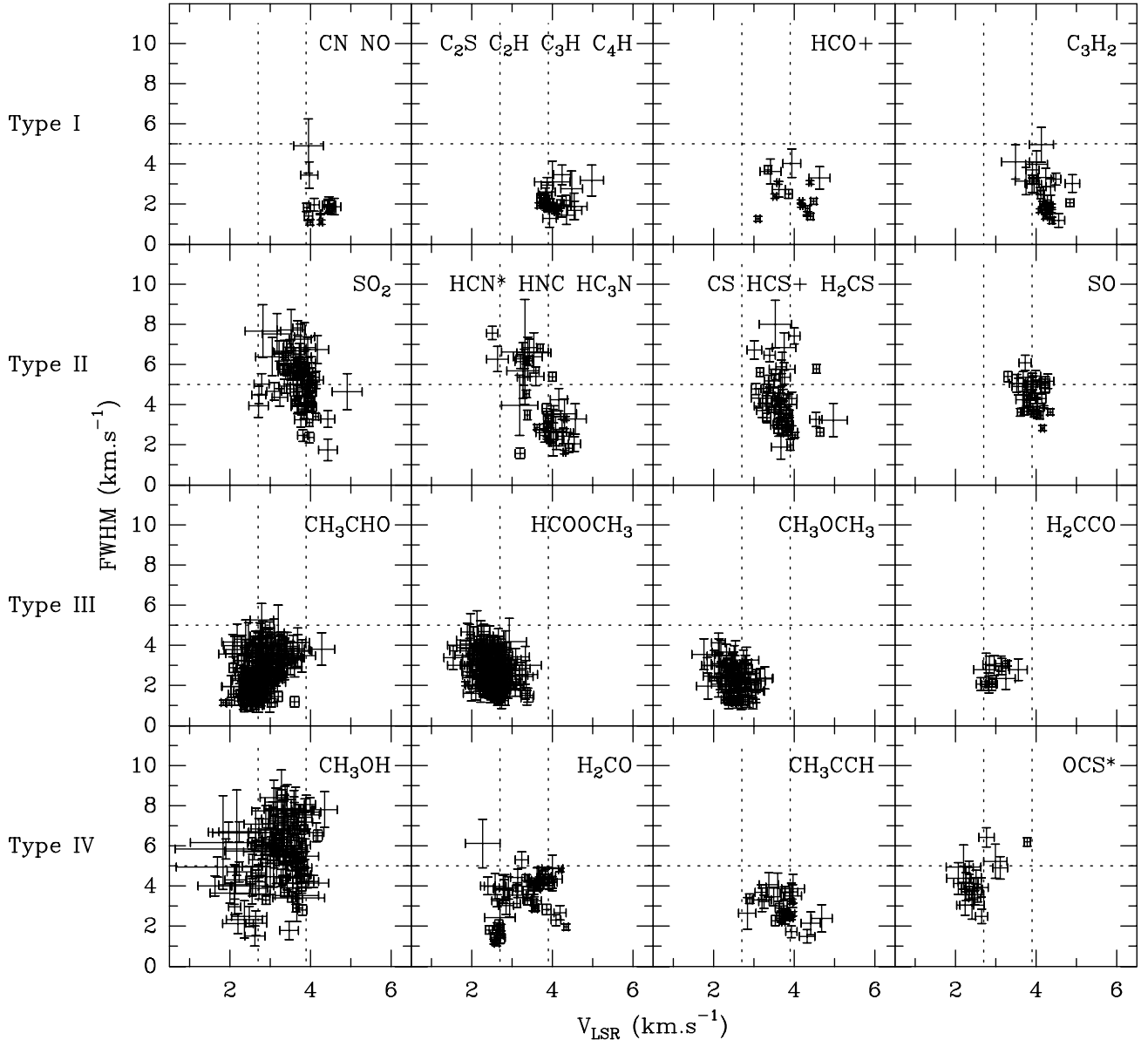


Fig. 5. Plots of the rest velocity v_{LSR} versus the FWHM, derived from the Gaussian fits of the lines (Table 4). All the detected species and the relevant isotopologues of Table 5 are plotted, except those in which the lines have obviously non Gaussian profiles (see text). In particular, the labels HCN^* and OCS^* mean that the main isotopologues of these species are not included, due to their non Gaussian profiles. The 1 sigma errorbars include fit and spectral resolution uncertainties. The vertical lines at $v_{\text{LSR}} = 2.7$ and 3.9 km.s^{-1} correspond to the velocity of the components B and A respectively (see §6). The horizontal line at 5 km.s^{-1} corresponds approximatively to the average of the line FWHM range.

species are associated only or predominantly with one of the two sources A and B, and others are observed in both sources. All studies agree in measuring broader lines towards A ($\sim 8 \text{ km.s}^{-1}$) than towards B ($\sim 3 \text{ km.s}^{-1}$). However, the situation about the rest velocity of the molecular emission in the two objects is more confused: there is some evidence that the two objects have different rest velocities (higher in source A than in source B), but this difference might also be due to absorption by the envelope according to Chandler et al. (2005) or self-absorption in optically thick lines from source B according to Bottinelli et al. (2004); Kuan et al. (2004) also report velocities somewhat higher in source A than in source B, with a dispersion larger than 2.5 km.s^{-1} from one species to another. According to Bisschop

et al. (2008), both A and B sources show emission at velocities between 1.5 and 2.5 km.s^{-1} ; Huang et al. (2005) mention two velocity components at 1.5 and 4.5 km.s^{-1} for source A and show emission from B peaking at $\sim 2 \text{ km.s}^{-1}$. It can be noted that all these studies use moderate spectral resolutions ($\sim 1 \text{ km.s}^{-1}$), deal with a small number of lines (often only one) for each species and, in some cases, suffer from poor signal to noise ratio for the weakest lines.

Table 7 summarizes, for each of the species classified according to their kinematical Type in Table 6, the results of interferometric observations towards the three components of IRAS16293 (sources A and B and envelope).

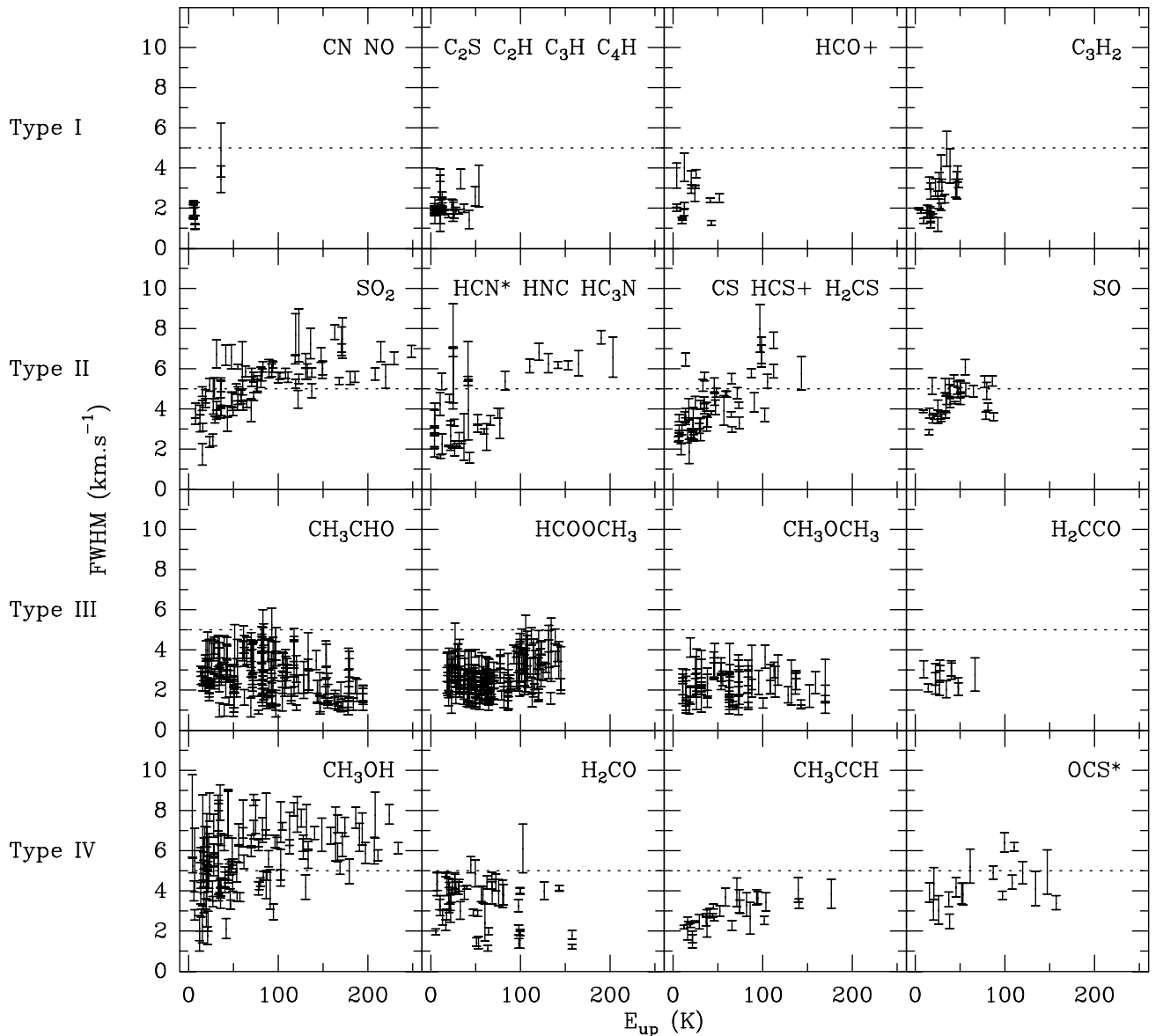


Fig. 6. Plots of the linewidth, FWHM, versus the energy of the upper level of the transition, E_{up} . The species are grouped as in Fig. 5. All the detected species and the relevant isotopologues of Table 5 are plotted, except those in which the lines have obviously non Gaussian profiles (see text). In particular, the labels HCN* and OCS* mean that the main isotopologues of these species are not included, due to their non Gaussian profiles. The 1 sigma errorbars include fit and spectral resolution uncertainties. The horizontal line at 5 km.s⁻¹ corresponds approximatively to the average of the line FWHM range.

c) Interpretation of the kinematical types

Based on published interferometric observations each species is assigned to one or two of the three components (source A, B and envelope). For example, CN has the Type I kinematical characteristics ($v_{\text{LSR}} \sim 4 \text{ km.s}^{-1}$ and $\text{FWHM} \sim 2 \text{ km.s}^{-1}$) and has only been detected associated with the envelope and was not detected in any of the two sources A and B. On the contrary, CH₃CHO has the characteristics of the Type III behavior ($v_{\text{LSR}} = 2.5\text{--}3 \text{ km.s}^{-1}$ and $\text{FWHM} \leq 4 \text{ km.s}^{-1}$) and has only been detected in the direction of source B. Some species of Table 6 (C₂H, C₃H, C₄H, C₂S, NO, HNC, HCS⁺ and CS) have not been observed with interferometers, to the best of our knowledge, so they are not reported in Table 7. The correspondence between the four Types of Table 6 and the interferometric observations presented in Table 7 suggests that the species belonging to the same kinematical Type

are associated with a spatially different source: envelope (Type I), source A (Type II), source B (Type III) and a mix of the three previous components (Type IV). It should be noted that the distribution of molecules in four kinematical types is not an artifact or a bias due to the survey pointing, which favors emission from source B compared to emission from source A at higher frequencies. Even excluding all lines observed at IRAM 30 m or JCMT telescopes with a HPBW larger than 14'', i.e. all lines with frequencies higher than 200 GHz, the v_{LSR} versus FWHM plots and the FWHM versus E_{up} plots show the same behavior.

1. Type I corresponds to molecules abundant in the cold envelope of IRAS16293. We cannot exclude that these species also emit in the densest parts of sources A and B but that this emission is strongly absorbed by the gas in the envelope. NO, which shows two broad and relatively bright lines with

Table 7. Correspondence between kinematical types and spatial distributions derived from interferometric observations

Type	Source A	Source B	Envelope	Refs.
Type I		(C ₃ H ₂)	CN	B2004
Type II	HCN	(HCN)		T2007
	HCN			H2005
	HC ₃ N			C2005
	SO	(SO)		C2005
	SO			H2005
	SO ₂			C2005
Type III	SO ₂	(SO ₂)		H2005
	H ₂ CS	(H ₂ CS)		H2005
				K2004
Type IV		CH ₃ CHO		B2008
		CH ₃ OCH ₃		C2005
	(CH ₃ OCH ₃)	CH ₃ OCH ₃		H2005
	(H ₂ CCO)	H ₂ CCO		K2004
		H ₂ CCO		B2008
		HCOOCH ₃		R2006
Type V	HCOOCH ₃	(HCOOCH ₃)		B2004
	HCOOCH ₃	HCOOCH ₃		K2004
	HCOOCH ₃			C2005
	CH ₃ OH			C2005
Type VI	CH ₃ OH	CH ₃ OH		K2004
	H ₂ CO	H ₂ CO		S2004
	H ₂ CO	H ₂ CO		C2005
	OCS	OCS		H2005

The first column reports the kinematical type of the species according to the definition given in Table 6. The columns 2, 3 and 4 report where the species has been detected: source A, B and envelope respectively. The species in parenthesis means that weaker emission has also been observed in the relevant component or that they are questionable identifications (see text). Last column reports the interferometric observations references; B2004: Bottinelli et al. (2004); B2008: Bisschop et al. (2008); C2005: Chandler et al. (2005); H2005: Huang et al. (2005); K2004: Kuan et al. (2004); R2006: Remijan & Hollis (2006); S2004: Schöier et al. (2004); T2007: Takakuwa et al. (2007).

E_{up} = 36 K, bright narrow lines with E_{up} = 7 K and barely detected lines with E_{up} = 19 K (not included in this paper), might be an example of such a situation, which deserves a detailed excitation study to come. The 343.8 GHz line associated with source B was identified by Kuan et al. (2004) as the C₃H₂ 23_{13,10} - 23_{12,11} transition (E_{low} = 790 K) but the CH₃CHO 18_{2,17} - 17_{2,16} transition (with E_{up} = 166 K) seems a more reasonable identification.

2. Type II identifies molecules prevalently associated with source A. A few exceptions, for which emission from source B is mentioned in the literature, deserve some attention. The identification by Huang et al. (2005) of a line to SO₂(v₂ = 1) associated with source B is also questionable given the very high upper energy level (E_{low} = 1800 K) of the transition, as is the attribution by Huang et al. (2005) of H₂CS emission to source B, as no map is shown for this species. Finally, SO emission is rather extended and associated with both sources A and B (Chandler et al. 2005). It is possible that part of the lines broadening is due to wings associated with the outflow, whereas the bulk of the emission is associated with the cold envelope (which would make SO rather a species of Type I). In addition, it should be noted that, without detailed excitation models which will be presented in subsequent studies, it

is not possible to exclude that, for some Type II species, the cold envelope contributes to the emission observed at low E_{up} and low FWHM.

3. Type III species have lines prevalently emitted by source B. HCOOCH₃, which has been observed both in source A and source B appears as a notable exception. Excitation modeling of this species will be discussed in detail in a subsequent paper. Several qualitative arguments may already contribute to explain why no lines with Type II characteristics are present in this study: (i) as the lines emitted by the source A are much broader than the lines emitted by the source B, those lines present a higher percentage of blending with nearby lines which excludes them from this study; (ii) in our large beam observations, emission from sources A and B are superposed; the narrow lines emitted from the source B appear "on the top of" broad lines emitted by the source A and are, thus, more easily detected; (iii) this second effect is enhanced by the pointing towards the source B.
4. Type IV species are a mixed bag. The species are present in both source A and B and, sometimes, even in the envelope. Depending on the intensity contribution, the lines can have a low or high v_{LSR} and FWHM. Therefore, Type IV species are not associated with any specific component.

Using the kinematic properties of the lines, we were able to propose general trends as whether the emission of the species originates from source A or source B although both sources are included in our single dish observations. Despite the fact that the kinematic differences are small, for example a difference in the v_{LSR} of not more than 1.5 km.s⁻¹, we were able to draw a general picture thanks to the large number of detected lines.

6.3. The dynamics of sources A and B

Having identified where the emission from the various species originates helps to clarify the nature of sources A and B. As noted in several previous works, A and B have apparently a different chemical composition: source B is brighter in complex organic molecules, while source A is brighter in simpler S- and N-bearing molecules (see Table 7). Furthermore, it was also noted that the FWHM of the lines arising in source A are broader than in source B.

Our analysis establishes two additional properties previously unrecognized (see discussion in 6.1): i) the two sources have different velocities (v_{LSR}) and ii) in the source A, the FWHM of the lines increases with increasing upper level energy (Fig. 6) whereas it remains constant in the source B.

Concerning the linewidths behavior, a related effect, the increase of FWHM with the excitation temperature, had already been observed by Schöier et al. (2002), but this represents a less direct probe of the gas kinematics, as it relied on modeling assumptions to derive the excitation temperatures. The increase of the lines FWHM with increasing excitation has been interpreted in two ways, either this is due to the effect of the infalling gas on the accreting protostellar object (Ceccarelli et al. (2003)), or the increased width is due to shocks caused by jet/wind interaction with the inner dense envelope (Schöier et al. (2002), Jørgensen et al. (2002)). The two interpretations predict different molecular emission distributions. However, the existing maps do not allow to distinguish these interpretations. In addition, to fully disentangle these two interpretations requires a detailed modeling of the source that is beyond the scope of this paper. At this stage, it can simply be said that the interpretation of the infalling gas (Ceccarelli et al. 2000b) would lead to reasonable

estimates of source A and source B central masses: for optically thin emission, the free-fall velocity may be estimated from the linewidth, assuming that the FWHM includes quadratically a turbulent width δ_{th} and the free-fall broadening; its analytic expression yields to the following expression of the core mass, where the widths are expressed in km.s⁻¹ and the radius r in AU:

$$M(M_\odot) = 1.4 \times 10^{-4} (FWHM^2 - \delta_{th}^2) r \quad (2)$$

Assuming that the turbulent width in the A and B cores external layers is close to that of the envelope static gas, we derive $\delta_{th} \sim 2$ km.s⁻¹ from the Type I species linewidths. According to the interferometric observations of Type II and Type III species reported in Table 7, both sources show a radius of $\sim 1.5''$ (i.e 180 AU at a distance of 120 pc). For core A, typical FWHM larger than ~ 6 km.s⁻¹ lead to a central mass of at least $0.8 M_\odot$, whereas for core B, where FWHM are smaller than ~ 3 km.s⁻¹, the central mass cannot exceed $0.1 M_\odot$. This assumes that the linewidths are due to collapsing envelopes rather than rotating disks. If they were, on the contrary, due to rotating disks, one would have to take into account the (unknown) inclination angle. The available interferometer observations, which barely spatially resolve the core A only (Bottinelli et al. 2004), do not allow to distinguish between these two possibilities. In the following, we will restrict the discussion to the infalling envelopes, for simplicity, but our conclusions substantially apply also to the disk case.

The difference between the v_{LSR} of both sources can be interpreted in the following way: the source B rotates around its companion, the source A; for a distance of 480 AU between cores A and B, and a core A mass of $0.8 M_\odot$, the rotation velocity of core B is 1.2 km.s⁻¹. The observed difference between A and B velocities (v_{LSR} of 3.9 and 2.7 km.s⁻¹ respectively) is thus perfectly consistent with this picture. Bottinelli et al. (2004) already discussed this possibility but did not have enough evidence for preferring it with respect to another hypothesis where the lines kinematics properties reflect opacity effects. The large number of lines and species observed in our survey allows to favor the dynamical issue.

7. Conclusions

We have presented the unbiased spectral survey of the 3, 2, 1 and 0.9 mm bands accessible from ground towards the Class 0 source IRAS16293. For that, we used the IRAM-30 m and JCMT-15 m telescopes, during about 300 hours of observations. This is the most sensitive survey ever published in these bands towards a solar type protostar.

The data have been released for public use in two CLASS files, which can be retrieved on the web site <http://www-laog.obs.ujf-grenoble.fr/heberges/timasss/>. The site also contains two accompanying files (reported in the On Line Material) providing informations about the calibration of the single receiver settings, obtained by comparing the survey lines with previously obtained observations.

The line density, ~ 20 lines/GHz, appears as high as in comparable surveys obtained towards high mass protostars (with the exception of SgrB2). More than one thousand unblended lines with $S/N \geq 3$ and upper energy levels lower than 250 K have been identified through the comparison with the JPL and CDMS catalogs. They correspond to 32 chemically distinct species, showing a chemical richness comparable to that of hot cores. The identification of 37 additional rare isotopologues and, specifically, numerous D-bearing molecules confirm that IRAS16293 has a

remarkably high abundance of deuterated species. The 3 mm–0.9 mm spectra are dominated by relatively simple molecules (CO, SO, H₂CO, SO₂ and CH₃OH). However, the numerous weaker lines emitted by larger molecules account for at least as much as the CO integrated line intensities.

The analysis of the profiles of this large set of identified lines, and specifically the central velocities and widths, gives clues to disentangle where each emission dominantly originates from: cold envelope (narrow lines at $V_{LSR} \approx 3.9$ km.s⁻¹), source A (broader lines at $V_{LSR} \approx 3.9$ km.s⁻¹) and source B (narrow lines at $V_{LSR} \approx 2.7$ km.s⁻¹). Furthermore, in source A, the line widths increase with the upper energy level of the transition. If this behavior is interpreted as due to gas infalling towards a central object, the core A mass is $\sim 1 M_\odot$ and the lower line widths observed towards source B set an upper limit to the mass of this source, $\leq 0.1 M_\odot$. The observed difference in the V_{LSR} , ~ 1.2 km.s⁻¹, is consistent with the source B rotating around the more massive source A. From a chemical point of view, the source B shows predominant emission from O-bearing complex molecules whereas N- and S- bearing molecules are strong emitters in the source A. In order to derive reliable estimates of the corresponding chemical abundances, it is necessary to carry out careful radiative transfer modeling. This is postponed to future articles.

Acknowledgements. We are deeply thankful to the IRAM staff and the successive TACs, and particularly to Clemens Thum, for his help in preparing and programming the observations at the IRAM-30 m telescope. We gracefully thank the JCMT staff, particularly Remo Tilanus and Jim Hogh, who were always able to quickly resolve problems. We thank Laurent Pagani for fruitful discussions about calibration problems. We are very thankful to the molecular databases JPL and CDMS, which were largely used for the work presented here as to the spectroscopic groups providing the data. This work has been supported by l'Agence Nationale pour la Recherche (ANR), France (contracts ANR-08-BLAN-022) and by the Ministère de la Recherche Scientifique et Université J. Fourier de Grenoble, France (PPF WAGOS). Finally, we warmly thanks the referee, Dr. J. Cernicharo, and the editor, Dr. M. Walmsley, who contributed to improve a lot this paper with numerous helpful comments.

References

- Belloche, A., Comito, C., Hieret, C., et al. 2007, in Molecules in Space and Laboratory
- Belov, S. 1995, Journal of Molecular Spectroscopy, 173, 380
- Belov, S. P., Tretyakov, M. Y., Kozin, I. N., et al. 1998, Journal of Molecular Spectroscopy, 191, 17
- Bergin, E. A., Phillips, T. G., Comito, C., et al. 2010, A&A, 521, L20+
- Bisschop, S. E., Jørgensen, J. K., Bourke, T. L., Bottinelli, S., & van Dishoeck, E. F. 2008, A&A, 488, 959
- Blake, G. A., van Dishoeck, E. F., Jansen, D. J., Groesbeck, T. D., & Mundy, L. G. 1994, ApJ, 428, 680
- Bocquet, R., Demaison, J., Cosloué, J., et al. 1999, Journal of Molecular Spectroscopy, 195, 345
- Bogey, M., Civiš, S., Delcroix, B., et al. 1997, Journal of Molecular Spectroscopy, 182, 85
- Bogey, M., Demuynick, C., & Destombes, J. L. 1985, A&A, 144, L15+
- Bogey, M., Demuynick, C., Destombes, J. L., & Dubus, H. 1987, Journal of Molecular Spectroscopy, 122, 313
- Bottinelli, S., Ceccarelli, C., Neri, R., et al. 2004, ApJ, 617, L69
- Bottinelli, S., Ceccarelli, C., Williams, J. P., & Lefloch, B. 2007, A&A, 463, 601
- Brown, R. D., Godfrey, P. D., McNaughton, D., & Yamanouchi, K. 1987, Molecular Physics, 62, 1429
- Brünken, S., Fuchs, U., Lewen, F., et al. 2004, Journal of Molecular Spectroscopy, 225, 152
- Brünken, S., Müller, H. S. P., Thorwirth, S., Lewen, F., & Winnewisser, G. 2006, Journal of Molecular Structure, 780, 3
- Butner, H. M., Charnley, S. B., Ceccarelli, C., et al. 2007, ApJ, 659, L137
- Camy-Peyret, C., Flaud, J., Lechuga-Fossat, L., & Johns, J. W. C. 1985, Journal of Molecular Spectroscopy, 109, 300
- Carvajal, M., Margulès, L., Tercero, B., et al. 2009, A&A, 500, 1109
- Castets, A., Ceccarelli, C., Loinard, L., Caux, E., & Lefloch, B. 2001, A&A, 375, 40

- Cazaux, S., Tielens, A. G. G. M., Ceccarelli, C., et al. 2003, *ApJ*, 593, L51
- Cazzoli, G., Cludi, L., & Puzzarini, C. 2006, *Journal of Molecular Structure*, 780, 260
- Cazzoli, G. & Puzzarini, C. 2005, *Journal of Molecular Spectroscopy*, 233, 280
- Cazzoli, G. & Puzzarini, C. 2008, *A&A*, 487, 1197
- Cazzoli, G., Puzzarini, C., & Gauss, J. 2005, *ApJS*, 159, 181
- Cazzoli, G., Puzzarini, C., & Lapinov, A. V. 2004, *ApJ*, 611, 615
- Ceccarelli, C. 2007, in *Molecules in Space and Laboratory*
- Ceccarelli, C., Bacmann, A., Boogert, A., et al. 2010, *A&A*, 521, L22+
- Ceccarelli, C., Castets, A., Caux, E., et al. 2000a, *A&A*, 355, 1129
- Ceccarelli, C., Castets, A., Loinard, L., Caux, E., & Tielens, A. G. G. M. 1998, *A&A*, 338, L43
- Ceccarelli, C., Loinard, L., Castets, A., Tielens, A. G. G. M., & Caux, E. 2000b, *A&A*, 357, L9
- Ceccarelli, C., Maret, S., Tielens, A. G. G. M., Castets, A., & Caux, E. 2003, *å*, 410, 587
- Chandler, C. J., Brogan, C. L., Shirley, Y. L., & Loinard, L. 2005, *ApJ*, 632, 371
- Chen, W., Novick, S. E., McCarthy, M. C., Gottlieb, C. A., & Thaddeus, P. 1995, *J. Chem. Phys.*, 103, 7828
- Cho, S. & Saito, S. 1998, *ApJ*, 496, L51+
- Clouthier, D. J., Huang, G., Adam, A. G., & Merer, A. J. 1994, *J. Chem. Phys.*, 101, 7300
- Comito, C., Schilke, P., Phillips, T. G., et al. 2005, *ApJS*, 156, 127
- Crimier, N., Ceccarelli, C., Maret, S., et al. 2010, *A&A*, 519, A65+
- Crovisier, J., Biver, N., Bockelée-Morvan, D., et al. 2004, in *IAU Symposium*, Vol. 202, *Planetary Systems in the Universe*, ed. A. Penny, 178–+
- de Graauw, T., Helmich, F. P., Phillips, T. G., et al. 2010, *A&A*, 518, L6+
- Demyk, K., Mäder, H., Tercero, B., et al. 2007, *A&A*, 466, 255
- Dore, L., Puzzarini, C., & Cazzoli, G. 2001, *Canadian Journal of Physics*, 79, 359
- Fusina, L., di Lonardo, G., Johns, J. W. C., & Halonen, L. 1988, *Journal of Molecular Spectroscopy*, 127, 240
- Goldsmith, P. F. 2001, *ApJ*, 557, 736
- Golubiatnikov, G. Y., Lapinov, A. V., Guarnieri, A., & Knöchel, R. 2005, *Journal of Molecular Spectroscopy*, 234, 190
- Guarnieri, A. & Huckauf, A. 2003, *Z. Naturforsch*, 58, 275
- Hatchell, J., Thompson, M. A., Millar, T. J., & MacDonald, G. H. 1998, *A&AS*, 133, 29
- Helmich, F. P. & van Dishoeck, E. F. 1997, *A&AS*, 124, 205
- Herbst, E. & van Dishoeck, E. F. 2009, *ARA&A*, 47, 427
- Huang, H., Kuan, Y., Charnley, S. B., et al. 2005, *Advances in Space Research*, 36, 146
- Johns, J. W. C. 1985, *Journal of the Optical Society of America B Optical Physics*, 2, 1340
- Jørgensen, J. K., Lahuis, F., Schöier, F. L., et al. 2005, *ApJ*, 631, L77
- Jørgensen, J. K., Schöier, F. L., & van Dishoeck, E. F. 2002, *A&A*, 389, 908
- Kim, E. & Yamamoto, S. 2003, *Journal of Molecular Spectroscopy*, 219, 296
- Kim, H., Cho, S., Chung, H., et al. 2000, *ApJS*, 131, 483
- Kim, S., Kim, H., Lee, Y., et al. 2006, *ApJS*, 162, 161
- Klapper, G., Lewen, F., Gendriesch, R., Belov, S. P., & Winnewisser, G. 2001, *Zeitschrift Naturforschung Teil A*, 56, 329
- Klapper, G., Surin, L., Lewen, F., et al. 2003, *ApJ*, 582, 262
- Klaus, T., Saleck, A. H., Belov, S. P., et al. 1996, *Journal of Molecular Spectroscopy*, 180, 197
- Kleiner, I., Lovas, F. J., & Godefroid, M. 1996, *Journal of Physical and Chemical Reference Data*, 25, 1113
- Klisch, E., Klaus, T., Belov, S. P., Winnewisser, G., & Herbst, E. 1995, *A&A*, 304, L5+
- Kuan, Y., Huang, H., Charnley, S. B., et al. 2004, *ApJ*, 616, L27
- Kutner, M. L. & Ulich, B. L. 1981, *ApJ*, 250, 341
- Lapinov, A. V., Golubiatnikov, G. Y., Markov, V. N., & Guarnieri, A. 2007, *Astronomy Letters*, 33, 121
- Lattanzi, V., Walters, A., Drouin, B. J., & Pearson, J. C. 2007, *ApJ*, 662, 771
- Lee, C. W., Cho, S., & Lee, S. 2001, *ApJ*, 551, 333
- Leguennec, M., Demaison, J., Wlodarczak, G., & Marsden, C. J. 1993, *Journal of Molecular Spectroscopy*, 160, 471
- Lohilahki, J. & Horneman, V. 2004, *Journal of Molecular Spectroscopy*, 228, 1
- Loinard, L., Castets, A., Ceccarelli, C., et al. 2000, *A&A*, 359, 1169
- Loinard, L., Torres, R. M., Mioduszewski, A. J., & Rodríguez, L. F. 2008, *ApJ*, 675, L29
- Lovas, F. J. & Suenram, R. D. 1982, *Journal of Molecular Spectroscopy*, 93, 416
- Lovas, F. J. & Suenram, R. D. 1987, *J. Chem. Phys.*, 87, 2010
- Lovas, F. J., Suenram, R. D., Ogata, T., & Yamamoto, S. 1992, *ApJ*, 399, 325
- MacDonald, G. H., Gibb, A. G., Habing, R. J., & Millar, T. J. 1996, *A&AS*, 119, 333
- Maeda, A., De Lucia, F. C., & Herbst, E. 2008, *Journal of Molecular Spectroscopy*, 251, 293
- Margulès, L., Lewen, F., Winnewisser, G., Botschwina, P., & Müller, H. S. P. 2003, *Physical Chemistry Chemical Physics (Incorporating Faraday Transactions)*, 5, 2770
- Margulès, L., Motyenko, R., Demyk, K., et al. 2009, *A&A*, 493, 565
- Meerts, W. L. & Dymanus, A. 1972, *Journal of Molecular Spectroscopy*, 44, 320
- Minowa, H., Satake, M., Hirota, T., et al. 1997, *ApJ*, 491, L63+
- Mizuno, A., Fukui, Y., Iwata, T., Nozawa, S., & Takano, T. 1990, *ApJ*, 356, 184
- Mollaaghataba, R., Gottlieb, C. A., Vrtilek, J. M., & Thaddeus, P. 1993, *J. Chem. Phys.*, 99, 890
- Müller, H. S. P., Drouin, B. J., & Pearson, J. C. 2009, *A&A*, 506, 1487
- Müller, H. S. P., Farhoomand, J., Cohen, E. A., et al. 2000a, *Journal of Molecular Spectroscopy*, 201, 1
- Müller, H. S. P., Gendriesch, R., Lewen, F., & Winnewisser, G. 2000b, *Zeitschrift Naturforschung Teil A*, 55, 486
- Müller, H. S. P., Gendriesch, R., Margulès, L., et al. 2000c, *Physical Chemistry Chemical Physics (Incorporating Faraday Transactions)*, 2, 3401
- Müller, H. S. P., Menten, K. M., & Mäder, H. 2004, *A&A*, 428, 1019
- Müller, H. S. P., Schlöder, F., Stutzki, J., & Winnewisser, G. 2005, *Journal of Molecular Structure*, 742, 215
- Müller, H. S. P., Thorwirth, S., Roth, D. A., & Winnewisser, G. 2001, *A&A*, 370, L49
- Müller, H. S. P., Winnewisser, G., Demaison, J., Perrin, A., & Valentini, A. 2000d, *Journal of Molecular Spectroscopy*, 200, 143
- Mundy, L. G., Wootten, A., Wilking, B. A., Blake, G. A., & Sargent, A. I. 1992, *ApJ*, 385, 306
- Neustock, W., Guarneri, A., & Demaison, G. 1990, *Z. Naturforsch*, 45, 702
- Nummelin, A., Bergman, P., Hjalmarson, A., et al. 1998, *ApJS*, 117, 427
- Nummelin, A., Bergman, P., Hjalmarson, Å., et al. 2000, *ApJS*, 128, 213
- Olofsson, A. O. H., Persson, C. M., Koning, N., et al. 2007, *A&A*, 476, 791
- Padovani, M., Walmsley, C. M., Tafalla, M., Galli, D., & Müller, H. S. P. 2009, *A&A*, 505, 1199
- Parise, B., Castets, A., Herbst, E., et al. 2004, *A&A*, 416, 159
- Parise, B., Caux, E., Castets, A., et al. 2005a, *A&A*, 431, 547
- Parise, B., Ceccarelli, C., & Maret, S. 2005b, *A&A*, 441, 171
- Parise, B., Ceccarelli, C., Tielens, A. G. M., et al. 2002, *A&A*, 393, L49
- Pech, G., Loinard, L., Chandler, C. J., et al. 2010, *ApJ*, 712, 1403
- Pickett, H. M., Poynter, I. R. L., Cohen, E. A., et al. 1998, *Journal of Quantitative Spectroscopy and Radiative Transfer*, 60, 883
- Pilbratt, G. L., Riedinger, J. R., Passvogel, T., et al. 2010, *A&A*, 518, L1+
- Pizzarello, S. & Huang, Y. 2005, *Geochim. Cosmochim. Acta*, 69, 599
- Remijan, A. J. & Hollis, J. M. 2006, *ApJ*, 640, 842
- Schilke, P., Benford, D. J., Hunter, T. R., Lis, D. C., & Phillips, T. G. 2001, *ApJS*, 132, 281
- Schilke, P., Groesbeck, T. D., Blake, G. A., & Phillips, T. G. 1997, *ApJS*, 108, 301
- Schmid-Burgk, J., Muders, D., Müller, H. S. P., & Bruppacher-Gatehouse, B. 2004, *A&A*, 419, 949
- Schöier, F. L., Jørgensen, J. K., van Dishoeck, E. F., & Blake, G. A. 2002, *A&A*, 390, 1001
- Schöier, F. L., Jørgensen, J. K., van Dishoeck, E. F., & Blake, G. A. 2004, *A&A*, 418, 185
- Spahn, H., Müller, H. S. P., Giesen, T. F., et al. 2008, *Chemical Physics*, 346, 132
- Takakuwa, S., Ohashi, N., Bourke, T. L., et al. 2007, *ApJ*, 662, 431
- Tercero, B., Cernicharo, J., Pardo, J. R., & Goicoechea, J. R. 2010, *A&A*, 517, A96+
- Thompson, M. A. & MacDonald, G. H. 1999, *A&AS*, 135, 531
- Thorwirth, S., Müller, H. S. P., Lewen, F., et al. 2003, *ApJ*, 585, L163
- Thorwirth, S., Müller, H. S. P., Lewen, F., Gendriesch, R., & Winnewisser, G. 2000a, *A&A*, 363, L37
- Thorwirth, S., Müller, H. S. P., & Winnewisser, G. 2000b, *Journal of Molecular Spectroscopy*, 204, 133
- van der Tak, F. F. S., Müller, H. S. P., Harding, M. E., & Gauss, J. 2009, *A&A*, 507, 347
- van Dishoeck, E. F., Blake, G. A., Jansen, D. J., & Groesbeck, T. D. 1995, *ApJ*, 447, 760
- Wakelam, V., Castets, A., Ceccarelli, C., et al. 2004, *A&A*, 413, 609
- White, G. J., Araki, M., Greaves, J. S., Ohishi, M., & Higginbottom, N. S. 2003, *A&A*, 407, 589
- Winnewisser, G., Belov, S. P., Klaus, T., & Schieder, R. 1997, *Journal of Molecular Spectroscopy*, 184, 468
- Wootten, A. 1989, *ApJ*, 337, 858
- Xu, L. & Lovas, F. J. 1997, *Journal of Physical and Chemical Reference Data*, 26, 17
- Yamamoto, S. & Saito, S. 1994, *J. Chem. Phys.*, 101, 5484

Table 2. Comparison of the spectral survey lines with previous observations.

Setting number	Species	Transition	Freq. (MHz)	$\int T_A^* dv$ survey (K.kms ⁻¹)	Ref.
				prev. obs.	
2	HDO	1 ₁₀ - 1 ₁₁	80578	0.507	0.4 (6)
11*	CH ₃ CCH	5 ₂ - 4 ₂	85450	0.188	0.18 (3)
11*	CH ₃ CCH	5 ₁ - 4 ₁	85455	0.411	0.5 (3)
11*	CH ₃ CCH	5 ₀ - 4 ₀	85457	0.524	0.54 (3)
14*	H ¹³ CO ⁺	1 - 0	86754	4.351	3.97 (12)
14*	H ¹³ CO ⁺	1 - 0	86754	4.351	4.56 (13)
14*	SiO	2 - 1	86846	1.910	1.9 (4)
14*	SiO	2 - 1	86846	1.910	2.04 (12)
14*	SiO	2 - 1	86846	1.910	2.23 (14)
14*	SiO	2 - 1	86846	1.910	2.16 (15)
19	HCO ⁺	1 - 0	89188	15.195	13.93 (13)
19	CH ₂ DOH	2 ₀₂ - 1 ₀₁ o ₁	89251	0.182	0.19 (10)
19	CH ₂ DOH	2 ₀₂ - 1 ₀₁ e ₀	89407	0.262	0.31 (10)
21	CH ₃ OCHO-E	8 ₀₈ - 7 ₀₇	90227	0.164	0.15 (3)
21	CH ₃ OCHO-A	8 ₀₈ - 7 ₀₇	90229	0.144	0.11 (3)
36	³⁴ SO	3 ₂ - 2 ₁	97715	0.791	1 (4)
38	CH ₃ OCHO-A	8 ₄₅ - 7 ₄₄	98682	0.248	0.22 (3)
38	CH ₃ OCHO-E	8 ₄₅ - 7 ₄₄	98711	0.118	0.14 (3)
60*	C ¹⁸ O	1 - 0	109782	9.900	9.02 (16)
60*	C ¹⁸ O	1 - 0	109782	9.900	7.35 (17)
60*	C ¹⁸ O	1 - 0	109782	9.900	8.7 (13)
61*	CH ₃ CN	6 ₄₀ - 5 ₄₀	110349	0.164	0.48 (3)
61*	CH ₃ CN	6 ₃₀ - 5 ₃₀	110364	0.189	0.88 (3)
61*	CH ₃ CN	6 ₂₀ - 5 ₂₀	110375	0.304	0.77 (3)
61*	CH ₃ CN	6 ₁₀ - 5 ₁₀ / 6 ₀₀ - 5 ₀₀	110382	0.695	2.02 (3)
62	D ₂ CO	2 ₁₂ - 1 ₁₁	110838	0.515	0.64 (15)
65	C ¹⁷ O	1 - 0	112359	2.855	3.07 (16)
65	C ¹⁷ O	1 - 0	112359	2.855	2.59 (17)
74	SiO	3 - 2	130268	1.361	4.86 (15)
74	SiO	3 - 2	130268	1.361	4.61 (14)
81	CH ₃ CHO-E	7 ₀₇ - 6 ₀₆	133830	0.383	0.41 (3)
81	CH ₃ CHO-A	7 ₀₇ - 6 ₀₆	133854	0.597	0.57 (3)
81	CH ₂ DOH	3 ₀₃ - 2 ₀₂ o ₁	133872	0.739	0.6 (10)
81	CH ₂ DOH	3 ₂₂ - 2 ₂₁ o ₁	133881	0.465	0.34 (10)
82	HDCO	2 ₁₁ - 1 ₁₀	134284	1.466	1.8 (9)
82	HDCO	2 ₁₁ - 1 ₁₀	134284	1.466	1.55 (15)
85	SO ₂	5 ₁₅ - 4 ₀₄	135696	3.115	4.6 (4)
85	SO ₂	5 ₁₅ - 4 ₀₄	135696	3.115	3.41 (12)
88	H ₂ ¹³ CO	2 ₁₂ - 1 ₁₁	137450	0.524	0.58 (9)
88	H ₂ ¹³ CO	2 ₁₂ - 1 ₁₁	137450	0.524	0.58 (15)
88	H ₂ ¹³ CO	2 ₁₂ - 1 ₁₁	137450	0.524	0.76 (15)
88	H ₂ ¹³ CO	2 ₁₂ - 1 ₁₁	137450	0.524	0.76 (15)
95	H ₂ CO	2 ₁₂ - 1 ₁₁	140839	19.242	16.6 (9)
95	H ₂ CO	2 ₁₂ - 1 ₁₁	140839	19.242	15.57 (15)
100	C ₂ H ₅ CN	16 _{5,12} - 15 _{5,11} / 16 _{5,11} - 15 _{5,10}	143406	0.256	0.55 (3)
101	CH ₃ OCH ₃	7 _{3,4,2} - 7 _{2,5,2}	143600	0.107	0.42 (3)
101	CH ₃ OCH ₃	7 _{3,4,1} - 7 _{2,5,1}	143603	0.414	0.31 (3)
101	CH ₃ OCH ₃	7 _{3,4,0} - 7 _{2,5,0}	143606	0.189	0.28 (3)
146	CHD ₂ OH	4 ₀ - 3 ₀ e ₀	166435	0.500	0.48 (10)
151	H ₂ S	1 ₁₀ - 1 ₀₁	168762	17.511	17.5 (4)
282*	H ₂ ¹³ CO	3 ₁₃ - 2 ₁₂	206132	1.752	1.6 (9)
282*	H ₂ ¹³ CO	3 ₁₃ - 2 ₁₂	206132	1.752	1.97 (15)
282*	H ₂ ¹³ CO	3 ₁₃ - 2 ₁₂	206132	1.752	2.19 (15)
282*	H ₂ ¹³ CO	3 ₁₃ - 2 ₁₂	206132	1.752	2.48 (15)
282*	SO	4 ₅ - 3 ₄	206176	21.367	36 (15)
285*	CH ₂ DOH	2 ₁₂ - 3 ₀₃ e ₀	207780	0.690	1.01 (10)
292*	H ₂ CO	3 ₁₃ - 2 ₁₂	211211	31.416	43.8 (9)
292*	H ₂ CO	3 ₁₃ - 2 ₁₂	211211	31.416	33 (15)
292*	H ₂ CO	3 ₁₃ - 2 ₁₂	211211	31.416	26.4 (16)
296	H ₂ ¹³ CO	3 ₂₂ - 2 ₂₁	213037	0.711	0.45 (15)
296	H ₂ ¹³ CO	3 ₂₁ - 2 ₂₀	213294	0.593	0.46 (15)
303	H ₂ S	2 ₂₀ - 2 ₁₁	216710	7.436	3 (4)
304	SiO	5 - 4	217104	4.524	4.83 (14)

Table 2. Continued.

Setting number	Species	Transition	Freq. (MHz)	$\int T_A^* dv$ (K.kms ⁻¹)	Ref.
				survey	prev. obs.
312	D ₂ CO	4 ₁₄ – 3 ₁₃	221191	1.274	1.6 (9)
316	CH ₂ DOH	5 ₂₃ – 4 ₁₄ e ₁	223071	0.972	1.13 (10)
316	CH ₂ DOH	5 ₃₃ – 4 ₃₂ o ₁	223153	1.204	0.58 (10)
316	CH ₂ DOH	5 ₂₃ – 4 ₂₂ e ₁	223315	0.717	0.38 (10)
321	HDO	3 ₁₂ – 2 ₂₁	225897	2.089	1.7 (6)
322	CH ₃ OCH ₃	1413	226346	1.685	0.89 (3)
323	CH ₃ CHO-E	12 _{0,12} – 11 _{0,11}	226551	0.809	0.49 (3)
323	CH ₃ OCHO-E	20 _{2,18} – 19 _{2,18}	226713	1.540	1.19 (3)
323	CH ₃ OCHO-A	20 _{2,19} – 19 _{2,18}	226718	0.707	0.49 (3)
323	CH ₃ OCHO-A	20 _{1,19} – 19 _{1,18}	226778	1.324	0.84 (3)
332	D ₂ CO	4 ₀₄ – 3 ₀₃	231410	3.334	2.43 (15)
332	D ₂ CO	4 ₀₄ – 3 ₀₃	231410	3.334	2.01 (16)
332	D ₂ CO	4 ₀₄ – 3 ₀₃	231410	3.334	1.92 (17)
332	D ₂ CO	4 ₀₄ – 3 ₀₃	231410	3.334	2.69 (13)
332	D ₂ CO	4 ₀₄ – 3 ₀₃	231410	3.340	3 (9)
332	CH ₃ CHO-A	12 ₄₈ – 11 ₄₇	231457	0.520	0.51 (3)
342	D ₂ CO	4 ₂₂ – 3 ₂₁	236102	1.718	1.86 (8)
342	D ₂ CO	4 ₂₂ – 3 ₂₁	236102	1.718	1.9 (9)
342	D ₂ CO	4 ₂₂ – 3 ₂₁	236102	1.710	1.9 (15)
353	HDO	2 ₁₁ – 2 ₁₂	241561	2.268	2 (6)
363*	HDCO	4 ₁₄ – 3 ₁₃	246925	2.067	8.43 (15)
363*	HDCO	4 ₁₄ – 3 ₁₃	246925	2.067	7.6 (9)
401	HDO	2 ₂₀ – 3 ₁₃	266161	0.214	0.21 (6)
434	C ¹⁸ O	3 – 2	329335	55.768	33.6 (11)
436	¹³ CH ₃ OH	7 ₁₇ – 6 ₁₆	330194	0.458	0.51 (5)
436	¹³ CH ₃ OH	7 ₃₄ – 6 ₃₃	330408	1.123	0.91 (5)
437	¹³ CO	3 – 2	330588	55.854	67.2 (11)
446	HDCO	5 ₁₄ – 4 ₁₃	335096	4.550	3.95 (2)
446	HDCO	5 ₁₄ – 4 ₁₃	335097	4.550	4.5 (9)
450	C ¹⁷ O	3 – 2	337061	12.481	11 (1)
450	CH ₃ OH	3 ₃ – 4 ₂ E ⁺	337136	0.826	1.05 (2)
452	H ₂ CS	21 _{1,10} – 9 _{1,9}	338081	1.723	2.4 (1)
455	³⁴ SO	8 ₉ – 7 ₈	339858	3.863	2.98 (1)
461	D ₂ CO	6 ₀₆ – 5 ₀₅	342522	1.875	1.9 (9)
461	CS	7 – 6	342883	38.535	51.4 (11)
462	H ₂ ¹³ CO	5 ₁₅ – 4 ₁₄	343325	3.181	1.37 (9)
464	SÖ	8 ₈ – 7 ₇	344311	18.647	18.1 (1)
470	SiO	8 – 7	347331	8.546	5.79 (1)
475	D ₂ CO	6 ₂₅ – 5 ₂₄	349631	1.506	1 (9)
479	H ₂ CO	5 ₁₅ – 4 ₁₄	351768	35.945	38.3 (9)
483	H ₂ ¹³ CO	5 ₀₅ – 4 ₀₄	353812	0.869	0.6 (9)
484	HCN	4 – 3	354505	41.068	63.4 (11)
485	H ₂ ¹³ CO	5 ₂₄ – 4 ₂₃	354899	0.557	0.3 (9)
490	SO ₂	15 _{4,12} – 15 _{3,13}	357241	3.603	3.29 (1)
490	SO ₂	11 ₄₈ – 11 ₃₉	357388	4.201	2.25 (1)
496	DCO ⁺	5 – 4	360170	3.135	4.02 (2)
501	HNC	4 – 3	362630	8.264	11.9 (11)
501	H ₂ CO	5 ₀₅ – 4 ₀₄	362736	18.394	28.9 (9)
503	H ₂ CO	5 ₂₄ – 4 ₂₃	363946	11.728	11.9 (9)

All observations are obtained with the same telescopes: IRAM 30 m from 80 to 280 GHz, JCMT from 328 to 366 GHz. The coordinates of the observed position are $\alpha(2000.0) = 16^{\text{h}}32^{\text{m}} 22.6^{\text{s}}$, $\delta(2000.0) = -24^{\circ} 28' 33''$; except for the settings numbers tagged with an asterisk that correspond to a slightly different position: $\alpha(2000.0) = 16^{\text{h}}32^{\text{m}} 22.7^{\text{s}}$, $\delta(2000.0) = -24^{\circ} 22' 13''$. References: ¹Blake et al. (1994); ²van Dishoeck et al. (1995); ³Cazaux et al. (2003); ⁴Wakelam et al. (2004); ⁵Parise et al. (2004); ⁶Parise et al. (2005a); ⁷Butner et al. (2007); ⁸Ceccarelli et al. (1998); ⁹Loinard et al. (2000); ¹⁰Parise et al. (2002); ¹¹Schöier et al. (2002), unpublished IRAM 30 m observations: ¹²June 1997, ¹³September 2000, ¹⁴April 1998, ¹⁵January 1999, ¹⁶March 2000, ¹⁷August 2000, ¹⁸March 1998.

Table 3. Comparison of the strong spectral survey lines simultaneously observed with different backends.

Setting number	Frequency (MHz)	$\int T_A^* dv$ (K.kms $^{-1}$)		Setting number	Frequency (MHz)	$\int T_A^* dv$ (K.kms $^{-1}$)		Setting number	Frequency (MHz)	$\int T_A^* dv$ (K.kms $^{-1}$)	
		VESPA	FB			VESPA	FB			VESPA	FB
73	129515	2.436	3.091	105	145603	11.325	11.266	136	161172	0.501	0.367
74	130268	1.361	5.378	106	146368	2.447	1.604	137	161603	0.462	0.713
75	130892	0.506	0.290	107	146968	28.254	27.119	138	162186	0.340	0.302
76	131015	1.432	2.062	108	147174	3.356	3.312	139	162530	0.779	0.900
77	131885	1.103	1.042	109	147944	0.600	0.904	140	163119	1.409	1.142
78	132246	0.510	0.948	110	148112	1.802	1.816	140	163162	0.610	0.617
79	132891	1.429	2.186	111	148807	0.327	0.304	141	163753	2.187	2.047
80	133355	0.226	0.337	112	149022	0.764	0.563	142	164138	0.432	0.448
81	133786	3.012	1.995	113	149533	1.211	1.282	144	165048	1.493	1.987
82	134284	1.499	2.367	114	150142	1.232	1.140	144	165369	1.444	1.939
83	134897	1.358	0.798	115	150852	2.651	2.765	145	165677	2.606	1.283
84	135298	1.361	2.372	116	151378	1.399	1.898	146	166167	2.838	2.476
85	135696	3.131	4.058	117	151861	0.627	1.278	147	166896	2.483	2.226
86	136464	1.975	1.792	119	152609	2.889	2.860	149	167909	3.481	3.193
87	136635	1.459	1.313	120	153282	1.263	1.175	150	168087	0.622	0.636
88	137450	0.512	0.868	121	153865	1.525	1.792	150	168092	0.576	0.584
89	137903	0.769	0.821	122	154426	1.347	1.227	151	168762	17.648	18.619
90	138178	16.594	18.887	123	154657	1.652	1.948	152	169114	2.601	2.574
91	138739	1.716	1.647	124	155321	1.468	1.111	153	169743	0.399	0.561
92	139484	1.490	1.696	125	155507	1.066	1.048	154	170268	2.965	3.644
94	140306	2.451	2.967	126	156128	1.296	1.337	155	170691	0.737	0.726
95	140839	18.764	15.396	127	156602	2.266	1.967	156	171183	1.604	2.101
96	141244	0.451	0.569	128	157246	1.859	2.994	157	171688	1.454	1.553
97	141984	0.537	0.502	129	157599	0.517	0.417	158	172181	18.028	14.817
98	142379	0.594	0.711	130	158108	2.840	3.706	159	172678	5.176	5.507
99	142769	0.628	0.495	130	158200	2.105	2.313	160	173506	7.830	8.033
100	143057	2.545	2.622	131	158972	13.990	11.328	161	173687	6.316	7.010
101	143866	2.455	2.390	132	159439	0.695	0.719	162	174345	1.860	1.973
102	144077	5.405	6.935	133	159777	0.594	1.009	163	174663	2.927	2.708
103	144616	4.056	3.609	134	160343	2.371	2.091				
104	145103	3.614	5.050	135	160828	4.805	4.875				

The two backends used in the 129-175 GHz range were the VESPA autocorrelator (0.32 MHz resolution) and the 1 MHz resolution Filter Banks (FB).

Table 4. Identified non-blended lines. The line characteristics are derived from Gaussian fits.

TAG	Species & Transition	Frequency (MHz)	E _{up} (K)	A _{ij} s ⁻¹	V ₀ (km s ⁻¹)	δ_{V_0} (km s ⁻¹)	FWHM (km s ⁻¹)	δ_{FWHM} (km s ⁻¹)	Int. δ_{Int} (K)	Flux (K.kms ⁻¹)	δ_{Flux} (K.kms ⁻¹)	comments
28503	CO (1-0)	115271.20	5.53	7.20E-08	5.90	0.23	7.49	0.54	10.718	0.667	108.94	11.98
28503	CO (2-1)	230538.00	16.60	6.91E-07	5.23	0.39	10.00	0.92	10.405	0.826	189.77	32.26
28503	CO (3-2)	345795.99	33.19	2.50E-06	6.65	0.40	10.91	0.94	14.595	1.087	307.10	55.28
29501	13CO (1-0)	110201.35	5.29	6.33E-08	4.34	0.06	2.82	0.14	3.148	0.135	11.92	1.31
29501	13CO (2-1)	220398.68	15.87	6.07E-07	3.84	0.10	5.03	0.22	5.440	0.210	48.19	8.19
29501	13CO (3-2)	330587.97	31.73	2.19E-06	3.63	0.47	4.55	1.13	6.493	1.377	55.92	10.07
30502	C ¹⁸ O (1-0)	109782.17	5.27	6.27E-08	3.92	0.03	2.19	0.06	3.362	0.081	9.88	1.09
30502	C ¹⁸ O (2-1)	219560.35	15.81	6.01E-07	3.57	0.04	3.28	0.10	4.842	0.131	27.88	4.74
30502	C ¹⁸ O (3-2)	329330.55	31.61	2.17E-06	3.67	0.13	3.22	0.30	4.891	0.396	29.79	5.36
29006	C ¹⁷ O (1-0)	112359.28	5.39	6.70E-08	4.24	0.25	4.45	0.60	0.511	0.059	3.07	0.34
29006	C ¹⁷ O (2-1)	224714.39	16.18	6.43E-07	3.62	0.02	3.66	0.05	1.576	0.020	10.32	1.75
29006	C ¹⁷ O (3-2)	337061.13	32.35	2.32E-06	3.66	0.09	3.15	0.22	2.010	0.121	12.07	2.17
48501	SO (2 ₂ -1 ₁)	86093.95	19.31	5.25E-06	4.03	0.09	3.50	0.20	0.804	0.041	3.63	0.4
48501	SO (2 ₃ -1 ₂)	99299.87	9.23	1.13E-05	4.19	0.02	3.88	0.06	1.930	0.020	9.86	1.09
48501	SO (5 ₄ -4 ₄)	100029.64	38.58	1.08E-06	4.14	0.10	4.30	0.23	0.191	0.009	1.09	0.12
48501	SO (3 ₂ -2 ₁)	109252.22	21.05	1.08E-05	4.35	0.06	3.63	0.15	0.449	0.016	2.19	0.24
48501	SO (3 ₃ -2 ₂)	129138.92	25.51	2.25E-05	4.09	0.08	3.46	0.18	2.361	0.108	11.39	1.94
48501	SO (6 ₅ -5 ₅)	136634.80	50.66	1.75E-06	4.23	0.11	5.11	0.27	0.200	0.009	1.44	0.25
48501	SO (3 ₄ -2 ₃)	138178.60	15.86	3.17E-05	3.92	0.11	3.79	0.25	3.069	0.174	16.50	2.81
48501	SO (4 ₃ -3 ₂)	158971.81	28.68	4.23E-05	3.96	0.08	3.57	0.18	2.594	0.113	13.74	2.34
48501	SO (4 ₄ -3 ₃)	172181.40	33.78	5.83E-05	4.00	0.08	3.72	0.18	3.161	0.131	18.00	3.06
48501	SO (7 ₆ -6 ₆)	174928.86	64.89	2.51E-06	3.78	0.11	4.89	0.28	0.257	0.012	1.94	0.33
48501	SO (5 ₄ -4 ₃)	206176.01	38.58	1.01E-04	3.99	0.12	4.89	0.33	2.489	0.098	20.49	3.48
48501	SO (5 ₅ -4 ₄)	215220.65	44.10	1.19E-04	4.00	0.02	4.31	0.05	2.919	0.024	21.76	3.70
48501	SO (5 ₆ -4 ₅)	219949.44	34.99	1.34E-04	3.86	0.10	4.48	0.26	4.467	0.210	35.18	5.98
48501	SO (6 ₅ -5 ₄)	251825.77	50.66	1.92E-04	3.80	0.10	4.49	0.27	3.066	0.144	27.27	4.64
48501	SO (6 ₆ -5 ₅)	258255.83	56.50	2.12E-04	4.21	0.12	4.96	0.33	2.139	0.093	21.58	3.67
48501	SO (6 ₇ -5 ₆)	261843.72	47.55	2.28E-04	4.23	0.10	4.83	0.24	4.960	0.202	49.49	8.41
48501	SO (3 ₃ -2 ₃)	339341.46	25.51	1.45E-05	3.77	0.09	4.19	0.25	3.391	0.149	27.20	4.92
48501	SO (8 ₇ -7 ₆)	340714.16	81.25	4.99E-04	3.78	0.07	4.10	0.18	3.886	0.133	30.54	5.50
48501	SO (8 ₈ -7 ₇)	344310.61	87.48	5.19E-04	3.61	0.07	3.62	0.19	2.539	0.104	17.71	3.19
48501	SO (8 ₉ -7 ₈)	346528.48	78.78	5.38E-04	3.71	0.07	3.66	0.18	4.665	0.179	32.93	5.93
50501	34SO (2 ₂ -1 ₁)	84410.69	19.23	4.95E-06	3.91	0.17	5.14	0.42	0.038	0.003	0.25	0.04
50501	34SO (3 ₄ -2 ₃)	135775.73	15.61	3.00E-05	4.16	0.05	2.83	0.13	0.321	0.012	1.28	0.22
50501	34SO (4 ₃ -3 ₂)	155506.80	28.37	3.96E-05	3.86	0.08	3.68	0.18	0.201	0.009	1.09	0.19
50501	34SO (4 ₄ -3 ₃)	168815.14	33.41	5.50E-05	4.29	0.15	5.17	0.36	0.212	0.017	1.49	0.26
50501	34SO (5 ₄ -4 ₃)	201846.48	38.06	9.47E-05	3.52	0.18	5.07	0.44	0.217	0.015	1.83	0.31
50501	34SO (5 ₅ -4 ₄)	211013.03	43.54	1.12E-04	3.99	0.12	5.42	0.28	0.199	0.010	1.85	0.32
50501	34SO (5 ₆ -4 ₅)	215839.92	34.38	1.26E-04	3.67	0.17	4.24	0.41	0.426	0.035	3.13	0.53
50501	34SO (6 ₅ -5 ₄)	246663.47	49.89	1.81E-04	3.93	0.18	4.99	0.43	0.124	0.009	1.19	0.21
50501	34SO (6 ₆ -5 ₅)	253207.02	55.69	2.00E-04	3.73	0.15	6.08	0.38	0.114	0.006	1.38	0.24
50501	34SO (6 ₇ -5 ₆)	256877.81	46.71	2.15E-04	3.91	0.12	5.05	0.31	0.464	0.023	4.73	0.80
50501	34SO (8 ₇ -7 ₆)	333900.98	79.86	4.69E-04	3.56	0.16	4.91	0.42	0.288	0.019	2.68	0.48
50501	34SO (8 ₈ -7 ₇)	337580.15	86.07	4.89E-04	3.30	0.10	5.40	0.25	0.302	0.012	3.12	0.56
50501	34SO (8 ₉ -7 ₈)	339857.27	77.34	5.08E-04	3.68	0.12	5.36	0.29	0.383	0.017	3.93	0.71

Table 4. Continued.

TAG	Species & Transition	Frequency (MHz)	Eup (K)	A _{ij} s ⁻¹	V _O δ _{ν_o} (km s ⁻¹)	FWHM δ _{FWM} (km s ⁻¹)	Int δ _{int} (K)	Flux δ _{Flux} (K km s ⁻¹)	comments
30591	o-H ₂ CO (6 _{1,5} -6 _{1,6})	101332.99	72.40	1.57E-06	3.14	0.18	4.43	0.42	0.111 0.009
30591	o-H ₂ CO (7 _{1,6} -7 _{1,7})	135030.44	97.63	2.79E-06	2.63	0.13	3.26	0.30	0.154 0.012
30591	o-H ₂ CO (2 _{1,2} -1 _{1,1})	140839.50	6.76	5.29E-05	4.00	0.24	4.34	0.57	3.051 0.343
30591	o-H ₂ CO (2 _{1,1} -1 _{1,0})	150498.33	7.45	6.46E-05	3.89	0.19	4.49	0.46	2.975 0.232
30591	o-H ₂ CO (8 _{1,7} -8 _{1,8})	173461.70	126.44	4.61E-06	2.40	0.18	4.01	0.44	0.137 0.013
30591	o-H ₂ CO (3 _{1,3} -2 _{1,2})	211211.47	16.90	2.27E-04	4.19	0.04	4.80	0.09	3.771 0.060
30591	o-H ₂ CO (3 _{1,2} -2 _{1,1})	225697.77	18.29	2.77E-04	3.65	0.25	4.36	0.59	4.646 0.543
30591	o-H ₂ CO (5 _{1,5} -4 _{1,4})	351768.65	47.29	1.20E-03	3.59	0.07	2.92	0.16	6.392 0.293
30591	o-H ₂ CO (5 _{3,3} -4 _{3,2})	364275.14	143.26	8.88E-04	3.49	0.06	4.16	0.13	1.166 0.033
30591	o-H ₂ CO (5 _{3,2} -4 _{3,1})	364288.88	143.26	8.88E-04	3.52	0.06	4.12	0.14	1.186 0.035
30581	p-H ₂ CO (2 _{0,2} -1 _{0,1})	145602.95	10.48	7.80E-05	3.52	0.21	3.26	0.50	2.428 0.324
30581	p-H ₂ CO (3 _{0,3} -2 _{0,2})	218222.19	20.96	2.81E-04	3.87	0.06	4.30	0.13	3.212 0.083
30581	p-H ₂ CO (3 _{2,2} -2 _{2,1})	218475.63	68.09	1.57E-04	3.75	0.08	4.75	0.18	1.036 0.034
30581	p-H ₂ CO (3 _{2,1} -2 _{2,0})	218760.07	68.11	1.57E-04	3.69	0.08	4.27	0.19	1.100 0.042
30581	p-H ₂ CO (5 _{0,5} -4 _{0,4})	362736.05	52.31	1.37E-03	3.56	0.07	2.87	0.15	3.320 0.153
30581	p-H ₂ CO (5 _{2,4} -4 _{2,3})	363945.89	99.54	1.16E-03	3.69	0.07	4.01	0.15	1.512 0.050
30581	p-H ₂ CO (5 _{2,3} -4 _{2,2})	365363.43	99.66	1.18E-03	3.62	0.06	3.98	0.15	1.337 0.044
31501	HDCO (6 _{1,5} -6 _{1,6})	112066.60	75.53	2.13E-06	2.82	0.27	3.91	0.65	0.042 0.006
31501	HDCO (2 _{1,1} -1 _{1,0})	134284.83	17.63	4.59E-05	3.86	0.11	2.82	0.26	0.366 0.029
31501	HDCO (7 _{1,6} -7 _{1,7})	149214.25	97.99	3.79E-06	2.67	0.10	2.05	0.25	0.079 0.008
31501	HDCO (3 _{1,2} -2 _{1,1})	201341.36	27.29	1.97E-04	3.82	0.15	4.47	0.36	0.557 0.039
31501	HDCO (4 _{1,4} -3 _{1,3})	246924.60	37.60	3.96E-04	3.54	0.14	3.91	0.33	0.275 0.020
31501	HDCO (4 _{0,4} -3 _{0,3})	256585.54	30.85	4.74E-04	3.92	0.13	4.13	0.31	0.842 0.054
31501	HDCO (4 _{2,3} -3 _{2,2})	257748.70	62.77	3.61E-04	3.76	0.14	4.42	0.32	0.231 0.014
31501	HDCO (4 _{3,2} -3 _{3,1})	258070.94	102.56	2.11E-04	2.27	0.43	6.12	1.21	0.105 0.015
31501	HDCO (4 _{1,3} -3 _{1,2})	2688292.02	40.17	5.09E-04	3.71	0.04	4.18	0.10	0.484 0.010
31501	HDCO (5 _{1,4} -4 _{1,3})	335096.78	56.25	1.04E-03	3.55	0.16	3.85	0.39	0.532 0.044
31503	H ₂ ¹³ CO (2 _{1,2} -1 _{1,1})	137449.95	21.72	4.93E-05	3.54	0.07	3.18	0.16	0.110 0.005
31503	H ₂ ¹³ CO (2 _{0,2} -1 _{0,1})	141983.74	10.22	7.25E-05	3.38	0.11	3.32	0.26	0.130 0.009
31503	H ₂ ¹³ CO (2 _{1,1} -1 _{1,0})	146635.67	22.38	5.99E-05	3.14	0.13	3.74	0.32	0.181 0.013
31503	H ₂ ¹³ CO (3 _{1,3} -2 _{1,2})	206131.63	31.62	2.11E-04	3.36	0.12	4.28	0.29	0.257 0.015
31503	H ₂ ¹³ CO (3 _{0,3} -2 _{0,2})	212811.18	20.44	2.61E-04	3.12	0.23	3.54	0.62	0.147 0.020
31503	H ₂ ¹³ CO (3 _{1,2} -2 _{1,1})	219908.52	32.94	2.56E-04	2.85	0.19	3.03	0.44	0.330 0.042
31503	H ₂ ¹³ CO (4 _{1,4} -3 _{1,3})	274762.11	44.80	5.47E-04	3.24	0.16	5.31	0.40	0.202 0.013
31503	H ₂ ¹³ CO (5 _{0,5} -4 _{0,4})	353811.87	51.02	1.27E-03	2.56	0.09	1.45	0.21	0.300 0.038
31503	H ₂ ¹³ CO (5 _{2,4} -4 _{2,3})	354898.59	98.41	1.08E-03	2.71	0.10	1.39	0.24	0.200 0.029
31503	H ₂ ¹³ CO (5 _{3,3} -4 _{3,2})	355190.90	157.52	8.25E-04	2.55	0.05	1.23	0.12	0.190 0.016
31503	H ₂ ¹³ CO (5 _{3,2} -4 _{3,1})	355202.60	157.52	8.25E-04	2.43	0.09	1.81	0.21	0.173 0.017
31503	H ₂ ¹³ CO (5 _{1,4} -4 _{1,3})	366270.15	64.59	1.36E-03	2.63	0.07	1.99	0.17	0.337 0.025
32592	o-D ₂ CO (3 _{0,3} -2 _{0,2})	174413.12	16.78	1.44E-04	4.09	0.12	2.30	0.27	0.510 0.052
32592	o-D ₂ CO (4 _{0,4} -3 _{0,3})	221410.23	27.88	3.47E-04	4.00	0.12	4.18	0.29	0.430 0.026
32592	o-D ₂ CO (4 _{2,2} -3 _{2,1})	236102.09	49.80	2.77E-04	4.00	0.26	4.87	0.67	0.171 0.018
32592	o-D ₂ CO (6 _{0,6} -5 _{0,5})	342522.13	58.12	1.17E-03	3.40	0.15	3.80	0.40	0.268 0.021
32592	o-D ₂ CO (6 _{2,5} -5 _{2,4})	349630.61	80.41	1.11E-03	2.78	0.24	3.86	0.69	0.214 0.026
32592	o-D ₂ CO (6 _{2,4} -5 _{2,3})	357871.46	81.21	1.19E-03	2.80	0.21	3.81	0.51	0.199 0.022
32582	p-D ₂ CO (2 _{1,2} -1 _{1,1})	110837.83	5.32	2.58E-05	4.34	0.06	1.96	0.15	0.194 0.013

Table 4. Continued.

TAG	Species & Transition	Frequency (MHz)	Eup (K)	A _{ij} s ⁻¹	V _O (km s ⁻¹)	δ_{V_O} (km s ⁻¹)	FWHM (km s ⁻¹)	δ_{FWHM} (km s ⁻¹)	Int δ_{Int} (K)	Flux (K km s ⁻¹)	δ_{Flux} (K km s ⁻¹)	comments
32582	p-D ₂ CO (3 _{1,3} -2 _{1,2})	166102.75	13.29	1.10E-04	4.19	0.15	2.66	0.36	0.280	0.032	1.12	0.19
32582	p-D ₂ CO (4 _{1,4} -3 _{1,3})	2211191.67	23.91	2.85E-04	3.89	0.14	4.22	0.36	0.182	0.012	1.35	0.23
32582	p-D ₂ CO (4 _{3,2} -3 _{3,1})	234293.36	68.57	1.58E-04	2.91	0.23	3.90	0.56	0.048	0.006	0.34	0.07
32582	p-D ₂ CO (4 _{1,3} -3 _{1,2})	245532.75	26.83	3.90E-04	3.62	0.19	4.41	0.50	0.073	0.006	0.62	0.11
32582	p-D ₂ CO (6 _{1,6} -5 _{1,5})	330674.35	53.03	1.02E-03	2.70	0.13	1.43	0.30	0.204	0.037	0.55	0.10
32582	p-D ₂ CO (6 _{3,4} -5 _{3,3})	351894.28	99.52	9.54E-04	2.73	0.07	1.92	0.16	0.157	0.011	0.58	0.11
32582	p-D ₂ CO (6 _{3,3} -5 _{3,2})	352243.69	99.55	9.56E-04	2.62	0.16	1.56	0.42	0.147	0.031	0.45	0.08
32503	H ₂ C ¹⁸ O (2 _{1,1} -1 _{1,0})	143213.07	22.18	5.58E-05	2.94	0.26	3.13	0.68	0.051	0.009	0.23	0.05
32503	H ₂ C ¹⁸ O (3 _{0,3} -2 _{0,2})	208006.44	19.97	2.44E-04	2.58	0.27	3.99	0.64	0.034	0.005	0.23	0.04
32503	H ₂ C ¹⁸ O (5 _{1,5} -4 _{1,4})	335815.93	60.23	1.05E-03	2.70	0.38	2.42	0.92	0.060	0.019	0.28	0.05
32503	H ₂ C ¹⁸ O (5 _{1,4} -4 _{1,3})	357741.05	63.39	1.26E-03	2.62	0.06	1.14	0.14	0.194	0.021	0.44	0.08
64502	SO ₂ (13 _{4,10} -14 _{3,11})	82951.94	122.97	1.26E-06	2.82	0.44	7.67	1.32	0.028	0.003	0.27	0.04
64502	SO ₂ (8 _{1,7} -8 _{0,8})	83688.09	36.72	6.82E-06	4.04	0.10	3.89	0.23	0.399	0.021	1.99	0.22
64502	SO ₂ (8 _{3,5} -9 _{2,8})	86639.09	55.20	1.34E-06	3.10	0.18	4.67	0.44	0.046	0.004	0.28	0.04
64502	SO ₂ (7 _{3,5} -8 _{2,6})	97702.33	47.84	1.81E-06	3.34	0.23	6.60	0.60	0.040	0.003	0.35	0.05
64502	SO ₂ (2 _{2,0} -3 _{1,3})	100878.10	12.59	1.03E-06	4.43	0.18	3.29	0.42	0.040	0.005	0.17	0.02
64502	SO ₂ (3 _{1,3} -2 _{0,2})	104029.42	7.74	1.01E-05	4.13	0.07	3.40	0.16	0.460	0.018	2.08	0.23
64502	SO ₂ (16 _{2,14} -15 _{3,13})	104033.58	137.53	3.17E-06	3.36	0.14	4.92	0.35	0.055	0.003	0.36	0.04
64502	SO ₂ (10 _{1,9} -10 _{0,10})	104239.29	54.71	1.12E-05	3.98	0.10	4.17	0.23	0.375	0.018	2.08	0.23
64502	SO ₂ (12 _{1,11} -1 _{1,2,10})	129105.83	76.41	9.03E-06	4.14	0.18	5.23	0.43	0.209	0.015	1.52	0.26
64502	SO ₂ (10 _{2,8} -10 _{1,9})	129514.81	60.93	2.50E-05	4.02	0.09	4.16	0.22	0.432	0.020	2.51	0.43
64502	SO ₂ (12 _{1,11} -12 _{0,12})	131014.86	76.41	1.86E-05	3.94	0.13	5.18	0.30	0.198	0.010	1.43	0.24
64502	SO ₂ (14 _{2,12} -14 _{1,13})	132744.86	108.12	2.93E-05	3.86	0.10	5.78	0.25	0.154	0.006	1.25	0.21
64502	SO ₂ (8 _{2,6} -8 _{1,7})	134004.86	43.15	2.50E-05	4.02	0.12	3.88	0.28	0.347	0.022	1.89	0.32
64502	SO ₂ (5 _{1,5} -4 _{0,4})	135696.02	15.66	2.21E-05	3.97	0.08	3.10	0.19	0.724	0.038	3.16	0.54
64502	SO ₂ (5 _{3,3} -6 _{2,4})	139355.06	35.89	3.85E-06	3.66	0.25	4.78	0.60	0.072	0.008	0.49	0.09
64502	SO ₂ (6 _{2,4} -6 _{1,5})	140306.17	29.20	2.53E-05	3.84	0.07	3.48	0.17	0.501	0.021	2.49	0.42
64502	SO ₂ (16 _{2,14} -16 _{1,15})	143057.11	137.53	3.57E-05	3.88	0.09	5.81	0.23	0.299	0.010	2.49	0.42
64502	SO ₂ (10 _{4,6} -11 _{3,9})	146550.08	89.84	5.90E-06	3.40	0.18	6.01	0.46	0.097	0.006	0.84	0.15
64502	SO ₂ (4 _{2,2} -4 _{1,3})	146605.52	19.03	2.47E-05	3.93	0.09	4.30	0.22	0.468	0.021	2.91	0.50
64502	SO ₂ (15 _{5,11} -16 _{4,12})	150381.10	171.68	6.95E-06	3.17	0.36	7.53	1.01	0.067	0.006	0.73	0.13
64502	SO ₂ (2 _{2,0} -2 _{1,1})	151378.63	12.59	1.87E-05	3.96	0.10	3.94	0.24	0.247	0.013	1.42	0.24
64502	SO ₂ (3 _{2,2} -3 _{1,3})	158199.74	15.34	2.53E-05	3.63	0.11	4.17	0.25	0.352	0.018	2.17	0.37
64502	SO ₂ (18 _{2,16} -18 _{1,17})	160342.99	170.76	4.69E-05	3.49	0.08	7.03	0.21	0.229	0.005	2.40	0.41
64502	SO ₂ (4 _{3,1} -5 _{2,4})	160543.06	31.29	4.32E-06	3.70	0.16	3.98	0.38	0.077	0.006	0.46	0.08
64502	SO ₂ (10 _{0,10} -9 ₁₉)	160827.88	49.71	3.95E-05	4.01	0.08	3.86	0.20	0.826	0.036	4.76	0.81
64502	SO ₂ (18 _{2,16} -17 _{3,15})	163119.38	170.76	1.35E-05	3.85	0.25	7.38	0.71	0.119	0.008	1.31	0.23
64502	SO ₂ (14 _{1,13} -14 _{0,14})	163605.53	101.75	3.01E-05	3.98	0.07	5.63	0.17	0.322	0.008	2.72	0.46
64502	SO ₂ (5 _{2,4} -5 _{1,5})	165144.65	23.59	3.12E-05	3.97	0.12	2.36	0.27	0.466	0.047	1.66	0.28
64502	SO ₂ (7 _{1,7} -6 _{0,6})	165225.45	27.08	4.13E-05	3.81	0.12	2.46	0.29	0.743	0.075	2.75	0.47
64502	SO ₂ (16 _{1,15} -16 _{0,16})	200809.18	130.67	4.70E-05	3.35	0.11	5.76	0.28	0.173	0.007	1.65	0.28
64502	SO ₂ (11 _{2,10} -11 _{1,11})	205300.57	70.22	5.32E-05	3.84	0.11	5.74	0.29	0.351	0.013	3.38	0.58
64502	SO ₂ (3 _{2,2} -2 _{1,1})	208700.34	15.34	6.72E-05	4.00	0.10	4.87	0.24	0.472	0.019	3.89	0.66
64502	SO ₂ (16 _{3,13} -16 _{2,14})	214689.39	147.84	9.90E-05	3.72	0.13	6.68	0.36	0.444	0.017	5.12	0.87
64502	SO ₂ (17 _{6,12} -18 _{5,13})	214728.29	228.96	1.89E-05	3.63	0.12	6.52	0.32	0.108	0.004	1.21	0.22
64502	SO ₂ (22 _{2,20} -22 _{1,20})	216643.30	248.45	9.27E-05	3.42	0.10	6.87	0.30	0.202	0.006	2.41	0.41

Table 4. Continued.

TAG	Species & Transition	Frequency (MHz)	Eup (K)	A _{ij} s ⁻¹	V _O δ _{ν_o} (km s ⁻¹)	FWHM δ _{FWM} (km s ⁻¹)	Int δ _{Int} (K)	Flux δ _{Flux} (K km s ⁻¹)	comments
64502	SO ₂ (11 _{1,1} -10 _{0,10})	221965.22	60.36	1.14E-04	3.99	0.14	5.06	0.35	0.838
64502	SO ₂ (6 _{1,2} -7 _{3,5})	223883.57	58.58	1.16E-05	3.65	0.15	4.62	0.36	0.080
64502	SO ₂ (20 _{0,-18} -19 _{3,17})	224264.81	207.76	3.94E-05	3.42	0.11	5.75	0.30	0.107
64502	SO ₂ (13 _{2,12} -13 _{1,13})	225153.70	92.99	6.52E-05	3.76	0.11	5.92	0.32	0.381
64502	SO ₂ (14 _{3,11} -14 _{2,12})	226300.03	118.99	1.07E-04	3.38	0.08	6.46	0.21	0.400
64502	SO ₂ (11 _{5,7} -12 _{4,8})	229347.63	122.01	1.91E-05	2.72	0.18	4.49	0.44	0.105
64502	SO ₂ (4 _{2,2} -3 _{1,3})	235151.72	19.03	7.69E-05	4.00	0.14	4.64	0.33	0.415
64502	SO ₂ (16 _{1,15} -15 _{2,14})	236216.69	130.67	7.50E-05	3.89	0.13	6.39	0.37	0.369
64502	SO ₂ (12 _{3,9} -12 _{2,10})	237068.83	93.96	1.14E-04	3.64	0.06	6.19	0.15	0.335
64502	SO ₂ (18 _{1,17} -18 _{0,18})	240942.79	163.07	7.02E-05	3.68	0.12	7.82	0.36	0.361
64502	SO ₂ (5 _{2,4} -4 _{1,3})	241615.80	23.59	8.45E-05	3.91	0.13	5.21	0.32	0.630
64502	SO ₂ (14 _{0,14} -13 _{1,13})	244254.22	93.90	1.64E-04	4.03	0.10	6.11	0.28	0.565
64502	SO ₂ (10 _{3,7} -10 _{2,8})	245563.42	72.71	1.19E-04	3.77	0.10	5.58	0.24	0.174
64502	SO ₂ (15 _{2,14} -15 _{1,15})	248057.40	119.33	8.05E-05	3.52	0.35	7.73	1.02	0.063
64502	SO ₂ (13 _{1,13} -12 _{0,12})	251199.67	82.18	1.76E-04	3.78	0.12	5.70	0.30	0.607
64502	SO ₂ (8 _{3,5} -8 _{2,6})	251210.58	55.20	1.20E-04	3.65	0.04	6.10	0.12	0.392
64502	SO ₂ (6 _{3,3} -6 _{2,4})	254280.54	41.40	1.14E-04	3.23	0.17	6.67	0.51	0.353
64502	SO ₂ (4 _{3,1} -4 _{2,2})	255553.30	31.29	9.28E-05	4.17	0.28	6.75	0.70	0.060
64502	SO ₂ (3 _{3,1} -3 _{2,2})	255958.04	27.62	6.62E-05	4.91	0.37	4.64	0.90	0.039
64502	SO ₂ (5 _{3,3} -5 _{2,4})	256246.95	35.89	1.07E-04	3.82	0.14	5.21	0.34	0.441
64502	SO ₂ (7 _{3,5} -7 _{2,6})	257099.97	47.84	1.22E-04	3.88	0.16	4.47	0.37	0.398
64502	SO ₂ (9 _{3,7} -9 _{2,8})	258942.20	63.47	1.32E-04	3.79	0.11	5.88	0.27	0.371
64502	SO ₂ (11 _{3,9} -11 _{2,10})	262256.91	82.80	1.41E-04	3.75	0.10	6.11	0.26	0.454
64502	SO ₂ (7 _{2,6} -6 _{1,5})	271529.01	35.50	1.11E-04	3.98	0.18	5.01	0.44	0.440
64502	SO ₂ (17 _{2,16} -17 _{1,17})	273752.82	149.22	9.97E-05	3.34	0.17	5.94	0.41	0.179
64502	SO ₂ (15 _{3,13} -15 _{2,14})	275240.18	132.54	1.64E-04	3.72	0.15	5.85	0.39	0.329
64502	SO ₂ (21 _{2,20} -21 _{1,21})	332091.43	219.53	1.51E-04	3.43	0.23	5.62	0.59	0.114
64502	SO ₂ (4 _{3,1} -3 _{2,2})	332505.24	31.29	3.29E-04	3.79	0.10	3.71	0.23	0.742
64502	SO ₂ (8 _{2,6} -7 _{1,7})	334673.35	43.15	1.27E-04	3.76	0.15	3.24	0.35	0.451
64502	SO ₂ (19 _{1,19} -18 _{0,18})	346652.17	168.14	5.22E-04	3.69	0.07	5.40	0.17	0.442
64502	SO ₂ (5 _{3,3} -4 _{2,2})	351257.22	35.89	3.36E-04	3.79	0.10	3.79	0.24	0.700
64502	SO ₂ (14 _{4,10} -14 _{3,11})	351873.87	135.87	3.43E-04	3.75	0.27	7.26	0.76	0.227
64502	SO ₂ (12 _{4,8} -12 _{3,9})	355045.52	111.00	3.40E-04	3.59	0.10	5.58	0.26	0.349
64502	SO ₂ (13 _{4,10} -13 _{3,11})	357165.39	122.97	3.51E-04	3.73	0.09	5.49	0.23	0.329
64502	SO ₂ (15 _{4,12} -15 _{3,13})	357241.19	149.68	3.62E-04	3.72	0.13	6.05	0.34	0.283
64502	SO ₂ (11 _{4,8} -11 _{3,9})	357387.58	99.95	3.38E-04	3.75	0.10	5.56	0.26	0.411
64502	SO ₂ (8 _{4,4} -8 _{3,5})	357581.45	72.36	3.06E-04	4.05	0.08	4.62	0.20	0.403
64502	SO ₂ (9 _{4,6} -9 _{3,7})	357671.82	80.64	3.20E-04	3.93	0.19	5.57	0.51	0.338
64502	SO ₂ (7 _{4,4} -7 _{3,5})	357892.44	65.01	2.87E-04	3.68	0.08	4.26	0.19	0.434
64502	SO ₂ (6 _{4,2} -6 _{3,3})	357925.85	58.58	2.60E-04	3.69	0.11	4.69	0.26	0.398
64502	SO ₂ (17 _{4,14} -17 _{3,15})	357962.91	180.11	3.73E-04	3.51	0.13	5.55	0.32	0.264
64502	SO ₂ (5 _{4,2} -5 _{3,3})	358013.15	53.07	2.18E-04	3.89	0.11	5.00	0.25	0.313
64502	SO ₂ (4 _{4,0} -4 _{3,1})	358037.89	48.48	1.45E-04	3.24	0.19	4.37	0.44	0.115
64502	SO ₂ (20 _{0,20} -19 _{1,19})	358215.63	185.33	5.83E-04	3.56	0.11	5.60	0.28	0.294
64502	SO ₂ (19 _{4,16} -19 _{3,17})	359770.68	214.26	3.85E-04	3.94	0.18	6.85	0.50	0.220
64502	SO ₂ (15 _{2,14} -14 _{1,13})	366214.47	119.33	3.04E-04	3.66	0.09	5.26	0.23	0.334
66002	³⁴ SO ₂ (3 _{1,3} -2 _{2,2})	102031.88	7.64	9.50E-06	3.68	0.16	3.91	0.37	0.030

Table 4. Continued.

TAG	Species & Transition	Frequency (MHz)	Eup (K)	A _{ij} s ⁻¹	V _O δ _{ν_o} (km s ⁻¹)	FWHM δ _{FWM} (km s ⁻¹)	Int δ _{int} (K)	Flux δ _{Flux} (K km s ⁻¹)	comments
66002	³⁴ SO ₂ (5 _{1,5} -4 _{0,4})	133471.47	15.54	2.11E-05	4.43	0.23	1.75	0.54	0.066
66002	³⁴ SO ₂ (6 _{2,4} -6 _{1,5})	134826.12	28.83	2.27E-05	2.79	0.19	5.03	0.52	0.056
66002	³⁴ SO ₂ (11 _{2,10} -11 _{1,11})	201376.42	69.74	4.96E-05	2.71	0.24	3.94	0.57	0.042
66002	³⁴ SO ₂ (11 _{1,11} -10 _{0,10})	219355.01	60.08	1.11E-04	3.05	0.40	6.39	0.95	0.057
32504	CH ₃ OH (7 _{2,6} -8 _{1,7} A ⁻)	80993.24	102.7	1.04E-06	3.59	0.44	7.43	1.01	0.032
32504	CH ₃ OH (5 _{-1,5} -4 _{+0,4} , E)	84521.17	40.39	1.97E-06	3.93	0.15	4.25	0.35	0.327
32504	CH ₃ OH (6 _{-2,5} -7 _{+1,7} E)	85568.08	74.66	1.13E-06	3.90	0.35	7.68	0.84	0.048
32504	CH ₃ OH (7 _{2,6} -6 _{3,3} A ⁻)	86615.60	102.7	6.85E-07	2.71	0.18	4.65	0.41	0.043
32504	CH ₃ OH (7 _{2,5} -6 _{3,4} A ⁺)	86902.95	102.72	6.92E-07	2.78	0.31	5.31	0.76	0.044
32504	CH ₃ OH (8 _{-4,5} -9 _{-3,7} E)	89505.81	171.46	7.65E-07	3.04	0.26	6.30	0.59	0.050
32504	CH ₃ OH (8 _{+3,5} -9 _{+2,7} E)	94541.77	131.28	1.29E-06	3.32	0.34	7.46	0.85	0.046
32504	CH ₃ OH (8 _{0,8} -7 _{1,7} A ⁺)	95169.46	83.54	4.26E-06	3.85	0.09	4.75	0.21	0.241
32504	CH ₃ OH (2 _{1,2} -1 _{1,1} A ⁺)	95914.31	21.44	2.49E-06	3.44	0.05	5.18	0.11	0.122
32504	CH ₃ OH (2 _{0,2} -1 _{0,1} A ⁺)	96741.38	6.97	3.41E-06	3.80	0.11	2.81	0.26	0.621
32504	CH ₃ OH (2 _{+0,2} -1 _{+0,1} E)	96744.55	20.09	3.41E-06	3.64	0.14	4.47	0.35	0.186
32504	CH ₃ OH (2 _{+1,1} -1 _{+1,0} E)	96755.51	28.01	2.62E-06	3.53	0.10	5.00	0.23	0.109
32504	CH ₃ OH (2 _{1,1} -1 _{1,0} A ⁻)	97582.80	21.56	2.63E-06	3.71	0.06	5.32	0.15	0.114
32504	CH ₃ OH (13 _{2,11} -12 _{3,9} A ⁺)	100638.90	233.61	1.69E-06	2.55	0.11	6.13	0.28	0.064
32504	CH ₃ OH (7 _{-2,6} -7 _{+1,6} E)	101293.34	90.91	3.73E-08	2.11	0.39	4.07	0.99	0.020
32504	CH ₃ OH (9 _{-2,8} -9 _{+1,8} E)	101737.17	130.4	1.08E-07	2.65	0.23	4.20	0.61	0.041
32504	CH ₃ OH (11 _{-2,10} -11 _{+1,0} E)	102658.05	179.19	2.65E-07	2.56	0.25	4.98	0.61	0.046
32504	CH ₃ OH (12 _{-2,11} -12 _{+1,1} E)	103381.15	207.08	3.98E-07	2.81	0.28	6.01	0.66	0.041
32504	CH ₃ OH (11 _{-1,11} -10 _{-2,9} E)	104300.41	158.64	1.96E-06	3.32	0.18	6.74	0.42	0.079
32504	CH ₃ OH (10 _{4,7} -11 _{3,8} A ⁻)	104354.82	207.99	1.57E-06	3.63	0.45	7.78	1.15	0.047
32504	CH ₃ OH (3 _{1,3} -4 _{0,4} A ⁺)	107013.80	28.35	6.13E-06	3.36	0.12	5.52	0.30	0.046
32504	CH ₃ OH (0 _{+0,0} -1 _{-1,1} E)	108893.96	13.13	1.47E-05	3.44	0.12	5.70	0.30	0.043
32504	CH ₃ OH (12 _{1,1} -11 _{2,10} A ⁻)	129433.41	197.08	4.69E-06	2.82	0.22	5.88	0.52	0.112
32504	CH ₃ OH (6 _{2,5} -7 _{1,6} A ⁺)	132621.94	86.46	4.26E-06	2.14	0.26	4.31	0.69	0.071
32504	CH ₃ OH (6 _{1,6} -5 _{0,5} E)	132890.69	54.31	7.75E-06	3.56	0.09	3.70	0.21	0.279
32504	CH ₃ OH (5 _{-2,4} -6 _{-1,6} E)	133605.50	60.73	4.01E-06	4.15	0.18	6.67	0.47	0.095
32504	CH ₃ OH (8 _{2,7} -7 _{3,4} A ⁻)	134896.96	121.27	3.00E-06	4.35	0.31	7.81	0.89	0.122
32504	CH ₃ OH (7 _{+3,4} -8 _{+2,6} E)	143169.50	112.71	4.13E-06	3.08	0.27	7.10	0.83	0.121
32504	CH ₃ OH (3 _{1,3} -2 _{1,2} A ⁺)	143865.80	28.35	1.07E-05	3.80	0.09	6.12	0.22	0.307
32504	CH ₃ OH (3 _{0,5} -2 _{0,2} E)	145093.71	27.05	1.23E-05	3.53	0.10	3.46	0.26	0.358
32504	CH ₃ OH (13 _{+0,13} -13 _{-1,13} E)	151860.32	223.82	1.15E-05	3.52	0.19	7.82	0.49	0.077
32504	CH ₃ OH (12 _{+0,12} -12 _{-1,12} E)	153281.24	193.79	1.29E-05	2.65	0.30	7.08	0.27	0.655
32504	CH ₃ OH (11 _{+0,11} -11 _{-1,11} E)	154425.78	166.05	1.42E-05	2.96	0.17	7.34	0.44	0.124
32504	CH ₃ OH (12 _{-1,12} -11 _{-2,10} E)	150884.58	186.43	5.86E-06	3.60	0.21	7.65	0.52	0.146
32504	CH ₃ OH (9 _{+0,9} -9 _{-1,9} E)	155997.52	117.46	1.67E-05	3.99	0.13	8.07	0.34	0.166
32504	CH ₃ OH (6 _{2,4} -7 _{1,7} A ⁺)	156127.70	86.47	6.54E-06	3.19	0.34	7.82	1.04	0.110
32504	CH ₃ OH (8 _{0,8} -8 _{-1,8} E)	156448.87	96.61	1.78E-05	3.45	0.13	6.46	0.30	0.205
32504	CH ₃ OH (2 _{1,2} -3 _{0,3} A ⁺)	156602.41	21.44	1.78E-05	3.73	0.10	5.46	0.24	0.278
32504	CH ₃ OH (7 _{+0,7} -7 _{-1,7} E)	156828.53	78.08	1.88E-05	3.78	0.08	6.40	0.19	0.270

Table 4. Continued.

TAG	Species & Transition	Frequency (MHz)	Eup (K)	A _{ij} s ⁻¹	V _O δ _{ν_o} (km s ⁻¹)	FWHM δ _{FWM} (km s ⁻¹)	Int δ _{int} (K)	Flux δ _{Flux} (K km s ⁻¹)	comments
32504	CH ₃ OH (6 _{+0,6} -6 _{-1,6} E)	157048.62	61.85	1.96E-05	3.33	0.14	5.44	0.34	0.232
32504	CH ₃ OH (5 _{+0,5} -5 _{-1,5} E)	157179.02	47.93	2.04E-05	3.62	0.13	5.24	0.32	0.260
32504	CH ₃ OH (4 _{+0,4} -4 _{-1,4} E)	157246.06	36.34	2.10E-05	3.74	0.09	4.34	0.22	0.290
32504	CH ₃ OH (2 _{+0,2} -2 _{-1,2} E)	157276.06	20.09	2.18E-05	3.86	0.17	4.90	0.42	0.332
32504	CH ₃ OH (1 _{+0,0} -1 _{+0,1} E)	165050.20	23.37	2.35E-05	3.14	0.27	8.18	0.71	0.112
32504	CH ₃ OH (2 _{+1,1} -2 _{+0,2} E)	165061.16	28.01	2.34E-05	3.20	0.22	7.24	0.58	0.142
32504	CH ₃ OH (3 _{+1,2} -3 _{+0,3} E)	165099.27	34.98	2.33E-05	3.09	0.34	8.41	0.88	0.125
32504	CH ₃ OH (4 _{+1,3} -4 _{+0,4} E)	165190.53	44.26	2.32E-05	3.37	0.39	7.85	1.11	0.130
32504	CH ₃ OH (4 _{+1,3} -4 _{+0,4} E)	165190.53	44.26	2.32E-05	3.42	0.40	7.84	1.20	0.130
32504	CH ₃ OH (6 _{+1,5} -6 _{+0,6} E)	165678.77	69.8	2.30E-05	4.18	0.11	6.51	0.27	0.294
32504	CH ₃ OH (7 _{+1,6} -7 _{+0,7} E)	166169.21	86.05	2.28E-05	3.84	0.09	6.82	0.22	0.274
32504	CH ₃ OH (8 _{+1,7} -8 _{+0,8} E)	166898.65	104.62	2.28E-05	3.78	0.08	7.22	0.19	0.228
32504	CH ₃ OH (9 _{+1,8} -9 _{+0,9} E)	167931.13	125.52	2.27E-05	3.70	0.17	7.63	0.44	0.237
32504	CH ₃ OH (10 _{+1,9} -10 _{-0,10} E)	169335.34	148.73	2.28E-05	3.45	0.27	6.79	0.83	0.162
32504	CH ₃ OH (3 _{+2,1} -2 _{+1,1} E)	170060.58	36.17	2.55E-05	3.78	0.10	3.97	0.23	0.494
32504	CH ₃ OH (11 _{+1,10} -11 _{+0,11} E)	171182.58	174.27	2.30E-05	3.86	0.19	7.19	0.48	0.169
32504	CH ₃ OH (7 _{+0,7} -6 _{+1,5} E)	172445.95	78.08	1.16E-05	3.60	0.11	6.28	0.27	0.195
32504	CH ₃ OH (10 _{0,10} -9 _{1,9} A ⁺)	198403.22	127.6	4.10E-05	3.53	0.12	6.28	0.31	0.131
32504	CH ₃ OH (8 _{4,4} -9 _{3,7} A ⁺)	201088.98	163.9	9.13E-06	3.07	0.54	6.84	1.34	0.086
32504	CH ₃ OH (5 _{2,3} -6 _{1,6} A ⁺)	201445.59	72.53	1.30E-05	3.29	0.11	8.52	0.28	0.139
32504	CH ₃ OH (1 _{1,1} -2 _{0,2} A ⁺)	205791.27	16.84	3.36E-05	3.52	0.09	5.74	0.21	0.227
32504	CH ₃ OH (1 _{+1,0} -0 _{+0,0} E)	213427.12	23.37	3.37E-05	3.50	0.10	5.46	0.25	0.208
32504	CH ₃ OH (5 _{+1,4} -4 _{+2,2} E)	216945.60	55.87	1.21E-05	3.31	0.16	6.82	0.52	0.150
32504	CH ₃ OH (4 _{+2,2} -3 _{+1,2} E)	218440.05	45.46	4.69E-05	3.81	0.11	5.07	0.28	0.139
32504	CH ₃ OH (8 _{-1,8} -7 _{+0,7} E)	229758.76	89.1	4.19E-05	3.38	0.16	5.60	0.40	0.385
32504	CH ₃ OH (3 _{-2,2} -4 _{-1,4} E)	230027.06	39.83	1.49E-05	3.27	0.16	6.42	0.41	0.121
32504	CH ₃ OH (10 _{-3,8} -11 _{-2,10} E)	232945.83	190.37	2.13E-05	2.73	0.28	6.67	0.70	0.128
32504	CH ₃ OH (5 _{1,5} -4 _{1,4} A ⁺)	239746.25	49.06	5.66E-05	3.27	0.18	4.40	0.42	0.293
32504	CH ₃ OH (5 _{3,2} -6 _{4,2} E)	240241.50	82.53	1.44E-05	3.34	0.24	7.03	0.61	0.146
32504	CH ₃ OH (5 _{0,5} -4 _{0,4} A ⁺)	241879.07	55.87	5.96E-05	3.77	0.15	5.82	0.42	0.496
32504	CH ₃ OH (5 _{+1,4} -4 _{+1,3} E)	241700.22	47.94	6.04E-05	3.76	0.10	5.19	0.25	0.641
32504	CH ₃ OH (5 _{0,5} -4 _{0,4} E)	241767.22	40.39	5.81E-05	3.85	0.16	4.56	0.39	1.088
32504	CH ₃ OH (5 _{-1,5} -4 _{-1,4} E)	241791.43	34.82	6.05E-05	4.08	0.12	4.22	0.30	1.248
32504	CH ₃ OH (5 _{2,3} -6 _{4,2} E)	241887.70	72.53	5.11E-05	3.51	0.16	7.04	0.46	0.299
32504	CH ₃ OH (5 _{2,3} -4 _{2,2} A ⁺)	243915.83	49.66	5.97E-05	3.68	0.10	5.35	0.24	0.499
32504	CH ₃ OH (5 _{1,4} -4 _{1,3} A ⁺)	247228.69	60.93	2.12E-05	3.36	0.36	7.58	0.95	0.061
32504	CH ₃ OH (8 _{3,5} -8 _{2,6} A [±])	251517.26	133.36	7.96E-05	3.04	0.07	6.27	0.19	0.271
32504	CH ₃ OH (6 _{+1,5} -5 _{+2,3} E)	265289.65	69.8	2.58E-05	3.01	0.09	5.92	0.22	0.173
32504	CH ₃ OH (5 _{2,3} -4 _{2,2} A ⁺)	251738.52	98.55	7.46E-05	3.24	0.10	6.40	0.27	0.301
32504	CH ₃ OH (8 _{3,6} -8 _{2,7} A [±])	251984.70	133.36	7.99E-05	3.00	0.19	5.56	0.44	0.244
32504	CH ₃ OH (2 _{+1,1} -1 _{+0,1} E)	261805.71	28.01	5.57E-05	3.87	0.13	6.04	0.31	0.349
32504	CH ₃ OH (6 _{+1,5} -5 _{+2,3} E)	335582.01	78.97	1.63E-04	3.32	0.08	4.26	0.19	0.238
32504	CH ₃ OH (5 _{2,3} -4 _{1,3} E)	338124.50	78.08	1.70E-04	3.42	0.14	4.14	0.33	0.319
32504	CH ₃ OH (7 _{1,7} -6 _{1,6} A ⁺)	338559.93	127.71	1.40E-04	2.87	0.24	6.19	0.60	0.151

Table 4. Continued.

TAG	Species & Transition	Frequency (MHz)	Eup (K)	A _{ij} s ⁻¹	V _O (km s ⁻¹)	δ_{V_O} (km s ⁻¹)	FWHM (km s ⁻¹)	δ_{FWHM} (km s ⁻¹)	Int δ_{Int} (K)	Flux (K km s ⁻¹)	δ_{Flux} (K km s ⁻¹)	comments
32504	CH ₃ OH (7 _{+3,4} -6 _{-3,3} E)	338583.20	112.71	1.39E-04	3.22	0.14	6.19	0.35	0.209	0.010	2.47	0.45
32504	CH ₃ OH (7 _{1,6} -6 _{1,5} A ⁻)	341415.64	80.09	1.71E-04	3.75	0.09	4.44	0.21	0.525	0.021	4.48	0.81
32504	CH ₃ OH (4 ₊₄ -3 _{-1,3} E)	350687.73	36.33	8.67E-05	3.16	0.12	6.55	0.29	0.498	0.019	6.33	1.14
32504	CH ₃ OH (1 _{1,1} -0 _{0,0} A ⁺)	350905.12	16.84	3.31E-04	3.85	0.14	4.54	0.33	0.599	0.037	5.27	0.95
32504	CH ₃ OH (13 _{0,13} -12 _{1,12} A ⁺)	355603.11	211.03	2.53E-04	3.18	0.11	5.77	0.27	0.270	0.010	3.04	0.55
32504	CH ₃ OH (4 ₊₃ -3 _{-3,3} E)	358605.80	44.26	1.32E-04	3.55	0.16	4.79	0.39	0.352	0.024	3.30	0.59
32504	CH ₃ OH (11 _{+0,11} -10 _{+1,9} E)	360848.86	166.05	1.21E-04	3.15	0.17	5.91	0.45	0.194	0.011	2.25	0.41
32504	CH ₃ OH (7 _{+2,5} -6 _{+1,5} E)	363739.82	87.26	1.71E-04	3.70	0.08	4.72	0.20	0.516	0.019	4.80	0.86
33502	¹³ CH ₃ OH (2 _{1,2} -1 _{1,1} A ⁺)	93619.46	21.30	2.32E-06	3.47	0.23	1.78	0.45	0.028	0.007	0.07	0.01
33502	¹³ CH ₃ OH (2 _{-1,2} -1 _{-1,1} E)	94405.16	12.40	2.38E-06	2.65	0.26	2.14	0.62	0.027	0.006	0.08	0.01
33502	¹³ CH ₃ OH (2 _{0,2} -1 _{0,1} A ⁺)	94407.13	6.80	3.17E-06	3.08	0.47	5.53	1.59	0.022	0.003	0.16	0.03
33502	¹³ CH ₃ OH (2 _{0,2} -1 _{0,1} A ⁺)	94411.02	19.91	3.17E-06	3.66	0.54	3.52	1.30	0.019	0.006	0.09	0.02
33502	¹³ CH ₃ OH (2 _{1,1} -1 _{1,0} A ⁻)	95208.66	21.41	2.44E-06	2.65	0.19	6.21	0.47	0.050	0.003	0.41	0.05
(*)	CH ₂ DOH (2 _{0,2} -1 _{0,1} o1)	141602.53	13.59	1.15E-05	2.72	0.21	3.89	0.54	0.066	0.007	0.36	0.07
(*)	CH ₂ DOH (2 _{0,2} -1 _{0,1} e1)	155695.81	94.59	1.77E-05	2.12	0.15	2.96	0.39	0.070	0.007	0.30	0.06
(*)	CH ₂ DOH (2 _{0,2} -1 _{0,1} e0)	235881.17	47.08	5.61E-05	2.90	0.09	3.31	0.23	0.088	0.005	0.54	0.10
(*)	CH ₂ DOH (5 _{1,4} -4 _{-1,3} A ⁻)	237983.38	48.82	5.54E-05	3.15	0.26	5.95	0.67	0.073	0.007	0.82	0.15
(*)	CH ₂ DOH (2 _{0,2} -1 _{0,1} o1)	89251.20	17.20		3.50	0.29	5.86	0.78	0.029	0.030	0.23	0.02
(*)	CH ₂ DOH (2 _{0,2} -1 _{0,1} e1)	89275.40	13.80		3.16	0.40	5.15	1.02	0.028	0.003	0.19	0.03
(*)	CH ₂ DOH (2 _{0,2} -1 _{0,1} e0)	89407.90	4.50		3.09	0.15	5.26	0.36	0.038	0.003	0.26	0.02
(*)	CH ₂ DOH (3 _{0,3} -2 _{0,2} e1)	133847.30	18.30		2.23	0.50	6.71	0.50	0.078	0.014	0.56	0.10
(*)	CH ₂ DOH (3 _{0,3} -2 _{0,2} o1)	133872.90	21.70		2.91	0.50	4.47	0.50	0.085	0.014	0.39	0.08
(*)	CH ₂ DOH (3 _{2,2} -2 _{2,1} o1)	133881.80	33.60		1.83	0.81	6.16	2.34	0.053	0.016	0.35	0.12
(*)	CH ₂ DOH (3 _{2,2} -2 _{2,1} e0)	134112.40	20.20		1.97	0.50	6.69	0.50	0.057	0.009	0.41	0.07
(*)	CH ₂ DOH (3 _{0,3} -2 _{0,2} e1)	134185.40	20.20		3.00	0.66	5.70	2.14	0.072	0.010	0.31	0.10
(*)	CH ₂ DOH (2 _{1,2} -3 _{0,3} e0)	207780.80	15.90		2.17	0.60	6.65	2.13	0.085	0.013	0.60	0.19
(*)	CH ₂ DOH (5 _{2,3} -4 _{-1,4} e1)	223071.30	33.60		2.89	1.02	5.75	2.25	0.081	0.020	0.99	0.30
(*)	CH ₂ DOH (5 _{2,3} -4 _{-2,2} e1)	223315.40	40.80		2.23	0.30	4.70	0.50	0.083	0.009	0.83	0.08
(*)	CH ₂ DOH (5 _{2,4} -4 _{-2,3} e0)	223422.30	33.60		3.87	0.35	7.54	0.80	0.095	0.025	1.26	0.12
(*)	CHD ₂ OH (2 _{0,-1} 1 ₀ e1)	83129.20	16.98		3.71	0.64	3.40	0.50	0.017	0.006	0.10	0.02
(*)	CHD ₂ OH (2 _{0,-1} 1 ₀ e0)	83289.50	4.17		3.28	0.74	7.74	2.05	0.020	0.006	0.20	0.04
(*)	CHD ₂ OH (4 _{2,-1} 3 ₂ e1)	166271.00	35.65		3.78	0.67	4.15	0.50	0.057	0.010	0.43	0.09
(*)	CHD ₂ OH (4 _{3,+} 3 _{3,-} e1)	166297.00	46.54		2.55	0.44	3.60	0.50	0.080	0.009	0.52	0.07
(*)	CHD ₂ OH (4 _{2,+} 3 ₂₊ e1)	166304.00	35.65		2.00	0.49	3.64	0.50	0.070	0.009	0.42	0.07
(*)	CHD ₂ OH (5 _{0,-4} 4 ₀ e1)	207771.00	33.63		1.90	1.26	5.85	0.50	0.051	0.013	0.51	0.13
(*)	CHD ₂ OH (5 _{3,-4} 4 ₃ e1)	207868.00	53.48		1.69	1.02	4.94	0.50	0.048	0.013	0.43	0.11
(*)	CH ₃ OD (3 _{1,-2} 3 ₀)	110475.80	15.40		2.36	0.45	2.33	0.93	0.016	0.005	0.06	0.02
(*)	CH ₃ OD (1 _{1,-1} 1 ₊)	133925.40	6.00		2.56	0.53	4.00	0.50	0.046	0.009	0.32	0.06
(*)	CH ₃ OD (5 _{1,+4} 4 ₊)	223308.60	26.80		1.63	0.42	4.00	0.50	0.052	0.009	0.83	0.14
(*)	CH ₃ OD (5 _{0,+4} 4 ₀)	226538.70	22.70		3.67	0.53	5.49	1.36	0.110	0.015	1.05	0.20
(*)	CD ₃ OH (4 _{1,-2} 2 ₁ E2)	156237.02	21.50		2.48	0.44	2.48	0.50	0.054	0.007	0.21	0.04
(*)	CD ₃ OH (4 _{2,-2} 2 ₂ A ⁻)	156239.30	42.00		2.20	0.38	2.12	0.50	0.051	0.007	0.17	0.04
(*)	CD ₃ OH (1 _{0,-1} 1 ₁ E2)	160753.93	12.20		2.62	0.25	1.50	0.50	0.047	0.011	0.10	0.03
29507	HCO ⁺ (1-0)	89188.53	4.28	4.19E-05	3.41	0.26	3.63	0.62	3.211	0.477	15.11	1.66
29507	HCO ⁺ (3-2)	267557.63	25.68	1.45E-03	3.35	0.09	3.71	0.21	8.559	0.430	69.33	11.79

Table 4. Continued.

TAG	Species & Transition	Frequency (MHz)	Eup (K)	A _{ij} s ⁻¹	V _O δ _{ν_o} (km s ⁻¹)	FWHM δ _{FWM} (km s ⁻¹)	Int δ _{int} (K)	Flux δ _{Flux} (K km s ⁻¹)	comments				
29507	HCO ⁺ (4-3)	356734.22	42.80	3.57E-03	3.10	0.05	1.27	0.12	24.109	1.904	59.73	10.75	self-abs
30504	H ¹³ CO ⁺ (1-0)	86754.29	4.16	3.85E-05	4.17	0.04	2.13	0.08	1.581	0.055	4.36	0.48	
30504	H ¹³ CO ⁺ (2-1)	173506.70	12.49	3.70E-04	4.48	0.07	2.14	0.15	2.347	0.146	7.71	1.31	
30504	H ¹³ CO ⁺ (3-2)	260255.34	24.98	1.34E-03	3.60	0.03	3.07	0.08	1.662	0.035	10.48	1.78	
30504	H ¹³ CO ⁺ (4-3)	346998.34	41.63	3.29E-03	3.52	0.05	2.39	0.11	1.943	0.079	8.97	1.61	
30510	DCO ⁺ (2-1)	144077.29	10.37	2.12E-04	4.32	0.01	1.44	0.03	2.638	0.052	5.44	0.92	
30510	DCO ⁺ (3-2)	216112.58	20.74	7.66E-04	4.39	0.03	3.08	0.09	1.082	0.023	5.78	0.98	
30510	DCO ⁺ (5-4)	360169.78	51.86	3.76E-03	3.86	0.09	2.51	0.22	0.616	0.046	3.04	0.55	
31506	HC ¹⁸ O ⁺ (1-0)	85162.22	4.09	3.64E-05	4.18	0.03	1.93	0.08	0.176	0.006	0.44	0.05	
31506	HC ¹⁸ O ⁺ (2-1)	170322.63	12.26	3.50E-04	4.33	0.06	1.78	0.15	0.293	0.021	0.80	0.14	
31506	HC ¹⁸ O ⁺ (3-2)	255479.39	24.52	1.27E-03	3.62	0.16	2.73	0.39	0.067	0.008	0.37	0.07	
31508	D ¹³ CO ⁺ (2-1)	141465.13	10.18	2.00E-04	4.40	0.07	1.38	0.16	0.163	0.016	0.32	0.06	
31508	D ¹³ CO ⁺ (3-2)	212194.49	20.37	7.25E-04	4.63	0.26	3.30	0.56	0.049	0.007	0.28	0.05	
30505	HC ¹⁷ O ⁺ (2-1)	174113.17	12.53	3.74E-04	3.94	0.22	4.03	0.71	0.056	0.006	0.35	0.07	
44501	CS (2-1)	97980.95	7.05	1.68E-05	3.88	0.08	3.54	0.18	3.393	0.150	15.80	1.74	small wings
44501	CS (3-2)	146969.03	14.11	6.07E-05	3.66	0.14	3.69	0.33	5.353	0.414	28.54	4.85	self-abs
44501	CS (5-4)	244935.56	35.27	2.98E-04	3.65	0.10	4.02	0.25	5.689	0.300	44.06	7.49	
44501	CS (7-6)	342882.85	65.83	8.40E-04	3.62	0.06	2.98	0.14	6.638	0.270	38.06	6.85	small wings
46501	C ³⁴ S (2-1)	96412.95	6.94	1.60E-05	3.83	0.05	2.80	0.13	0.548	0.021	2.01	0.22	
46501	C ³⁴ S (3-2)	144617.10	13.88	5.78E-05	3.68	0.07	3.40	0.17	0.834	0.036	4.08	0.69	
46501	C ³⁴ S (5-4)	241016.09	34.70	2.84E-04	3.58	0.06	4.44	0.15	1.102	0.031	9.27	1.58	
46501	C ³⁴ S (7-6)	337396.46	64.77	8.00E-04	3.44	0.06	3.74	0.13	0.808	0.025	5.77	1.04	
45501	¹³ CS (2-1)	92494.31	6.66	1.41E-05	3.86	0.08	3.00	0.19	0.213	0.012	0.83	0.09	
45501	¹³ CS (3-2)	138739.33	13.32	5.11E-05	3.80	0.12	3.59	0.27	0.331	0.022	1.69	0.29	
45501	¹³ CS (5-4)	231220.68	33.29	2.51E-04	3.38	0.12	5.18	0.29	0.459	0.022	4.35	0.74	
45501	¹³ CS (6-5)	277455.41	46.61	4.40E-04	3.73	0.12	4.48	0.29	0.215	0.012	2.14	0.37	
45502	C ³³ S (2-1)	97172.06	7.00	1.64E-05	4.64	0.09	2.63	0.20	0.093	0.006	0.32	0.04	
45502	C ³³ S (3-2)	145755.73	13.99	5.92E-05	3.39	0.14	6.46	0.32	0.124	0.005	1.16	0.20	hf structure
45502	C ³³ S (5-4)	242913.61	34.98	2.91E-04	3.15	0.09	5.61	0.21	0.318	0.010	3.41	0.58	
45502	C ³³ S (7-6)	340052.58	65.28	8.19E-04	3.54	0.11	5.51	0.26	0.217	0.009	2.29	0.41	self abs
27501	HCN (1-0)	88631.60	4.25	2.41E-05	4.46	0.33	9.50	0.79	1.765	0.127	21.71	2.39	hf structure
27501	HCN (3-2)	265886.43	25.52	8.36E-04	3.00	0.22	5.94	0.51	2.812	0.209	35.12	5.97	
27501	HCN (4-3)	354505.48	42.54	2.05E-03	3.25	0.26	5.73	0.60	3.637	0.331	40.65	7.32	
28002	H ¹³ CN (1 ₂ -0 ₁)	863340.18	4.14	2.22E-05	3.88	0.09	2.91	0.25	0.284	0.009	1.04	0.12	hf structure
28002	H ¹³ CN (1 ₁ -0 ₁)	863338.77	4.14	2.22E-05	3.84	0.06	2.87	0.17	0.191	0.005	0.75	0.09	hf structure
28002	H ¹³ CN (1 ₀ -0 ₁)	863342.27	4.14	2.22E-05	3.81	0.13	2.46	0.33	0.079	0.008	0.25	0.03	hf structure
28002	H ¹³ CN (3-2)	259011.82	24.86	6.48E-04	3.32	0.58	6.63	2.62	0.600	0.080	8.16	1.39	
28002	H ¹³ CN (4-3)	345339.76	41.44	1.90E-03	4.00	0.09	5.39	0.23	0.664	0.022	6.90	1.24	
28509	DCN (2-1)	144828.00	10.43	1.27E-04	4.16	0.21	4.24	0.56	0.635	0.062	3.88	0.66	
28509	DCN (3-2)	217238.54	20.85	4.57E-04	3.36	0.07	4.54	0.19	0.440	0.013	3.49	0.59	
28509	DCN (5-4)	362045.75	52.13	2.25E-03	3.38	0.06	3.48	0.24	0.570	0.015	3.90	0.70	odd profile
28003	HC ¹⁵ N (1-0)	86054.96	4.13	2.20E-05	4.03	0.18	3.51	0.43	0.114	0.012	0.51	0.06	
28003	HC ¹⁵ N (2-1)	172107.96	12.39	2.11E-04	3.29	0.16	5.37	0.41	0.228	0.014	1.88	0.32	
28003	HC ¹⁵ N (3-2)	258157.10	24.78	7.65E-04	3.70	0.07	6.81	0.21	0.186	0.003	2.57	0.45	

Table 4. Continued.

TAG	Species & Transition	Frequency (MHz)	E _{up} (K)	A _{ij} s ⁻¹	V _O (km s ⁻¹)	δ_{V_O} (km s ⁻¹)	FWHM (km s ⁻¹)	δ_{FWHM} (km s ⁻¹)	Int δ_{Int} (K)	Flux (K km s ⁻¹)	δ_{Flux} (K km s ⁻¹)	comments
28003	HC ¹⁵ N (4-3)	344200.32	41.30	1.88E-03	3.39	0.36	6.38	0.99	0.122	0.012	1.49	0.27
44003	CH ₃ CHO (5 _{1,5} -4 _{1,4} A)	93580.86	15.75	2.53E-05	3.15	0.23	2.52	0.56	0.041	0.008	0.13	0.02
44003	CH ₃ CHO (5 _{1,5} -4 _{1,4} E)	93595.28	15.82	2.53E-05	3.14	0.17	2.70	0.40	0.046	0.006	0.16	0.02
44003	CH ₃ CHO (5 _{0,5} -4 _{0,4} E)	95947.34	13.93	2.84E-05	2.88	0.13	2.60	0.32	0.053	0.006	0.18	0.02
44003	CH ₃ CHO (5 _{0,5} -4 _{0,4} A)	95963.38	13.84	2.84E-05	2.82	0.11	2.93	0.25	0.061	0.005	0.24	0.03
44003	CH ₃ CHO (5 _{2,4} -4 _{2,3} A)	96274.20	22.93	2.41E-05	2.66	0.05	2.26	0.11	0.055	0.002	0.16	0.02
44003	CH ₃ CHO (5 _{4,1} -4 _{4,0} E)	96353.16	49.99	1.04E-05	2.40	0.12	2.43	0.28	0.035	0.004	0.11	0.02
44003	CH ₃ CHO (5 _{4,2} -4 _{4,1} E)	96360.78	49.95	1.04E-05	2.67	0.15	2.19	0.34	0.028	0.004	0.08	0.01
44003	CH ₃ CHO (5 _{3,2} -4 _{3,1} E)	96368.35	34.26	1.85E-05	3.35	0.19	3.58	0.52	0.048	0.005	0.22	0.03
44003	CH ₃ CHO (5 _{3,2} -4 _{3,1} A)	96371.75	34.26	1.85E-05	2.59	0.16	2.31	0.39	0.033	0.005	0.10	0.02
44003	CH ₃ CHO (5 _{3,3} -4 _{3,2} E)	96384.40	34.16	1.85E-05	3.27	0.43	3.53	1.13	0.033	0.008	0.16	0.02
44003	CH ₃ CHO (5 _{2,4} -4 _{2,3} E)	96425.62	22.91	2.41E-05	2.83	0.09	1.88	0.21	0.055	0.005	0.13	0.02
44003	CH ₃ CHO (5 _{2,3} -4 _{2,2} E)	96475.54	23.03	2.42E-05	3.03	0.13	2.15	0.29	0.048	0.006	0.13	0.02
44003	CH ₃ CHO (5 _{2,3} -4 _{2,2} A)	96632.63	22.96	2.44E-05	2.84	0.16	2.20	0.37	0.041	0.006	0.12	0.02
44003	CH ₃ CHO (5 _{1,4} -4 _{1,3} E)	98863.33	16.59	2.99E-05	3.15	0.05	2.35	0.11	0.064	0.003	0.20	0.02
44003	CH ₃ CHO (5 _{1,4} -4 _{1,3} A)	98900.95	16.51	2.99E-05	3.10	0.11	2.46	0.25	0.057	0.005	0.19	0.02
44003	CH ₃ CHO (6 _{1,6} -5 _{1,5} A)	112248.73	21.13	4.50E-05	3.08	0.18	3.06	0.46	0.062	0.007	0.26	0.04
44003	CH ₃ CHO (6 _{1,6} -5 _{1,5} E)	112254.52	21.21	4.50E-05	2.91	0.10	2.70	0.23	0.083	0.006	0.30	0.04
44003	CH ₃ CHO (6 _{0,6} -5 _{0,5} E)	114940.19	19.45	4.96E-05	3.23	0.16	4.02	0.45	0.068	0.005	0.37	0.04
44003	CH ₃ CHO (6 _{0,6} -5 _{0,5} A)	114959.91	19.35	4.96E-05	3.31	0.12	3.16	0.29	0.067	0.005	0.29	0.03
44003	CH ₃ CHO (6 _{2,5} -5 _{2,4} A)	115493.94	28.48	4.48E-05	3.21	0.19	4.10	0.54	0.049	0.005	0.27	0.04
44003	CH ₃ CHO (7 _{0,7} -6 _{0,6} E)	133830.49	25.87	7.92E-05	2.93	0.06	2.36	0.14	0.119	0.006	0.39	0.07
44003	CH ₃ CHO (7 _{0,7} -6 _{0,6} A)	133854.10	25.78	7.92E-05	3.69	0.30	3.74	0.79	0.114	0.014	0.60	0.11
44003	CH ₃ CHO (7 _{2,6} -6 _{2,5} A)	134694.45	34.94	7.42E-05	3.34	0.19	3.11	0.50	0.078	0.010	0.34	0.06
44003	CH ₃ CHO (7 _{6,1} -6 _{6,0} E)	134877.32	107.11	2.15E-05	3.18	0.20	2.15	0.47	0.040	0.008	0.12	0.02
44003	CH ₃ CHO (7 _{5,2} -6 _{5,1} E)	134900.24	82.29	3.98E-05	2.50	0.13	1.54	0.31	0.068	0.012	0.15	0.03
44003	CH ₃ CHO (7 _{5,3} -6 _{5,2} E)	134905.47	82.25	3.98E-05	2.66	0.10	1.63	0.22	0.095	0.011	0.22	0.04
44003	CH ₃ CHO (7 _{4,3} -6 _{4,2} E)	134922.26	62.02	5.47E-05	2.57	0.17	3.65	0.47	0.072	0.007	0.37	0.06
44003	CH ₃ CHO (7 _{4,4} -6 _{4,3} E)	134933.40	61.97	5.47E-05	2.74	0.17	1.64	0.39	0.075	0.015	0.17	0.03
44003	CH ₃ CHO (7 _{3,5} -6 _{3,4} A)	134963.33	46.28	6.64E-05	2.90	0.16	2.02	0.38	0.056	0.009	0.16	0.03
44003	CH ₃ CHO (7 _{3,4} -6 _{3,3} E)	134973.05	46.29	6.64E-05	2.45	0.13	2.87	0.32	0.065	0.006	0.26	0.04
44003	CH ₃ CHO (7 _{3,4} -6 _{3,3} A)	134987.26	46.29	6.64E-05	2.56	0.12	2.72	0.26	0.082	0.007	0.33	0.06
44003	CH ₃ CHO (19 _{2,17} -19 _{1,18} A)	135272.97	187.63	1.23E-05	2.60	0.23	1.99	0.55	0.064	0.015	0.18	0.03
44003	CH ₃ CHO (7 _{2,5} -6 _{2,4} E)	135476.68	35.09	7.40E-05	2.96	0.11	2.85	0.27	0.089	0.007	0.36	0.06
44003	CH ₃ CHO (8 _{0,8} -7 _{0,7} A)	138284.88	28.92	8.57E-05	2.99	0.21	2.56	0.50	0.069	0.012	0.25	0.04
44003	CH ₃ CHO (8 _{1,8} -7 _{1,7} A)	138319.75	28.85	8.57E-05	3.30	0.12	4.11	0.33	0.072	0.004	0.42	0.07
44003	CH ₃ CHO (8 _{7,1} -7 _{7,0} E)	149507.55	34.59	1.10E-04	3.37	0.20	3.80	0.56	0.109	0.012	0.60	0.11
44003	CH ₃ CHO (6 _{1,6} -5 _{0,5} A)	152048.58	21.13	1.28E-05	2.90	0.33	4.00	0.88	0.054	0.009	0.31	0.06
44003	CH ₃ CHO (6 _{2,5} -6 _{1,6} A)	152635.07	33.10	1.18E-04	2.72	0.29	3.95	0.78	0.072	0.011	0.42	0.08
44003	CH ₃ CHO (8 _{7,1} -7 _{7,0} A)	153004.35	28.48	1.04E-05	2.71	0.12	2.50	0.29	0.035	0.004	0.13	0.03
44003	CH ₃ CHO (8 _{7,1} -7 _{7,0} E)	154131.38	143.81	2.86E-05	2.76	0.11	1.59	0.25	0.060	0.008	0.14	0.03
44003	CH ₃ CHO (8 _{7,1} -7 _{7,0} A)	154145.47	143.74	2.86E-05	2.03	0.23	1.94	0.54	0.077	0.018	0.22	0.04
44003	CH ₃ CHO (8 _{6,2} -7 _{6,1} A)	154151.99	114.50	5.35E-05	2.97	0.14	1.94	0.54	0.077	0.018	0.22	0.04
44003	CH ₃ CHO (8 _{6,3} -7 _{6,2} E)	154173.84	114.41	5.35E-05	2.32	0.10	1.56	0.24	0.073	0.010	0.17	0.03
44003	CH ₃ CHO (8 _{5,3} -7 _{5,2} E)	154182.91	89.69	7.45E-05	2.93	0.28	3.74	0.74	0.046	0.007	0.25	0.05
44003	CH ₃ CHO (8 _{5,4} -7 _{5,3} E)	154188.54	89.65	7.45E-05	2.68	0.17	2.02	0.40	0.075	0.013	0.22	0.04

Table 4. Continued.

TAG	Species & Transition	Frequency (MHz)	Eup (K)	A _{ij} s ⁻¹	V _O δ _{ν_o} (km s ⁻¹)	FWHM δ _{FWM} (km s ⁻¹)	Int δ _{int} (K)	Flux δ _{Flux} (K km s ⁻¹)	comments
44003	CH ₃ CHO (8 _{4,4} -7 _{4,3} A)	154201.47	69.49	9.18E-05	2.75	0.07	2.82	0.115	0.006
44003	CH ₃ CHO (8 _{3,6} -7 _{3,5} A)	154274.72	53.69	1.05E-04	3.01	0.08	3.36	0.20	0.077
44003	CH ₃ CHO (8 _{3,5} -7 _{3,4} E)	154296.57	53.69	1.05E-04	2.51	0.10	1.90	0.24	0.092
44003	CH ₃ CHO (8 _{2,6} -7 _{2,5} E)	155179.64	42.54	1.15E-04	3.07	0.17	2.83	0.43	0.013
44003	CH ₃ CHO (8 _{2,6} -7 _{2,5} A)	155342.11	42.50	1.17E-04	3.07	0.16	3.17	0.41	0.086
44003	CH ₃ CHO (8 _{1,7} -7 _{1,6} E)	157937.75	36.50	1.29E-04	3.27	0.14	2.60	0.35	0.112
44003	CH ₃ CHO (8 _{1,7} -7 _{1,6} A)	157974.71	36.43	1.29E-04	3.14	0.19	2.86	0.45	0.097
44003	CH ₃ CHO (8 _{2,7} -8 _{1,8} E)	159691.61	42.33	1.08E-05	2.74	0.32	3.47	0.81	0.031
44003	CH ₃ CHO (10 _{0,10} -9 _{1,9} A)	162043.81	50.44	1.57E-05	2.68	0.08	2.46	0.19	0.054
44003	CH ₃ CHO (10 _{0,10} -9 _{1,9} E)	162371.09	50.53	1.57E-05	2.72	0.21	1.41	0.50	0.046
44003	CH ₃ CHO (9 _{1,9} -8 _{1,8} E)	164727.07	50.64	1.21E-05	2.29	0.07	2.36	0.17	0.066
44003	CH ₃ CHO (9 _{2,8} -9 _{1,9} E)	167980.42	27.42	1.75E-05	2.73	0.16	3.90	0.44	0.070
44003	CH ₃ CHO (7 _{1,7} -6 _{0,6} A)	168088.65	42.73	1.57E-04	4.28	0.32	3.81	0.81	0.111
44003	CH ₃ CHO (9 _{1,9} -8 _{1,8} E)	168093.48	42.66	1.57E-04	3.18	0.17	3.08	0.42	0.115
44003	CH ₃ CHO (9 _{1,9} -8 _{1,8} A)	171296.97	41.32	1.68E-04	2.53	0.20	2.10	0.48	0.102
44003	CH ₃ CHO (9 _{0,9} -8 _{0,8} A)	173388.23	185.90	3.67E-05	2.43	0.17	2.22	0.39	0.040
44003	CH ₃ CHO (9 _{8,1} -8 _{8,0} E)	173453.47	122.74	9.73E-05	2.65	0.19	2.29	0.45	0.067
44003	CH ₃ CHO (9 _{6,4} -8 _{6,3} E)	173594.97	62.02	1.56E-04	2.74	0.15	4.29	0.44	0.077
44003	CH ₃ CHO (9 _{3,7} -8 _{3,6} A)	174982.61	50.94	1.70E-04	3.61	0.17	2.85	0.43	0.090
44003	CH ₃ CHO (9 _{2,7} -8 _{2,6} E)	197094.46	54.48	2.56E-04	3.26	0.50	3.43	1.10	0.077
44003	CH ₃ CHO (10 _{1,9} -9 _{1,8} E)	198062.33	105.90	1.88E-05	3.56	0.25	3.36	0.49	0.027
44003	CH ₃ CHO (14 _{2,13} -14 _{1,14} E)	198698.17	42.73	3.03E-05	3.50	0.36	3.36	0.84	0.015
44003	CH ₃ CHO (9 _{1,9} -8 _{0,8} E)	199332.25	179.21	3.23E-05	2.90	0.44	2.80	1.13	0.036
44003	CH ₃ CHO (18 _{3,15} -18 _{2,16} A)	205161.94	61.54	2.90E-04	2.81	0.31	4.40	0.81	0.080
44003	CH ₃ CHO (11 _{1,11} -10 _{1,10} E)	205170.70	61.46	2.90E-04	3.01	0.11	4.13	0.29	0.065
44003	CH ₃ CHO (11 _{1,11} -10 _{1,10} A)	208267.03	60.43	3.05E-04	3.22	0.19	3.95	0.49	0.065
44003	CH ₃ CHO (16 _{3,13} -16 _{2,14} A)	208730.58	146.56	3.46E-05	3.07	0.24	2.28	0.59	0.052
44003	CH ₃ CHO (11 _{2,10} -10 _{2,9} A)	211243.10	69.99	3.09E-04	3.68	0.29	4.14	0.72	0.070
44003	CH ₃ CHO (11 _{2,10} -10 _{2,9} E)	211273.76	70.00	3.09E-04	3.57	0.28	3.82	0.69	0.064
44003	CH ₃ CHO (11 _{0,11} -10 _{1,10} A)	212021.55	142.16	2.27E-04	2.77	0.21	3.49	0.47	0.049
44003	CH ₃ CHO (11 _{0,11} -10 _{1,10} E)	212059.55	117.44	2.56E-04	2.63	0.20	3.93	0.50	0.060
44003	CH ₃ CHO (11 _{5,7} -10 _{5,6} E)	212066.05	117.41	2.56E-04	2.29	0.39	3.59	0.92	0.059
44003	CH ₃ CHO (11 _{4,8} -10 _{4,7} A)	212128.40	97.25	2.81E-04	3.55	0.15	3.58	0.37	0.061
44003	CH ₃ CHO (11 _{6,6} -10 _{6,5} E)	212134.15	97.25	2.81E-04	2.28	0.20	3.96	0.47	0.056
44003	CH ₃ CHO (11 _{5,6} -10 _{5,5} E)	212151.90	97.18	2.81E-04	2.46	0.34	4.30	0.82	0.056
44003	CH ₃ CHO (11 _{4,8} -10 _{4,7} E)	212171.48	97.14	2.81E-04	2.77	0.27	4.46	0.64	0.053
44003	CH ₃ CHO (11 _{3,9} -10 _{3,8} A)	212257.12	81.47	3.00E-04	2.82	0.10	4.39	0.27	0.081
44003	CH ₃ CHO (11 _{2,9} -10 _{2,8} E)	212384.72	81.39	2.99E-04	2.95	0.17	4.35	0.43	0.064
44003	CH ₃ CHO (11 _{4,7} -10 _{4,6} A)	212400.95	81.48	3.00E-04	2.99	0.11	4.85	0.32	0.079
44003	CH ₃ CHO (11 _{3,8} -10 _{3,7} E)	214443.39	51.62	3.93E-05	2.39	0.67	3.57	1.70	0.034
44003	CH ₃ CHO (10 _{1,1} -9 _{0,9} A)	214800.80	70.60	3.24E-04	3.01	0.28	3.35	0.67	0.130
44003	CH ₃ CHO (11 _{2,9} -10 _{2,8} E)	214845.02	70.57	3.25E-04	3.79	0.33	3.48	0.81	0.112
44003	CH ₃ CHO (11 _{3,9} -10 _{3,8} E)	215604.58	18.40	1.48E-05	2.55	0.40	2.86	0.89	0.032
44003	CH ₃ CHO (14 _{2,2} -3 _{1,2} E)	216435.02	134.36	2.31E-05	2.35	0.21	2.48	0.48	0.035
44003	CH ₃ CHO (16 _{2,15} -16 _{1,16} A)	216534.44	117.68	3.32E-05	2.84	0.26	2.24	0.53	0.041
44003	CH ₃ CHO (14 _{3,11} -14 _{2,12} E)	216581.94	64.87	3.41E-04	3.36	0.21	4.11	0.53	0.084
44003	CH ₃ CHO (11 _{1,10} -10 _{1,9} E)	216630.22	64.81	3.41E-04	3.03	0.13	3.62	0.34	0.069
44003	CH ₃ CHO (11 _{1,10} -10 _{1,9} A)	223649.88	72.27	3.78E-04	3.03	0.31	3.61	0.75	0.089

Table 4. Continued.

TAG	Species & Transition	Frequency (MHz)	Eup (K)	A _{ij} s ⁻¹	V _O (km s ⁻¹)	δ_{V_O} (km s ⁻¹)	FWHM (km s ⁻¹)	δ_{FWHM} (km s ⁻¹)	Int δ_{Int} (K)	Flux (K km s ⁻¹)	δ_{Flux} (K km s ⁻¹)	comments
44003	CH ₃ CHO (12 _{1,12} -11 _{1,11} A)	223660.42	72.20	3.78E-04	2.63	0.32	3.66	0.79	0.103	0.018	0.67	0.12
44003	CH ₃ CHO (12 _{3,9} -12 _{2,10} E)	223909.92	92.61	2.95E-05	2.47	0.20	2.08	0.74	0.039	0.011	0.14	0.03
44003	CH ₃ CHO (13 _{0,13} -12 _{1,12} A)	226256.31	83.06	4.91E-05	2.72	0.10	2.25	0.46	0.070	0.012	0.29	0.05
44003	CH ₃ CHO (13 _{0,13} -12 _{1,12} E)	226487.69	83.14	4.90E-05	2.75	0.47	4.00	1.12	0.057	0.013	0.41	0.08
44003	CH ₃ CHO (12 _{0,12} -11 _{0,11} E)	226551.59	71.39	3.94E-04	2.55	0.21	2.36	0.42	0.196	0.032	0.83	0.14
44003	CH ₃ CHO (12 _{0,12} -11 _{0,11} A)	226592.71	71.31	3.94E-04	2.68	0.12	2.37	0.25	0.155	0.015	0.66	0.11
44003	CH ₃ CHO (11 _{3,8} -11 _{2,9} E)	226857.71	81.48	2.78E-05	2.95	0.33	3.08	0.77	0.086	0.019	0.48	0.08
44003	CH ₃ CHO (11 _{3,8} -11 _{2,9} A)	227514.36	81.49	3.90E-05	2.43	0.12	1.55	0.16	0.072	0.006	0.20	0.04
44003	CH ₃ CHO (12 _{2,11} -11 _{2,10} A)	230301.88	81.04	4.04E-04	2.79	0.21	3.93	0.55	0.063	0.007	0.45	0.08
44003	CH ₃ CHO (12 _{6,7} -11 _{6,6} E)	231310.46	153.26	3.16E-04	2.12	0.26	3.79	0.66	0.068	0.010	0.47	0.09
44003	CH ₃ CHO (12 _{5,7} -11 _{5,6} E)	231363.29	128.54	3.48E-04	2.55	0.34	2.51	0.92	0.067	0.020	0.31	0.06
44003	CH ₃ CHO (12 _{5,8} -11 _{5,7} E)	231369.74	128.51	3.48E-04	2.42	0.09	2.30	0.46	0.083	0.013	0.35	0.07
44003	CH ₃ CHO (12 _{4,9} -11 _{4,8} A)	231456.80	108.35	3.75E-04	2.93	0.29	2.67	0.57	0.085	0.016	0.42	0.08
44003	CH ₃ CHO (12 _{4,8} -11 _{4,7} A)	231467.49	108.36	3.75E-04	2.72	0.08	3.49	0.20	0.083	0.004	0.53	0.10
44003	CH ₃ CHO (12 _{4,8} -11 _{4,7} E)	231484.29	108.29	3.75E-04	2.63	0.19	3.56	0.46	0.078	0.008	0.51	0.09
44003	CH ₃ CHO (12 _{3,1} -11 _{3,9} A)	231595.18	92.58	3.96E-04	2.33	0.18	1.60	0.33	0.117	0.019	0.34	0.06
44003	CH ₃ CHO (12 _{3,1} -11 _{3,9} E)	231748.89	92.51	3.94E-04	2.88	0.40	2.62	0.90	0.112	0.034	0.54	0.10
44003	CH ₃ CHO (12 _{3,1} -11 _{3,9} E)	231847.62	92.61	3.94E-04	2.65	0.04	1.94	0.07	0.107	0.003	0.38	0.07
44003	CH ₃ CHO (12 _{3,9} -11 _{3,8} E)	231968.42	92.63	3.98E-04	2.79	0.29	5.27	0.81	0.153	0.016	1.48	0.26
44003	CH ₃ CHO (12 _{3,9} -11 _{3,8} A)	232269.137	22.93	3.10E-05	2.48	0.25	1.89	0.42	0.041	0.008	0.14	0.03
44003	CH ₃ CHO (5 _{2,4} -4 _{1,3} A)	2322981.31	23.03	1.34E-05	3.69	0.34	3.70	0.82	0.031	0.006	0.21	0.05
44003	CH ₃ CHO (5 _{2,3} -4 _{1,3} E)	2323845.39	39.81	3.38E-05	2.64	0.24	4.04	0.66	0.065	0.006	0.48	0.09
44003	CH ₃ CHO (6 _{3,3} -6 _{2,4} E)	234795.46	81.87	4.28E-04	3.42	0.31	3.82	0.82	0.062	0.010	0.44	0.08
44003	CH ₃ CHO (12 _{2,10} -11 _{2,9} E)	234825.83	81.84	4.28E-04	3.11	0.10	2.27	0.21	0.053	0.005	0.22	0.05
44003	CH ₃ CHO (12 _{2,10} -11 _{2,9} A)	238092.28	71.28	4.26E-05	3.36	0.42	3.29	1.00	0.052	0.013	0.32	0.06
44003	CH ₃ CHO (10 _{3,8} -10 _{2,9} A)	238677.10	92.51	3.41E-05	2.36	0.27	3.25	0.64	0.046	0.008	0.28	0.05
44003	CH ₃ CHO (12 _{3,10} -12 _{1,11} E)	239106.30	81.47	4.37E-05	2.79	0.24	2.54	0.79	0.039	0.010	0.19	0.05
44003	CH ₃ CHO (13 _{3,9} -11 _{2,10} A)	242010.29	104.62	4.61E-05	2.40	0.44	1.56	0.59	0.039	0.007	0.12	0.03
44003	CH ₃ CHO (13 _{1,1} -12 _{1,12} E)	2421106.02	83.89	4.81E-04	3.33	0.25	3.58	0.64	0.089	0.012	0.61	0.11
44003	CH ₃ CHO (13 _{1,1} -12 _{1,12} A)	2421118.14	83.82	4.81E-04	3.09	0.27	4.63	0.68	0.087	0.010	0.77	0.14
44003	CH ₃ CHO (13 _{0,1} -12 _{0,12} E)	244789.26	83.14	4.99E-04	2.96	0.27	3.20	0.67	0.070	0.012	0.43	0.08
44003	CH ₃ CHO (13 _{0,1} -12 _{0,12} A)	244832.18	83.06	4.99E-04	3.20	0.68	4.12	1.88	0.062	0.019	0.49	0.09
44003	CH ₃ CHO (12 _{1,1} -11 _{0,11} E)	244853.65	72.27	6.20E-05	2.82	0.20	2.09	0.40	0.051	0.009	0.21	0.04
44003	CH ₃ CHO (14 _{0,14} -13 _{1,13} E)	247341.32	95.76	6.63E-05	2.82	0.35	3.44	0.97	0.042	0.008	0.28	0.05
44003	CH ₃ CHO (6 _{2,5} -5 _{1,4} A)	249284.54	28.48	3.62E-05	3.19	0.16	2.54	0.30	0.034	0.004	0.17	0.04
44003	CH ₃ CHO (13 _{4,10} -12 _{4,9} A)	250795.66	120.39	8.70E-04	3.35	0.28	3.06	0.67	0.080	0.015	0.48	0.09
44003	CH ₃ CHO (13 _{3,11} -12 _{3,10} A)	250934.55	104.62	5.10E-04	2.95	0.21	2.28	0.44	0.034	0.006	0.15	0.04
44003	CH ₃ CHO (13 _{3,11} -12 _{3,10} E)	251095.44	104.56	5.05E-04	2.70	0.12	2.69	0.25	0.082	0.007	0.43	0.08
44003	CH ₃ CHO (13 _{1,12} -12 _{1,11} E)	251489.29	104.70	5.14E-04	2.67	0.13	3.59	0.30	0.068	0.005	0.48	0.09
44003	CH ₃ CHO (13 _{3,10} -12 _{3,9} A)	254827.18	94.10	5.51E-04	2.58	0.15	2.25	0.37	0.083	0.012	0.37	0.06
44003	CH ₃ CHO (13 _{2,11} -12 _{2,10} A)	254850.50	94.08	5.51E-04	2.70	0.32	3.85	0.77	0.070	0.012	0.54	0.09
44003	CH ₃ CHO (13 _{2,11} -12 _{2,10} E)	255326.98	88.45	5.64E-04	2.07	0.23	3.99	0.56	0.029	0.003	0.23	0.05
44003	CH ₃ CHO (13 _{1,13} -12 _{0,12} A)	260694.05	83.82	7.73E-05	2.61	0.08	1.81	0.28	0.081	0.010	0.30	0.05
44003	CH ₃ CHO (15 _{0,15} -14 _{1,14} E)	267893.38	109.25	8.70E-05	2.08	0.10	2.88	0.23	0.076	0.005	0.46	0.08
44003	CH ₃ CHO (13 _{2,11} -12 _{2,10} E)	269864.17	178.33	5.49E-04	2.27	0.21	2.24	0.76	0.074	0.020	0.36	0.08
44003	CH ₃ CHO (14 _{6,8} -13 _{6,7} E)	269899.81	178.24	5.49E-04	2.74	0.22	3.54	0.54	0.079	0.010	0.60	0.12
44003	CH ₃ CHO (14 _{6,9} -13 _{6,8} E)	269991.32	153.53	5.88E-04	2.37	0.31	3.56	0.72	0.087	0.015	0.66	0.13
44003	CH ₃ CHO (14 _{5,10} -13 _{5,9} E)	269997.52	153.50	5.87E-04	2.57	0.13	2.90	0.28	0.104	0.009	0.65	0.12

Table 4. Continued.

TAG	Species & Transition	Frequency (MHz)	Eup (K)	Aij s ⁻¹	V _O (km s ⁻¹)	δ_{V_O} (km s ⁻¹)	FWHM (km s ⁻¹)	δ_{FWHM} (km s ⁻¹)	Int δ_{Int} (K)	Flux (K km s ⁻¹)	δ_{Flux} (K km s ⁻¹)	comments
44003	CH ₃ CHO (14 _{4,11} -13 _{4,10} A)	270145.42	133.36	6.20E-04	2.44	0.32	2.71	0.83	0.122	0.031	0.71	0.13
44003	CH ₃ CHO (14 _{4,11} -13 _{3,10} E)	270212.78	133.26	6.19E-04	3.00	0.37	3.96	0.91	0.112	0.022	0.95	0.18
44003	CH ₃ CHO (14 _{3,12} -13 _{3,11} A)	270271.70	117.60	6.44E-04	2.18	0.38	4.16	0.91	0.112	0.021	1.00	0.18
44003	CH ₃ CHO (14 _{3,12} -13 _{3,11} E)	270415.84	117.54	6.37E-04	2.95	0.30	3.89	0.78	0.102	0.016	0.86	0.16
44003	CH ₃ CHO (14 _{3,11} -13 _{3,10} E)	270963.26	117.68	6.41E-04	2.46	0.10	2.41	0.25	0.100	0.009	0.52	0.10
44003	CH ₃ CHO (15 _{1,15} -14 _{1,14} E)	278924.43	109.78	7.40E-04	3.02	0.17	2.87	0.41	0.065	0.008	0.41	0.09
44003	CH ₃ CHO (15 _{1,15} -14 _{1,14} A)	278939.44	109.71	7.40E-04	2.34	0.14	3.22	0.34	0.075	0.007	0.54	0.11
44003	CH ₃ CHO (17 _{3,15} -16 _{3,14} A)	328231.53	162.07	1.18E-03	2.92	0.11	1.56	0.26	0.162	0.023	0.48	0.09
44003	CH ₃ CHO (11 _{4,8} -11 _{3,9} E)	328237.67	97.14	1.05E-04	2.66	0.15	0.98	0.31	0.129	0.036	0.24	0.05
44003	CH ₃ CHO (11 _{4,7} -11 _{3,8} A)	328242.99	97.25	1.07E-04	2.89	0.14	1.61	0.38	0.085	0.015	0.26	0.05
44003	CH ₃ CHO (17 _{4,14} -16 _{4,13} A)	328259.00	177.83	1.15E-03	2.21	0.09	1.22	0.22	0.110	0.017	0.25	0.05
44003	CH ₃ CHO (17 _{3,15} -16 _{3,14} E)	328361.96	177.75	1.14E-03	2.62	0.09	0.97	0.18	0.164	0.028	0.30	0.06
44003	CH ₃ CHO (11 _{4,8} -11 _{3,9} A)	328385.99	177.84	1.15E-03	2.49	0.23	1.30	0.54	0.097	0.035	0.24	0.05
44003	CH ₃ CHO (13 _{4,10} -13 _{3,11} A)	328520.34	120.39	1.11E-04	1.98	0.06	1.13	0.13	0.069	0.007	0.15	0.03
44003	CH ₃ CHO (11 _{4,8} -11 _{3,9} A)	328797.19	97.25	1.07E-04	1.84	0.06	1.14	0.13	0.083	0.008	0.18	0.03
44003	CH ₃ CHO (10 _{4,7} -10 _{3,8} A)	328927.15	87.07	1.05E-04	2.69	0.18	1.54	0.45	0.077	0.018	0.23	0.04
44003	CH ₃ CHO (17 _{4,14} -16 _{4,13} E)	328946.84	49.95	6.93E-05	2.36	0.07	0.91	0.22	0.082	0.016	0.14	0.03
44003	CH ₃ CHO (5 _{4,2} -5 _{3,3} E)	328970.47	45.32	4.61E-05	2.64	0.07	1.46	0.20	0.069	0.007	0.19	0.04
44003	CH ₃ CHO (4 _{4,1} -4 _{3,2} E)	329040.02	77.81	1.02E-04	2.33	0.06	0.91	0.10	0.118	0.012	0.20	0.04
44003	CH ₃ CHO (9 _{4,6} -9 _{3,7} A)	329046.77	69.49	9.72E-05	2.99	0.19	1.14	0.47	0.120	0.042	0.26	0.05
44003	CH ₃ CHO (8 _{4,4} -8 _{3,5} A)	3291602.53	146.65	1.25E-03	3.03	0.09	1.13	0.21	0.117	0.018	0.25	0.05
44003	CH ₃ CHO (17 _{1,16} -16 _{1,15} E)	331680.47	146.60	1.25E-03	2.62	0.17	1.28	0.47	0.129	0.032	0.32	0.06
44003	CH ₃ CHO (4 _{4,1} -4 _{3,2} E)	331916.57	34.26	1.17E-04	2.71	0.14	1.02	0.35	0.116	0.034	0.22	0.04
44003	CH ₃ CHO (5 _{3,3} -4 _{2,2} A)	333941.28	155.22	1.28E-03	2.51	0.05	1.36	0.12	0.144	0.011	0.37	0.07
44003	CH ₃ CHO (18 _{1,18} -17 _{1,17} E)	333959.74	155.15	1.28E-03	2.28	0.22	2.32	0.52	0.111	0.021	0.49	0.09
44003	CH ₃ CHO (18 _{0,18} -17 _{0,17} A)	334904.64	152.63	1.28E-03	2.74	0.24	1.92	0.62	0.149	0.026	0.55	0.10
44003	CH ₃ CHO (17 _{2,15} -16 _{2,14} E)	334931.81	152.61	1.28E-03	2.46	0.12	1.89	0.28	0.124	0.016	0.45	0.08
44003	CH ₃ CHO (18 _{0,18} -17 _{0,17} E)	335317.99	154.93	1.30E-03	2.43	0.05	1.48	0.13	0.143	0.011	0.40	0.07
44003	CH ₃ CHO (18 _{0,18} -17 _{1,17} A)	335358.84	154.85	1.29E-03	2.62	0.06	1.26	0.15	0.154	0.015	0.37	0.07
44003	CH ₃ CHO (9 _{2,7} -8 _{1,8} A)	339976.01	50.91	5.43E-05	2.90	0.20	1.59	0.46	0.065	0.017	0.20	0.04
44003	CH ₃ CHO (17 _{2,15} -16 _{2,14} A)	341464.93	155.22	1.95E-04	2.52	0.14	1.95	0.34	0.120	0.017	0.45	0.08
44003	CH ₃ CHO (18 _{2,17} -17 _{2,16} E)	343780.08	166.47	1.38E-03	3.20	0.10	1.45	0.25	0.077	0.011	0.22	0.04
44003	CH ₃ CHO (18 _{2,17} -17 _{2,16} A)	343803.08	166.46	1.38E-03	2.78	0.08	1.18	0.20	0.108	0.016	0.24	0.05
44003	CH ₃ CHO (18 _{3,16} -17 _{3,15} E)	347563.58	178.71	1.41E-03	2.55	0.12	1.88	0.28	0.121	0.016	0.44	0.08
44003	CH ₃ CHO (18 _{1,18} -17 _{0,17} E)	347650.37	194.51	1.38E-03	2.34	0.25	1.59	0.61	0.109	0.035	0.34	0.06
44003	CH ₃ CHO (18 _{2,17} -17 _{2,16} E)	347756.85	194.44	1.36E-03	2.71	0.11	1.55	0.27	0.131	0.020	0.39	0.07
44003	CH ₃ CHO (18 _{4,14} -17 _{4,13} E)	347830.95	194.47	1.36E-03	2.48	0.16	1.85	0.39	0.127	0.023	0.45	0.08
44003	CH ₃ CHO (18 _{3,16} -17 _{3,15} A)	347838.99	194.54	1.38E-03	2.24	0.14	1.73	0.35	0.143	0.024	0.48	0.09
44003	CH ₃ CHO (18 _{4,15} -17 _{4,14} A)	350134.53	179.18	1.44E-03	2.98	0.12	2.74	0.31	0.177	0.015	0.94	0.17
44003	CH ₃ CHO (18 _{3,15} -17 _{3,14} A)	350134.53	179.21	1.44E-03	3.13	0.18	3.10	0.46	0.168	0.019	1.01	0.18
44003	CH ₃ CHO (18 _{1,17} -17 _{1,16} E)	350362.91	163.46	1.47E-03	2.33	0.13	1.37	0.30	0.137	0.026	0.37	0.07
44003	CH ₃ CHO (18 _{1,17} -17 _{1,16} A)	350445.94	163.42	1.47E-03	2.55	0.04	1.89	0.09	0.192	0.008	0.70	0.13
44003	CH ₃ CHO (18 _{2,12} -12 _{2,11} E)	350572.18	93.02	9.70E-05	2.71	0.24	1.74	0.63	0.088	0.021	0.30	0.06
44003	CH ₃ CHO (13 _{2,12} -12 _{2,11} A)	351574.51	93.01	9.83E-05	2.80	0.10	1.44	0.25	0.114	0.015	0.32	0.06
44003	CH ₃ CHO (6 _{3,3} -5 _{2,4} A)	351588.98	39.81	1.25E-04	2.50	0.14	1.00	0.30	0.123	0.033	0.24	0.05
44003	CH ₃ CHO (19 _{0,19} -18 _{0,18} A)	3534813.01	169.66	1.52E-03	2.65	0.18	1.97	0.43	0.124	0.024	0.47	0.09
44003	CH ₃ CHO (18 _{2,16} -17 _{2,15} E)	354845.88	169.64	1.52E-03	3.61	0.11	1.19	0.26	0.149	0.028	0.35	0.06

Table 4. Continued.

TAG	Species & Transition	Frequency (MHz)	Eup (K)	A _{ij} s ⁻¹	V _O δ _{ν_o} (km s ⁻¹)	FWHM δ _{FWM} (km s ⁻¹)	Int δ _{Int} (K)	Flux δ _{Flux} (K km s ⁻¹)	comments
44003	CH ₃ CHO (19 _{1,19} -18 _{0,18} A)	358507.80	172.06	2.31E-04	2.62	0.12	1.40	0.105	0.29
44003	CH ₃ CHO (19 _{2,18} -18 _{2,17} A)	362561.10	183.86	1.62E-03	2.60	0.12	1.31	0.123	0.32
46509	H ₂ CS (3 _{1,3} -2 _{1,2})	101477.81	22.91	1.26E-05	3.79	0.06	2.59	0.14	0.248
46509	H ₂ CS (3 _{0,3} -2 _{0,2})	103040.45	9.89	1.48E-05	3.88	0.10	2.96	0.24	0.154
46509	H ₂ CS (3 _{1,2} -2 _{1,1})	104617.04	23.21	1.38E-05	3.81	0.10	2.71	0.23	0.229
46509	H ₂ CS (4 _{1,4} -3 _{1,3})	135298.26	29.40	3.27E-05	3.59	0.11	3.03	0.25	0.320
46509	H ₂ CS (4 _{0,4} -3 _{0,3})	137371.21	16.48	3.65E-05	3.94	0.14	2.63	0.32	0.177
46509	H ₂ CS (4 _{1,3} -3 _{1,2})	139483.68	29.91	3.58E-05	3.85	0.11	3.30	0.27	0.324
46509	H ₂ CS (5 _{1,5} -4 _{1,4})	169114.08	37.52	6.68E-05	3.68	0.09	4.10	0.22	0.421
46509	H ₂ CS (5 _{0,5} -4 _{0,4})	171688.12	24.72	7.28E-05	3.94	0.13	4.31	0.31	0.221
46509	H ₂ CS (5 _{1,4} -4 _{1,3})	174345.22	38.27	7.32E-05	3.32	0.10	3.34	0.24	0.367
46509	H ₂ CS (6 _{1,6} -5 _{1,5})	202924.05	47.26	1.19E-04	3.30	0.15	4.08	0.36	0.357
46509	H ₂ CS (6 _{0,6} -5 _{0,5})	205987.86	34.61	1.28E-04	3.34	0.13	4.32	0.29	0.215
46509	H ₂ CS (6 _{2,5} -5 _{2,4})	206054.17	87.28	1.14E-04	4.55	0.08	5.79	0.22	0.152
46509	H ₂ CS (6 _{1,5} -5 _{1,4})	209200.62	48.31	1.30E-04	3.32	0.09	4.80	0.22	0.354
46509	H ₂ CS (7 _{1,7} -6 _{1,6})	236727.02	58.62	1.92E-04	3.66	0.06	4.73	0.15	0.494
46509	H ₂ CS (7 _{0,7} -6 _{0,6})	240266.87	46.14	2.05E-04	3.51	0.15	5.19	0.35	0.287
46509	H ₂ CS (7 _{2,6} -6 _{2,5})	240382.05	98.82	1.88E-04	3.01	0.18	6.73	0.46	0.108
46509	H ₂ CS (7 _{2,5} -6 _{2,4})	240549.07	98.84	1.89E-04	3.75	0.29	6.84	0.75	0.092
46509	H ₂ CS (7 _{1,6} -6 _{1,5})	244048.50	60.03	1.20E-04	3.42	0.06	4.73	0.15	0.380
46509	H ₂ CS (8 _{1,7} -7 _{1,6})	270521.93	71.60	2.90E-04	3.05	0.12	4.78	0.28	0.421
46509	H ₂ CS (8 _{1,8} -7 _{1,7})	274703.35	112.00	2.89E-04	3.68	0.13	5.89	0.34	0.083
46509	H ₂ CS (8 _{2,7} -7 _{2,6})	274953.74	112.03	2.90E-04	4.00	0.14	7.43	0.40	0.094
46509	H ₂ CS (8 _{2,6} -7 _{2,5})	278887.66	73.41	3.18E-04	3.62	0.06	4.20	0.15	0.271
46509	H ₂ CS (8 _{1,7} -7 _{1,6})	338083.20	102.43	5.77E-04	3.21	0.14	3.70	0.34	0.237
46509	H ₂ CS (10 _{1,10} -9 _{1,9})	342946.42	90.59	6.08E-04	3.12	0.19	4.33	0.48	0.154
46509	H ₂ CS (10 _{0,10} -9 _{0,9})	343813.17	143.38	5.88E-04	3.70	0.32	5.77	0.83	0.086
46509	H ₂ CS (10 _{2,8} -9 _{2,7})	348534.36	105.19	6.32E-04	3.76	0.14	5.37	0.35	0.430
47505	H ₂ CS (10 _{1,9} -9 _{1,8})	97632.20	22.54	1.12E-05	4.97	0.35	3.23	0.83	0.013
47505	H ₁₃ CS (3 _{1,3} -2 _{1,2})	167543.38	37.29	6.49E-05	4.54	0.15	3.27	0.36	0.075
47505	H ₁₃ CS (5 _{1,4} -4 _{1,3})	227760.42	56.90	1.71E-04	3.32	0.31	3.93	0.74	0.025
47505	H ₁₃ CS (7 _{1,7} -6 _{1,6})	231280.89	97.06	1.68E-04	3.53	0.40	8.01	1.19	0.155
47504	HDCS (3 _{1,3} -2 _{1,2})	91171.07	17.74	9.12E-06	3.87	0.19	4.00	0.53	0.032
47504	HDCS (5 _{1,4} -4 _{1,3})	92981.60	8.93	1.09E-05	3.90	0.08	1.99	0.27	0.057
47504	HDCS (3 _{0,3} -2 _{0,2})	94828.49	18.09	1.03E-05	3.67	0.24	1.88	0.60	0.028
47504	HDCS (3 _{1,2} -2 _{1,1})	151927.54	30.86	4.83E-05	3.62	0.20	2.97	0.55	0.044
47504	HDCS (5 _{1,5} -4 _{1,4})	154885.03	22.31	5.33E-05	3.81	0.12	3.19	0.35	0.050
60503	OCS (7-6)	85139.10	16.34	1.71E-06	3.22	0.10	5.09	0.25	0.222
60503	OCS (8-7)	97301.21	21.01	2.58E-06	3.11	0.14	4.59	0.33	0.277
60503	OCS (9-8)	109463.06	26.27	3.70E-06	3.08	0.11	4.61	0.26	0.139
60503	OCS (11-10)	133785.90	38.53	6.82E-06	3.20	0.15	4.75	0.34	0.456
60503	OCS (12-11)	145946.81	45.53	8.88E-06	2.91	0.14	4.59	0.34	0.423
60503	OCS (13-12)	158107.36	53.12	1.13E-05	2.84	0.15	4.04	0.36	0.477
60503	OCS (14-13)	170267.49	61.29	1.42E-05	3.20	0.19	5.02	0.47	0.385
60503	OCS (17-16)	206745.16	89.31	2.56E-05	2.94	0.18	5.21	0.43	0.580
60503	OCS (18-17)	218903.36	99.81	3.04E-05	2.90	0.20	5.34	0.49	0.615
60503	OCS (19-18)	231060.99	110.90	3.58E-05	3.07	0.15	5.22	0.36	0.606

Table 4. Continued.

TAG	Species & Transition	Frequency (MHz)	E _{up} (K)	A _{ij} s ⁻¹	V _O (km s ⁻¹)	δ_{V_O} (km s ⁻¹)	FWHM (km s ⁻¹)	δ_{FWHM} (km s ⁻¹)	Int δ_{Int} (K)	Flux (K km s ⁻¹)	δ_{Flux} (K km s ⁻¹)	comments
60503	OCS (20-19)	243218.04	122.57	4.18E-05	3.00	0.12	5.94	0.29	0.503	0.020	5.71	0.97
60503	OCS (21-20)	255374.46	134.83	4.84E-05	4.10	0.50	7.05	1.38	0.047	0.006	0.66	0.12
62505	OC ³⁴ S (7-6)	83057.97	15.94	1.59E-06	2.64	0.17	3.93	0.48	0.062	0.005	0.31	0.04
62505	OC ³⁴ S (8-7)	94922.80	20.50	2.40E-06	2.24	0.21	3.05	0.51	0.066	0.009	0.26	0.03
62505	OC ³⁴ S (11-10)	130515.73	37.58	6.33E-06	2.55	0.15	3.57	0.37	0.112	0.009	0.56	0.10
62505	OC ³⁴ S (13-12)	154242.78	51.82	1.05E-05	2.34	0.19	3.87	0.52	0.137	0.013	0.78	0.14
62505	OC ³⁴ S (17-16)	201691.98	87.12	2.37E-05	2.34	0.10	4.92	0.33	0.144	0.006	1.17	0.20
62505	OC ³⁴ S (18-17)	213553.06	97.37	2.82E-05	2.35	0.08	3.78	0.21	0.177	0.008	1.15	0.20
62505	OC ³⁴ S (19-18)	225413.64	108.19	3.32E-05	2.51	0.13	4.43	0.35	0.163	0.010	1.29	0.23
62505	OC ³⁴ S (20-19)	237273.64	119.58	3.88E-05	3.11	0.18	4.90	0.56	0.141	0.010	1.29	0.22
62505	OC ³⁴ S (23-22)	272849.96	157.16	5.92E-05	2.48	0.15	3.41	0.35	0.133	0.012	0.99	0.18
61502	O ¹³ CS (8-7)	96988.12	20.95	2.56E-06	2.07	0.29	4.38	0.79	0.033	0.004	0.19	0.03
61502	O ¹³ CS (9-8)	109110.85	26.18	3.66E-06	2.41	0.30	3.05	0.71	0.034	0.007	0.14	0.03
61502	O ¹³ CS (11-10)	133355.42	38.40	6.76E-06	2.65	0.15	2.49	0.36	0.090	0.011	0.31	0.06
61502	O ¹³ CS (12-11)	145477.20	45.38	8.80E-06	2.26	0.19	4.18	0.48	0.082	0.007	0.49	0.09
61502	O ¹³ CS (13-12)	157598.62	52.95	1.12E-05	2.45	0.22	3.85	0.54	0.101	0.011	0.58	0.10
61502	O ¹³ CS (14-13)	169719.65	61.09	1.41E-05	2.99	0.29	5.23	0.85	0.072	0.008	0.57	0.11
61502	O ¹³ CS (18-17)	218199.00	99.49	3.01E-05	2.77	0.19	6.42	0.48	0.098	0.006	1.10	0.19
61502	O ¹³ CS (19-18)	220317.53	110.54	3.54E-05	3.78	0.08	6.20	0.21	0.098	0.002	1.11	0.19
61502	O ¹³ CS (21-20)	254552.73	134.40	4.80E-05	2.26	0.30	4.12	0.85	0.076	0.011	0.63	0.11
61502	O ¹³ CS (22-21)	266669.38	147.19	5.52E-05	2.20	0.43	4.94	1.10	0.048	0.009	0.50	0.10
60003	HCOOCH ₃ (7 _{2,6} -6 _{2,5} E)	84449.17	19.00	7.96E-06	2.75	0.25	2.30	0.58	0.017	0.004	0.05	0.02
60003	HCOOCH ₃ (7 _{2,6} -6 _{2,5} A)	84454.75	18.98	7.96E-06	2.66	0.24	3.31	0.59	0.025	0.004	0.11	0.02
60003	HCOOCH ₃ (7 _{4,4} -6 _{4,3} A)	86210.06	27.15	6.24E-06	2.93	0.43	4.18	1.16	0.024	0.005	0.13	0.03
60003	HCOOCH ₃ (7 _{4,4} -6 _{4,3} A)	86250.55	27.15	6.25E-06	2.82	0.20	2.63	0.48	0.023	0.004	0.08	0.02
60003	HCOOCH ₃ (7 _{4,4} -6 _{4,2} A)	86268.74	22.53	7.50E-06	3.25	0.27	2.45	0.69	0.028	0.006	0.09	0.02
60003	HCOOCH ₃ (7 _{3,5} -6 _{3,4} E)	87161.29	22.58	7.81E-06	2.72	0.33	3.01	0.82	0.040	0.009	0.15	0.02
60003	HCOOCH ₃ (7 _{3,4} -6 _{3,3} A)	88843.19	17.96	9.82E-06	3.09	0.36	2.85	1.00	0.035	0.009	0.13	0.02
60003	HCOOCH ₃ (7 _{1,6} -6 _{1,5} E)	88851.61	17.94	9.82E-06	2.71	0.15	2.77	0.35	0.033	0.004	0.12	0.02
60003	HCOOCH ₃ (7 _{1,6} -6 _{1,5} A)	89314.66	20.15	1.02E-05	2.37	0.38	3.00	1.08	0.034	0.009	0.13	0.02
60003	HCOOCH ₃ (8 _{1,8} -7 _{1,7} E)	90145.72	19.68	9.74E-06	2.49	0.17	2.01	0.38	0.045	0.007	0.12	0.02
60003	HCOOCH ₃ (7 _{2,5} -6 _{2,4} E)	90156.47	19.67	9.75E-06	1.99	0.20	1.61	0.38	0.028	0.006	0.06	0.02
60003	HCOOCH ₃ (8 _{0,8} -7 _{0,7} E)	90227.66	20.08	1.05E-05	3.35	0.28	2.55	0.69	0.033	0.008	0.11	0.02
60003	HCOOCH ₃ (8 _{2,7} -7 _{2,6} E)	96070.73	23.61	1.20E-05	2.84	0.13	3.22	0.31	0.043	0.004	0.18	0.02
60003	HCOOCH ₃ (8 _{0,2} -7 _{0,1} E)	98270.50	45.15	6.05E-06	2.76	0.34	3.08	0.85	0.017	0.004	0.07	0.02
60003	HCOOCH ₃ (7 _{2,5} -6 _{2,4} A)	98424.21	37.86	8.47E-06	2.75	0.14	2.39	0.32	0.034	0.004	0.11	0.02
60003	HCOOCH ₃ (8 _{3,3} -7 _{3,2} E)	98435.80	37.84	8.47E-06	2.61	0.20	3.04	0.54	0.040	0.005	0.16	0.02
60003	HCOOCH ₃ (8 _{3,3} -7 _{3,2} A)	98606.86	27.26	1.20E-05	2.49	0.15	3.56	0.40	0.031	0.003	0.15	0.02
60003	HCOOCH ₃ (8 _{3,6} -7 _{3,5} A)	98611.16	27.24	1.20E-05	2.67	0.24	3.00	0.65	0.045	0.007	0.18	0.02
60003	HCOOCH ₃ (8 _{4,5} -7 _{4,4} A)	98682.62	31.89	1.05E-05	2.63	0.14	3.36	0.35	0.047	0.004	0.21	0.03
60003	HCOOCH ₃ (8 _{4,5} -7 _{4,4} E)	98712.00	31.90	1.02E-05	2.52	0.14	1.96	0.31	0.040	0.006	0.10	0.02
60003	HCOOCH ₃ (8 _{3,6} -7 _{3,5} E)	98747.91	31.91	1.02E-05	2.58	0.10	2.40	0.27	0.030	0.002	0.09	0.02
60003	HCOOCH ₃ (8 _{4,4} -7 _{4,3} A)	98792.29	31.89	1.05E-05	2.34	0.40	3.20	1.33	0.035	0.008	0.15	0.02
60003	HCOOCH ₃ (8 _{4,5} -7 _{4,4} E)	100294.60	27.41	1.26E-05	2.37	0.09	2.62	0.21	0.035	0.002	0.12	0.02
60003	HCOOCH ₃ (8 _{3,5} -7 _{3,4} A)	100308.18	27.40	1.26E-05	2.62	0.13	2.81	0.33	0.034	0.003	0.13	0.02
60003	HCOOCH ₃ (8 _{1,7} -7 _{1,6} E)	100482.24	22.78	1.43E-05	2.47	0.20	3.36	0.51	0.034	0.004	0.15	0.02

Table 4. Continued.

TAG	Species & Transition	Frequency (MHz)	Eup (K)	A _{ij} s ⁻¹	V ₀ (km s ⁻¹)	δ_{V_0} (km s ⁻¹)	FWHM (km s^{-1})	δ_{FWHM} (km s^{-1})	Int δ_{Int} (K)	Flux (K km s^{-1})	δ_{Flux} (K km s^{-1})	comments
60003	HCOOCH ₃ (8 _{2,6} -7 ₅ E)	103466.57	24.65	1.52E-05	2.16	0.14	3.57	0.36	0.041	0.003	0.20	0.03
60003	HCOOCH ₃ (8 _{2,6} -7 ₅ A)	103478.66	24.63	1.52E-05	2.47	0.16	2.90	0.37	0.039	0.004	0.15	0.02
60003	HCOOCH ₃ (9 _{3,3} -8 _{6,2} E)	110652.81	50.46	1.10E-05	2.38	0.19	2.04	0.45	0.036	0.007	0.10	0.01
60003	HCOOCH ₃ (10 _{1,10} -9 _{1,9} E)	110788.66	30.27	1.97E-05	2.31	0.23	2.50	0.57	0.053	0.010	0.18	0.02
60003	HCOOCH ₃ (10 _{1,10} -9 _{1,9} A)	110790.53	30.26	1.97E-05	2.20	0.30	3.49	0.79	0.038	0.004	0.18	0.02
60003	HCOOCH ₃ (9 _{5,4} -8 _{5,3} E)	110873.96	43.18	1.38E-05	2.39	0.15	2.60	0.45	0.036	0.004	0.12	0.01
60003	HCOOCH ₃ (9 _{5,5} -8 _{5,4} E)	110882.33	43.16	1.38E-05	2.82	0.19	2.39	0.53	0.029	0.004	0.09	0.01
60003	HCOOCH ₃ (9 _{5,4} -8 _{5,3} A)	110890.26	43.16	1.38E-05	2.59	0.25	1.87	0.63	0.023	0.006	0.06	0.01
60003	HCOOCH ₃ (10 _{0,10} -9 _{0,9} E)	111169.90	30.25	1.99E-05	2.35	0.14	3.57	0.47	0.058	0.004	0.28	0.04
60003	HCOOCH ₃ (10 _{0,10} -9 _{0,9} A)	111171.63	30.23	1.99E-05	2.72	0.41	3.25	1.06	0.047	0.008	0.20	0.04
60003	HCOOCH ₃ (9 _{4,6} -8 _{4,5} A)	111195.96	37.22	1.62E-05	2.54	0.20	2.49	0.56	0.047	0.007	0.16	0.03
60003	HCOOCH ₃ (9 _{4,6} -8 _{4,5} E)	111223.49	37.23	1.53E-05	2.56	0.20	2.00	0.46	0.037	0.007	0.10	0.02
60003	HCOOCH ₃ (9 _{5,5} -8 _{4,4} A)	111453.30	37.24	1.63E-05	2.74	0.14	2.18	0.37	0.043	0.006	0.13	0.03
60003	HCOOCH ₃ (9 ₈ -8 ₇ A)	111682.19	28.12	1.98E-05	2.74	0.29	2.00	0.67	0.027	0.008	0.07	0.02
60003	HCOOCH ₃ (9 _{5,6} -8 _{5,5} E)	113743.11	32.87	1.92E-05	2.66	0.19	2.53	0.47	0.060	0.009	0.21	0.02
60003	HCOOCH ₃ (9 _{3,6} -8 _{3,5} A)	113756.61	32.86	1.92E-05	2.70	0.23	2.50	0.69	0.050	0.009	0.17	0.02
60003	HCOOCH ₃ (10 _{2,8} -9 _{2,7} E)	129296.36	36.45	3.06E-05	2.55	0.09	2.31	0.20	0.081	0.006	0.26	0.05
60003	HCOOCH ₃ (10 _{2,8} -9 _{2,7} A)	129310.57	36.43	3.06E-05	2.74	0.14	1.67	0.38	0.054	0.007	0.12	0.02
60003	HCOOCH ₃ (12 _{0,12} -11 _{1,11} E)	131914.52	42.44	5.10E-06	3.08	0.12	1.76	0.29	0.049	0.007	0.12	0.02
60003	HCOOCH ₃ (12 _{1,12} -11 _{1,11} E)	132105.51	42.44	3.38E-05	2.47	0.25	3.00	0.94	0.061	0.008	0.25	0.05
60003	HCOOCH ₃ (12 _{1,12} -11 _{1,11} A)	132107.20	42.43	3.38E-05	2.46	0.34	2.00	0.86	0.056	0.012	0.16	0.03
60003	HCOOCH ₃ (12 _{0,12} -11 _{0,11} E)	132245.13	42.44	3.39E-05	2.37	0.23	3.26	0.68	0.067	0.009	0.31	0.06
60003	HCOOCH ₃ (12 _{0,12} -11 _{0,11} A)	132246.73	42.42	3.39E-05	2.70	0.22	2.78	0.49	0.050	0.004	0.19	0.04
60003	HCOOCH ₃ (12 _{1,12} -11 _{0,11} E)	132436.11	42.44	5.16E-06	2.25	0.19	2.49	0.47	0.033	0.005	0.11	0.02
60003	HCOOCH ₃ (12 _{1,12} -11 _{0,11} A)	132437.49	42.43	5.16E-06	2.33	0.57	2.69	1.31	0.022	0.005	0.08	0.02
60003	HCOOCH ₃ (11 _{1,10} -10 _{1,9} A)	132928.74	40.38	3.36E-05	2.70	0.28	2.00	0.81	0.052	0.014	0.15	0.03
60003	HCOOCH ₃ (11 _{3,9} -10 _{3,8} A)	135101.63	44.96	3.37E-05	2.46	0.18	2.23	0.43	0.053	0.009	0.17	0.03
60003	HCOOCH ₃ (11 _{8,3} -10 _{8,2} E)	135143.06	81.42	1.72E-05	1.86	0.04	2.08	0.10	0.045	0.002	0.13	0.02
60003	HCOOCH ₃ (12 _{0,12} -11 _{0,11} E)	135156.25	81.40	1.72E-05	2.70	0.35	2.00	0.87	0.043	0.016	0.12	0.02
60003	HCOOCH ₃ (11 _{8,4} -10 _{8,3} E)	135541.48	62.86	2.59E-05	3.18	0.21	2.50	0.50	0.052	0.009	0.19	0.03
60003	HCOOCH ₃ (11 _{6,5} -10 _{6,4} A)	135921.95	55.60	2.95E-05	2.21	0.19	2.32	0.47	0.063	0.010	0.21	0.04
60003	HCOOCH ₃ (11 _{5,7} -10 _{5,6} A)	135942.98	55.61	2.92E-05	1.89	0.12	2.68	0.29	0.052	0.005	0.20	0.03
60003	HCOOCH ₃ (11 _{4,8} -10 _{4,7} A)	136282.60	49.70	3.25E-05	2.69	0.07	3.83	0.19	0.072	0.003	0.39	0.07
60003	HCOOCH ₃ (11 _{4,7} -10 _{4,6} E)	137293.18	49.81	3.31E-05	2.83	0.06	3.06	0.16	0.054	0.002	0.23	0.04
60003	HCOOCH ₃ (11 _{4,7} -10 _{4,6} A)	137313.33	49.80	3.33E-05	2.52	0.07	1.49	0.16	0.050	0.005	0.10	0.02
60003	HCOOCH ₃ (11 _{3,8} -10 _{3,7} A)	141260.42	45.75	3.87E-05	2.89	0.11	2.59	0.27	0.079	0.007	0.29	0.06
60003	HCOOCH ₃ (11 _{2,9} -10 _{2,8} E)	141652.99	43.25	4.06E-05	2.34	0.24	2.00	0.56	0.126	0.030	0.36	0.06
60003	HCOOCH ₃ (13 _{0,13} -12 _{0,12} E)	142815.48	49.29	4.29E-05	2.60	0.07	2.68	0.21	0.106	0.005	0.41	0.07
60003	HCOOCH ₃ (13 _{0,13} -12 _{0,12} A)	142817.02	49.27	4.29E-05	2.66	0.36	2.00	0.94	0.095	0.026	0.27	0.05
60003	HCOOCH ₃ (13 _{1,13} -12 _{0,12} E)	142924.51	49.29	6.59E-06	2.90	0.21	2.21	0.64	0.089	0.019	0.25	0.05
60003	HCOOCH ₃ (13 _{1,13} -12 _{0,12} A)	142925.91	49.28	6.59E-06	2.98	0.20	2.50	0.49	0.088	0.008	0.31	0.06
60003	HCOOCH ₃ (12 _{1,11} -11 _{1,10} E)	143234.20	47.27	4.22E-05	2.43	0.12	2.96	0.32	0.085	0.007	0.36	0.07
60003	HCOOCH ₃ (13 _{0,13} -12 _{0,12} A)	143240.51	47.25	4.23E-05	2.44	0.19	2.60	0.51	0.078	0.009	0.29	0.05
60003	HCOOCH ₃ (13 _{1,13} -12 _{0,12} E)	147325.39	112.37	1.45E-05	2.64	0.17	2.21	0.40	0.050	0.008	0.16	0.03
60003	HCOOCH ₃ (12 _{0,13} -11 _{0,12} E)	147397.07	99.78	2.09E-05	2.29	0.09	4.28	0.24	0.100	0.004	0.62	0.11
60003	HCOOCH ₃ (12 _{8,4} -11 _{8,3} E)	147524.31	88.50	2.65E-05	2.54	0.12	2.25	0.31	0.064	0.006	0.23	0.05
60003	HCOOCH ₃ (12 _{8,5} -11 _{8,4} E)	147538.64	88.49	2.65E-05	2.54	0.11	2.46	0.28	0.064	0.006	0.18	0.04
60003	HCOOCH ₃ (12 _{6,6} -11 _{6,5} A)	148045.82	69.96	3.62E-05	2.47	0.33	2.00	0.72	0.067	0.009	0.19	0.04

Table 4. Continued.

TAG	Species & Transition	Frequency (MHz)	Eup (K)	Aij s ⁻¹	V _O (km s ⁻¹)	δ_{V_O} (km s ⁻¹)	FWHM (δ_{FWHM} km s ⁻¹)	Int δ_{Int} (K)	Flux (δ_{Flux} K km s ⁻¹)	comments
60003	HCOOCH ₃ (12 _{5,8} -11 _{5,7} A)	148516.04	62.73	4.03E-05	2.34	0.07	1.67	0.16	0.079	0.007
60003	HCOOCH ₃ (12 _{5,8} -11 _{5,7} E)	148545.01	62.74	3.87E-05	2.58	0.22	2.07	0.60	0.076	0.015
60003	HCOOCH ₃ (12 _{5,7} -11 _{5,6} E)	148614.84	62.76	3.88E-05	2.27	0.18	2.00	0.44	0.085	0.016
60003	HCOOCH ₃ (12 _{5,7} -11 _{5,6} A)	148664.52	62.74	4.04E-05	2.27	0.15	2.50	0.39	0.072	0.009
60003	HCOOCH ₃ (12 _{4,9} -11 _{4,8} E)	148797.79	56.86	4.35E-05	2.23	0.21	3.07	0.80	0.077	0.010
60003	HCOOCH ₃ (12 _{4,9} -11 _{4,8} A)	148805.94	56.84	4.35E-05	2.37	0.12	2.48	0.30	0.085	0.009
60003	HCOOCH ₃ (13 _{1,12} -12 _{2,11} E)	149065.24	54.64	5.23E-06	2.53	0.04	1.41	0.09	0.046	0.002
60003	HCOOCH ₃ (13 _{1,12} -12 _{2,11} A)	149074.31	54.62	5.23E-06	3.37	0.15	1.38	0.36	0.031	0.006
60003	HCOOCH ₃ (12 _{4,8} -11 _{4,7} A)	150618.30	57.03	4.52E-05	2.42	0.23	2.00	0.63	0.094	0.021
60003	HCOOCH ₃ (13 _{2,12} -12 _{2,11} A)	151956.62	54.76	5.05E-05	2.77	0.07	1.96	0.17	0.052	0.004
60003	HCOOCH ₃ (14 _{1,14} -13 _{0,13} A)	153460.91	56.64	8.26E-06	2.64	0.24	2.00	0.64	0.065	0.015
60003	HCOOCH ₃ (12 _{2,10} -11 _{2,9} E)	153553.23	50.62	5.19E-05	2.65	0.11	2.07	0.31	0.072	0.008
60003	HCOOCH ₃ (12 _{5,10} -11 _{2,9} A)	153566.92	50.60	5.20E-05	2.22	0.30	2.00	0.83	0.065	0.019
60003	HCOOCH ₃ (12 _{3,9} -11 _{3,8} A)	155002.32	53.19	5.21E-05	2.47	0.08	1.78	0.18	0.074	0.006
60003	HCOOCH ₃ (13 _{2,12} -11 ₁₁ E)	156397.53	54.78	6.11E-06	2.16	0.14	2.07	0.34	0.041	0.006
60003	HCOOCH ₃ (13 _{3,11} -13 _{1,10} E)	158693.72	59.64	5.61E-05	2.84	0.11	2.27	0.27	0.093	0.006
60003	HCOOCH ₃ (13 _{3,11} -13 _{1,10} A)	158704.39	59.63	5.61E-05	2.51	0.14	2.09	0.36	0.107	0.014
60003	HCOOCH ₃ (13 _{10,3} -11 _{10,2} E)	159654.88	120.05	2.48E-05	2.79	0.11	1.78	0.26	0.044	0.005
60003	HCOOCH ₃ (13 _{10,4} -11 _{10,3} E)	159670.85	120.03	2.48E-05	2.85	0.09	1.65	0.22	0.068	0.008
60003	HCOOCH ₃ (13 _{6,7} -12 _{7,5} E)	160178.94	86.26	4.35E-05	2.29	0.10	2.72	0.31	0.055	0.004
60003	HCOOCH ₃ (13 _{6,7} -12 _{6,6} E)	160578.37	77.68	4.86E-05	2.43	0.14	2.70	0.36	0.080	0.008
60003	HCOOCH ₃ (13 _{6,8} -12 _{6,7} A)	160585.83	77.67	4.86E-05	2.26	0.11	3.67	0.34	0.079	0.004
60003	HCOOCH ₃ (13 _{6,8} -12 _{6,7} E)	160591.25	77.67	4.86E-05	2.49	0.20	3.15	0.54	0.081	0.010
60003	HCOOCH ₃ (13 _{6,7} -12 _{6,6} A)	160602.04	77.67	4.86E-05	2.39	0.10	3.42	0.33	0.083	0.005
60003	HCOOCH ₃ (13 _{5,9} -12 _{5,8} E)	161171.47	70.47	5.13E-05	2.63	0.12	3.05	0.33	0.100	0.007
60003	HCOOCH ₃ (13 _{4,10} -12 _{4,9} E)	161262.46	64.59	5.66E-05	2.10	0.26	2.00	0.73	0.093	0.023
60003	HCOOCH ₃ (13 _{4,10} -12 _{4,9} A)	161273.36	64.58	5.66E-05	2.75	0.23	2.99	0.58	0.086	0.007
60003	HCOOCH ₃ (13 _{5,8} -12 _{5,7} E)	161416.14	70.50	5.15E-05	2.32	0.18	2.00	0.44	0.075	0.014
60003	HCOOCH ₃ (13 _{5,8} -12 _{5,7} A)	161458.22	70.49	5.35E-05	2.49	0.06	2.24	0.18	0.106	0.005
60003	HCOOCH ₃ (14 _{2,13} -13 _{2,12} A)	162775.27	62.57	6.24E-05	2.51	0.11	3.33	0.29	0.121	0.008
60003	HCOOCH ₃ (14 _{1,13} -13 _{1,12} E)	163829.68	62.50	6.37E-05	2.71	0.04	1.40	0.09	0.086	0.005
60003	HCOOCH ₃ (15 _{0,15} -14 _{1,14} E)	163925.85	64.52	1.02E-05	2.75	0.07	1.72	0.19	0.061	0.005
60003	HCOOCH ₃ (15 _{0,15} -14 _{1,14} A)	163927.37	64.50	1.02E-05	2.72	0.21	2.00	0.55	0.035	0.008
60003	HCOOCH ₃ (15 _{1,15} -14 _{1,14} E)	163960.39	64.52	6.53E-05	2.59	0.03	2.06	0.07	0.126	0.003
60003	HCOOCH ₃ (15 _{1,15} -14 _{1,14} A)	163961.88	64.50	6.54E-05	2.83	0.46	2.00	0.99	0.141	0.024
60003	HCOOCH ₃ (15 _{0,15} -14 _{0,14} E)	163987.45	64.52	6.54E-05	2.57	0.07	1.68	0.21	0.110	0.009
60003	HCOOCH ₃ (15 _{0,15} -14 _{0,14} A)	163988.91	64.50	6.54E-05	2.66	0.24	2.00	0.64	0.105	0.021
60003	HCOOCH ₃ (15 _{1,15} -14 _{1,14} A)	164023.42	64.50	1.02E-05	2.94	0.06	2.75	0.14	0.067	0.003
60003	HCOOCH ₃ (13 _{5,10} -12 _{3,9} E)	164205.98	64.92	5.98E-05	2.14	0.14	3.16	0.36	0.071	0.024
60003	HCOOCH ₃ (13 _{4,9} -12 _{4,8} E)	164223.82	64.91	5.98E-05	2.58	0.07	1.81	0.17	0.063	0.005
60003	HCOOCH ₃ (13 _{2,11} -12 _{2,1} E)	164955.70	58.53	6.46E-05	2.02	0.25	2.50	0.67	0.036	0.007
60003	HCOOCH ₃ (13 _{5,10} -12 _{3,9} E)	168495.07	61.29	6.78E-05	2.44	0.17	2.55	0.42	0.087	0.012
60003	HCOOCH ₃ (13 _{4,9} -12 _{3,9} A)	168513.75	61.28	6.78E-05	2.14	0.25	3.00	0.67	0.091	0.011
60003	HCOOCH ₃ (13 _{4,9} -12 _{4,8} A)	170233.27	67.81	6.99E-05	2.39	0.06	1.64	0.14	0.087	0.006
60003	HCOOCH ₃ (14 _{3,12} -13 _{3,11} E)	170244.09	67.80	6.99E-05	2.81	0.12	2.00	0.33	0.081	0.009
60003	HCOOCH ₃ (6 _{3,3} -5 _{3,3} E)	170458.42	23.02	6.05E-06	2.74	0.17	1.25	0.41	0.055	0.015
60003	HCOOCH ₃ (14 _{10,5} -13 _{10,4} E)	172032.76	128.29	3.73E-05	2.20	0.09	3.10	0.22	0.083	0.005
60003	HCOOCH ₃ (14 _{9,5} -13 _{9,4} E)	172157.64	115.71	4.48E-05	3.16	0.05	2.17	0.14	0.068	0.003

Table 4. Continued.

TAG	Species & Transition	Frequency (MHz)	Eup (K)	Aij s ⁻¹	V _O (km s ⁻¹)	δ_{V_O} (km s ⁻¹)	FWHM (δ_{FWHM} km s ⁻¹)	Int δ_{Int} (K)	Flux (δ_{Flux} K km s ⁻¹)	comments
60003	HCOOCH ₃ (14 _{8,6} -13 _{8,5} E)	172364.37	104.45	5.16E-05	2.63	0.19	2.30	0.52	0.080	0.012
60003	HCOOCH ₃ (14 _{8,7} -13 _{8,6} E)	172380.95	104.44	5.16E-05	2.37	0.16	2.64	0.41	0.080	0.010
60003	HCOOCH ₃ (15 _{1,14} -14 _{2,13} A)	172393.49	70.85	8.93E-06	2.93	0.15	2.50	0.40	0.058	0.005
60003	HCOOCH ₃ (14 _{6,8} -13 _{6,7} E)	173185.19	86.00	6.32E-05	2.62	0.05	1.60	0.12	0.096	0.006
60003	HCOOCH ₃ (14 _{6,9} -13 _{6,8} E)	173194.27	85.98	6.32E-05	2.56	0.18	3.29	0.53	0.075	0.007
60003	HCOOCH ₃ (14 _{6,8} -13 _{6,7} A)	173218.68	85.98	6.35E-05	2.44	0.12	2.15	0.29	0.079	0.009
60003	HCOOCH ₃ (15 _{1,14} -14 _{1,13} E)	174209.80	70.86	7.69E-05	2.85	0.09	2.75	0.26	0.078	0.005
60003	HCOOCH ₃ (15 _{1,14} -14 _{1,13} A)	174215.56	70.85	7.70E-05	2.59	0.10	2.37	0.26	0.108	0.009
60003	HCOOCH ₃ (14 _{5,9} -13 _{5,8} E)	174377.41	78.87	6.83E-05	2.78	0.07	1.72	0.22	0.102	0.008
60003	HCOOCH ₃ (18 _{1,12} -18 _{6,13} E)	174995.67	133.72	5.36E-06	3.33	0.12	1.60	0.29	0.061	0.009
60003	HCOOCH ₃ (17 _{3,15} -16 _{3,14} A)	176525.62	112.91	7.10E-06	3.39	0.15	1.51	0.35	0.077	0.016
60003	HCOOCH ₃ (16 _{7,9} -16 _{6,10} A)	198636.78	104.45	9.73E-05	2.86	0.47	2.77	0.99	0.026	0.008
60003	HCOOCH ₃ (16 _{6,10} -15 _{6,9} E)	200936.16	97.52	1.10E-04	2.46	0.32	3.00	0.83	0.063	0.014
60003	HCOOCH ₃ (16 _{5,11} -15 _{5,10} E)	200956.37	97.51	1.10E-04	2.40	0.21	2.42	0.45	0.063	0.010
60003	HCOOCH ₃ (16 _{5,11} -15 _{5,10} A)	203864.21	95.55	1.22E-04	3.33	0.40	3.00	0.94	0.144	0.014
60003	HCOOCH ₃ (17 _{3,15} -16 _{3,14} A)	205501.70	98.96	1.28E-04	2.50	0.19	3.42	0.43	0.077	0.007
60003	HCOOCH ₃ (18 _{2,17} -17 _{2,16} A)	205663.74	98.96	1.28E-04	2.24	0.52	3.00	1.30	0.081	0.030
60003	HCOOCH ₃ (18 _{2,17} -17 _{1,16} E)	205669.41	98.94	1.28E-04	2.41	0.19	2.88	0.44	0.075	0.010
60003	HCOOCH ₃ (18 _{1,17} -17 _{1,16} A)	206247.92	92.59	1.24E-04	2.24	0.19	3.78	0.47	0.059	0.006
60003	HCOOCH ₃ (16 _{4,12} -15 _{4,11} E)	206619.48	89.25	1.28E-04	2.37	0.11	2.24	0.20	0.081	0.007
60003	HCOOCH ₃ (16 _{3,13} -15 _{3,12} A)	206719.92	95.26	1.28E-04	2.87	0.09	3.90	0.25	0.075	0.004
60003	HCOOCH ₃ (17 _{2,15} -16 _{2,14} A)	209918.52	101.43	1.31E-04	1.94	0.49	3.73	1.32	0.078	0.021
60003	HCOOCH ₃ (17 _{4,14} -16 _{4,13} E)	210434.51	123.02	1.16E-04	2.85	0.34	2.74	0.57	0.047	0.009
60003	HCOOCH ₃ (17 _{7,10} -16 _{7,9} E)	210442.75	123.01	1.17E-04	2.58	0.14	4.08	0.33	0.056	0.004
60003	HCOOCH ₃ (17 _{7,11} -16 _{7,10} A)	210451.40	123.01	1.16E-04	2.12	0.14	4.11	0.33	0.052	0.004
60003	HCOOCH ₃ (17 _{2,15} -16 _{2,14} E)	210463.20	123.01	1.17E-04	2.56	0.25	3.83	0.61	0.049	0.006
60003	HCOOCH ₃ (17 _{6,12} -16 _{6,11} E)	211266.10	114.57	1.21E-04	2.31	0.19	4.09	0.46	0.048	0.005
60003	HCOOCH ₃ (17 _{6,11} -16 _{6,10} A)	211575.13	114.59	1.25E-04	1.95	0.55	3.00	1.34	0.078	0.029
60003	HCOOCH ₃ (17 _{5,13} -16 _{5,12} E)	211771.08	107.49	1.30E-04	1.97	0.39	3.50	1.03	0.076	0.016
60003	HCOOCH ₃ (17 _{7,11} -16 _{7,10} E)	211874.86	107.48	1.31E-04	2.84	0.59	3.43	1.29	0.052	0.004
60003	HCOOCH ₃ (17 _{4,14} -16 _{4,13} A)	214652.63	107.81	1.36E-04	2.05	0.33	4.06	0.86	0.085	0.014
60003	HCOOCH ₃ (17 _{6,11} -16 _{7,10} A)	214792.55	105.86	1.44E-04	2.20	0.44	3.00	1.08	0.138	0.041
60003	HCOOCH ₃ (18 _{2,16} -17 _{2,15} E)	216830.20	105.68	1.48E-04	2.13	0.51	4.26	1.46	0.057	0.011
60003	HCOOCH ₃ (17 _{5,13} -16 _{5,12} A)	216838.89	105.67	1.48E-04	2.57	0.25	3.37	0.59	0.062	0.008
60003	HCOOCH ₃ (17 _{3,14} -16 _{3,13} E)	218280.90	99.73	1.51E-04	2.66	0.13	4.47	0.36	0.086	0.005
60003	HCOOCH ₃ (17 _{3,14} -16 _{3,13} A)	218297.89	99.72	1.51E-04	2.46	0.09	4.18	0.23	0.091	0.004
60003	HCOOCH ₃ (17 _{4,13} -16 _{4,12} E)	220166.89	103.15	1.52E-04	3.00	0.22	3.31	0.52	0.058	0.008
60003	HCOOCH ₃ (17 _{4,13} -16 _{4,12} A)	220190.29	103.15	1.52E-04	1.54	0.23	3.39	0.60	0.065	0.010
60003	HCOOCH ₃ (18 _{2,16} -17 _{2,15} A)	222657.32	37.86	1.58E-05	2.31	0.41	3.00	0.95	0.032	0.009
60003	HCOOCH ₃ (18 _{5,3} -7 _{4,3} E)	224609.38	125.37	1.52E-04	2.18	0.18	2.93	0.45	0.071	0.009
60003	HCOOCH ₃ (18 _{6,12} -17 _{6,11} A)	224615.04	116.70	1.67E-04	2.69	0.22	3.38	0.58	0.088	0.011
60003	HCOOCH ₃ (19 _{3,17} -18 _{3,16} E)	225608.82	116.70	1.67E-04	2.69	0.22	3.38	0.58	0.088	0.011
60003	HCOOCH ₃ (17 _{4,13} -16 _{4,12} A)	226713.06	120.22	1.72E-04	2.45	0.37	4.00	0.96	0.147	0.027
60003	HCOOCH ₃ (18 _{4,15} -17 _{4,14} E)	226718.69	120.21	1.72E-04	2.23	0.21	3.07	0.53	0.130	0.019
60003	HCOOCH ₃ (18 _{5,3} -7 _{4,3} E)	228628.88	118.79	1.66E-04	2.60	0.30	2.86	0.79	0.093	0.011
60003	HCOOCH ₃ (18 _{6,12} -17 _{6,11} A)	228651.40	118.78	1.66E-04	2.33	0.22	2.57	0.50	0.111	0.019
60003	HCOOCH ₃ (18 _{3,17} -17 _{3,16} E)	229405.02	110.74	1.75E-04	1.96	0.22	3.11	0.47	0.083	0.011
60003	HCOOCH ₃ (18 _{3,15} -17 _{3,14} E)	235844.54	145.04	1.71E-04	2.25	0.11	2.28	0.28	0.076	0.008

Table 4. Continued.

TAG	Species & Transition	Frequency (MHz)	Eup (K)	A _{ij} s ⁻¹	V _O (km s ⁻¹)	δ_{V_O} (km s ⁻¹)	FWHM (km s ⁻¹)	δ_{FWHM} (km s ⁻¹)	Int δ_{Int} (K)	Flux (K km s ⁻¹)	δ_{Flux} (K km s ⁻¹)	comments
60003	HCOOCH ₃ (19, ₁₃ -18 _{7,12} E)	235865.97	145.04	1.67E-04	2.24	0.42	3.00	1.17	0.049	0.012	0.27	0.06
60003	HCOOCH ₃ (21, _{1,20} -20, _{1,19} E)	237344.87	131.61	1.98E-04	2.25	0.19	4.44	0.53	0.093	0.007	0.77	0.14
60003	HCOOCH ₃ (21, _{1,20} -20, _{1,19} A)	237350.39	131.60	1.98E-04	2.23	0.60	3.89	1.33	0.085	0.010	0.62	0.11
60003	HCOOCH ₃ (21, _{2,20} -20, _{1,19} E)	237393.21	131.61	2.69E-05	2.53	0.27	3.81	0.69	0.052	0.008	0.37	0.08
60003	HCOOCH ₃ (19, _{3,16} -18 _{3,15} A)	240034.67	122.25	2.01E-04	2.11	0.19	3.54	0.52	0.097	0.010	0.65	0.12
60003	HCOOCH ₃ (20, _{5,16} -19 _{5,15} E)	249031.00	141.57	2.18E-04	1.86	0.15	3.83	0.40	0.051	0.004	0.38	0.07
60003	HCOOCH ₃ (20, _{3,17} -19 _{3,16} A)	250258.38	134.26	2.28E-04	1.97	0.57	4.00	1.58	0.060	0.016	0.47	0.09
60003	HCOOCH ₃ (20, _{5,15} -19 _{5,14} E)	257226.61	142.79	2.42E-04	2.67	0.34	3.50	0.92	0.055	0.011	0.39	0.08
60003	HCOOCH ₃ (20, _{4,16} -19 _{4,15} E)	259499.90	138.67	2.54E-04	2.30	0.14	4.68	0.37	0.105	0.004	1.00	0.18
60003	HCOOCH ₃ (20, _{4,16} -19 _{4,15} A)	259521.81	138.67	2.54E-04	2.07	0.14	3.56	0.38	0.084	0.006	0.61	0.12
60003	HCOOCH ₃ (8, _{7,1} -7 _{6,1} E)	278094.52	53.78	4.39E-05	2.21	0.17	3.28	0.45	0.048	0.005	0.35	0.09
60003	HCOOCH ₃ (13, ₆ -12 _{6,6} E)	339152.69	86.26	5.21E-05	2.66	0.13	1.37	0.30	0.052	0.010	0.14	0.03
60003	HCOOCH ₃ (13, _{7,7} -12 _{6,6} A)	339185.91	86.24	5.22E-05	2.64	0.31	1.81	0.80	0.030	0.010	0.10	0.02
44505	SiO (2-1)	86846.96	6.25	2.93E-05	4.87	0.14	4.57	0.32	0.358	0.021	2.07	0.23
44505	SiO (3-2)	130268.61	12.50	1.06E-04	4.34	0.08	4.62	0.19	0.224	0.009	5.38	0.86
44505	SiO (4-3)	173688.31	20.84	2.60E-04	4.97	0.13	6.05	0.32	0.623	0.035	5.98	1.02
44505	SiO (5-4)	217104.98	31.26	5.20E-04	4.39	0.11	5.99	0.27	0.810	0.030	8.49	1.44
44505	SiO (6-5)	260518.02	43.76	9.12E-04	4.06	0.10	6.38	0.23	0.813	0.017	18.60	3.16
44505	SiO (8-7)	347330.58	75.02	2.20E-03	3.79	0.10	5.79	0.23	0.825	0.025	9.23	1.66
27002	HNC (1-0)	90663.59	4.35	2.69E-05	4.30	0.30	3.54	0.74	1.624	0.277	7.47	0.82
27002	HNC (3-2)	271981.14	26.11	9.34E-04	3.90	0.07	3.31	0.17	2.262	0.099	16.19	2.75
27002	HNC (4-3)	362630.30	43.51	2.30E-03	3.20	0.12	1.57	0.27	2.741	0.413	8.48	1.53
28508	DNC (2-1)	152609.77	10.99	1.54E-04	4.30	0.03	1.63	0.09	1.233	0.050	2.94	0.50
28508	DNC (3-2)	228910.49	21.97	5.57E-04	4.32	0.04	3.31	0.10	0.333	0.006	2.00	0.34
28005	H ¹³ C (1-0)	87090.85	4.18	1.87E-05	4.41	0.09	1.83	0.22	0.443	0.045	1.05	0.12
28005	H ¹³ C (2-1)	174179.41	12.54	1.79E-04	4.10	0.18	2.26	0.50	0.339	0.053	1.18	0.20
28005	H ¹³ C (3-2)	261263.31	25.08	6.48E-04	3.27	0.40	5.69	1.39	0.158	0.017	1.85	0.32
28005	H ¹³ C (4-3)	348340.27	41.80	1.59E-03	3.19	0.45	3.96	1.50	0.099	0.019	0.76	0.14
51501	HC ₃ N (9-8)	81881.47	19.65	4.21E-05	3.94	0.02	2.16	0.04	0.889	0.015	2.46	0.27
51501	HC ₃ N (10-9)	90979.02	24.02	5.81E-05	3.95	0.02	2.11	0.04	0.845	0.015	2.31	0.25
51501	HC ₃ N (11-10)	100076.39	28.82	7.77E-05	3.95	0.02	2.21	0.06	0.751	0.017	2.19	0.24
51501	HC ₃ N (12-11)	109173.63	34.06	1.01E-04	3.87	0.03	2.35	0.06	0.296	0.006	0.93	0.11
51501	HC ₃ N (15-14)	136464.41	52.40	1.99E-04	3.94	0.07	3.01	0.17	0.464	0.022	1.97	0.34
51501	HC ₃ N (16-15)	145560.96	59.38	2.42E-04	3.62	0.06	2.87	0.13	0.415	0.017	1.72	0.29
51501	HC ₃ N (17-16)	154657.28	66.80	2.91E-04	3.88	0.10	3.43	0.24	0.329	0.020	1.66	0.28
51501	HC ₃ N (18-17)	163753.39	74.66	3.46E-04	3.86	0.11	3.80	0.25	0.377	0.022	2.15	0.37
51501	HC ₃ N (19-18)	172849.30	82.96	4.08E-04	3.59	0.20	5.41	0.47	0.284	0.021	2.36	0.40
51501	HC ₃ N (22-21)	200135.39	110.46	6.35E-04	3.21	0.14	6.15	0.34	0.161	0.008	1.64	0.28
51501	HC ₃ N (23-22)	209230.23	120.51	7.26E-04	3.43	0.18	6.84	0.42	0.186	0.010	2.16	0.37
51501	HC ₃ N (24-23)	218324.72	130.98	8.26E-04	3.30	0.20	6.29	0.48	0.207	0.014	2.28	0.39
51501	HC ₃ N (25-24)	227418.90	141.90	9.35E-04	3.36	0.07	6.20	0.17	0.206	0.005	2.30	0.39
51501	HC ₃ N (26-25)	236512.79	153.25	1.05E-03	3.42	0.10	6.18	0.23	0.198	0.006	2.29	0.39
51501	HC ₃ N (27-26)	245606.32	165.04	1.18E-03	2.64	0.27	6.27	0.63	0.068	0.006	0.82	0.14
51501	HC ₃ N (29-28)	263792.31	189.92	1.46E-03	2.51	0.14	7.57	0.33	0.297	0.011	4.69	0.80
51501	HC ₃ N (30-29)	272884.75	203.02	1.62E-03	3.54	0.42	6.58	1.00	0.100	0.013	1.43	0.26
52005	DC ₃ N (10 ₁₁ -9 ₁₀)	84429.83	22.29	4.63E-05	4.08	0.27	2.68	0.73	0.052	0.009	0.18	0.03

Table 4. Continued.

TAG	Species & Transition	Frequency (MHz)	Eup (K)	A _{ij} s ⁻¹	V _O δ _{ν_o} (km s ⁻¹)	FWHM δ _{FWM} (km s ⁻¹)	Int δ _{int} (K)	Flux δ _{Flux} (K km s ⁻¹)	comments
52005	DC ₃ N (11 ₁₂ -10 ₁₁)	92872.39	26.74	6.19E-05	4.55	0.15	2.04	0.37	0.053
52005	DC ₃ N (12 ₁₃ -11 ₁₂)	101314.83	31.61	8.06E-05	4.27	0.14	2.43	0.39	0.041
52005	DC ₃ N (13 ₁₄ -12 ₁₃)	109757.14	36.87	1.03E-04	4.02	0.43	2.60	1.16	0.071
52005	DC ₃ N (17 ₁₈ -16 ₁₇)	143524.87	62.00	2.32E-04	4.24	0.28	2.60	0.66	0.061
52005	DC ₃ N (19 ₂₀ -18 ₁₉)	160407.68	76.99	3.25E-04	4.57	0.27	3.29	0.76	0.024
34502	H ₂ S (1 _{1,0} -1 _{0,1})	168762.76	27.88	2.68E-05	3.92	0.19	4.84	0.45	2.420
34502	H ₂ S (2 _{2,0} -2 _{1,1})	216710.44	83.98	4.87E-05	3.18	0.06	4.95	0.15	0.862
35001	HDS(1 _{0,1} -0 _{0,0})	244555.58	11.74	1.25E-05	3.44	0.44	3.89	1.19	0.058
35001	HDS(2 _{0,2} -1 _{1,1})	332378.71	34.67	6.00E-05	2.66	0.13	0.93	0.36	0.146
38082	o-c-C ₃ H ₂ (3 _{1,2} -3 _{0,3})	82966.20	13.70	1.09E-05	4.16	0.06	2.01	0.13	0.184
38082	o-c-C ₃ H ₂ (2 _{1,2} -1 _{0,1})	85338.89	4.10	2.55E-05	4.21	0.02	1.98	0.04	0.625
38082	o-c-C ₃ H ₂ (4 _{3,2} -4 _{2,3})	85656.43	26.72	1.67E-05	4.28	0.10	2.21	0.23	0.079
38082	o-c-C ₃ H ₂ (3 _{1,2} -2 _{2,1})	145089.60	13.70	7.43E-05	4.10	0.04	1.66	0.10	0.566
38082	o-c-C ₃ H ₂ (4 _{1,4} -3 _{0,3})	150851.91	16.96	1.80E-04	4.38	0.04	1.92	0.09	0.956
38082	o-c-C ₃ H ₂ (3 _{3,0} -2 _{2,1})	216278.76	17.12	2.81E-04	4.36	0.11	2.86	0.41	0.183
38082	o-c-C ₃ H ₂ (5 _{1,4} -4 _{2,3})	217940.05	33.07	4.42E-04	4.12	0.08	2.47	0.21	0.223
38082	o-c-C ₃ H ₂ (4 _{3,2} -3 _{2,1})	227169.13	26.72	3.42E-04	4.24	0.19	3.33	0.46	0.180
38082	o-c-C ₃ H ₂ (3 _{2,1} -2 _{1,2})	244222.13	15.82	6.48E-05	4.49	0.12	3.25	0.30	0.088
38082	o-c-C ₃ H ₂ (5 _{2,3} -4 _{3,2})	249054.37	38.67	4.57E-04	3.49	0.35	4.10	0.86	0.052
38082	o-c-C ₃ H ₂ (7 _{0,7} -6 _{1,6})	251314.34	48.32	9.34E-04	3.92	0.09	3.24	0.21	0.289
38082	o-c-C ₃ H ₂ (6 _{2,5} -5 _{1,4})	251527.30	45.14	7.41E-04	3.95	0.18	2.99	0.45	0.154
38082	o-c-C ₃ H ₂ (4 _{4,1} -3 _{3,0})	265759.44	29.87	7.98E-04	3.90	0.17	3.02	0.43	0.126
38082	o-c-C ₃ H ₂ (5 _{5,0} -4 _{4,1})	349263.98	46.63	1.81E-03	3.75	0.27	3.15	0.68	0.113
38092	p-c-C ₃ H ₂ (4 _{2,2} -4 _{1,3})	80723.17	28.82	1.46E-05	4.01	0.27	3.98	0.67	0.032
38092	p-c-C ₃ H ₂ (2 _{0,2} -1 _{1,1})	82093.56	6.43	2.07E-05	4.30	0.02	1.82	0.08	0.287
38092	p-c-C ₃ H ₂ (3 _{2,2} -3 _{1,3})	84727.70	16.14	1.14E-05	4.31	0.06	1.93	0.15	0.074
38092	p-c-C ₃ H ₂ (2 _{2,0} -1 _{1,1})	150436.55	9.71	5.88E-05	4.23	0.05	1.37	0.12	0.193
38092	p-c-C ₃ H ₂ (4 _{0,4} -3 _{1,3})	150820.67	19.31	1.80E-04	4.38	0.03	1.64	0.08	0.407
38092	p-c-C ₃ H ₂ (3 _{2,2} -2 _{1,1})	155518.30	16.14	1.22E-04	4.28	0.06	1.63	0.14	0.282
38092	p-c-C ₃ H ₂ (4 _{2,2} -3 _{3,1})	204788.93	28.82	1.36E-04	4.84	0.10	2.06	0.18	0.077
38092	p-c-C ₃ H ₂ (5 _{2,4} -4 _{1,3})	218160.44	35.42	4.44E-04	4.13	0.30	4.96	0.87	0.094
38092	p-c-C ₃ H ₂ (6 _{1,5} -5 _{2,4})	251508.69	47.49	7.41E-04	3.91	0.16	3.70	0.40	0.055
39003	c-C ₃ HD (4 _{0,4} -3 _{1,3})	135640.90	17.39	1.09E-04	4.26	0.09	1.48	0.21	0.144
39003	c-C ₃ HD (4 _{1,4} -3 _{0,3})	136370.91	17.39	1.11E-04	4.39	0.06	1.18	0.16	0.172
39003	c-C ₃ HD (5 _{0,5} -4 _{1,4})	166112.36	25.37	2.13E-04	4.56	0.15	1.18	0.34	0.088
39003	c-C ₃ HD (5 _{1,5} -4 _{0,4})	166250.12	25.37	2.13E-04	4.10	0.08	2.66	0.19	0.084
39003	c-C ₃ HD (4 _{2,3} -3 _{1,2})	173911.59	22.49	1.52E-04	4.90	0.18	3.03	0.44	0.087
46008	CH ₃ OCH ₃ (1 _{1,1,0} -1 _{1,0,11} AA)	82460.38	62.92	2.16E-06	1.76	0.29	3.55	0.77	0.022
46008	CH ₃ OCH ₃ (4 _{2,2} -4 _{1,3} EE)	82688.77	14.74	2.31E-06	2.92	0.25	2.10	0.59	0.021
46008	CH ₃ OCH ₃ (1 _{4,2,12} -1 _{4,1,13} EE)	83098.92	102.85	3.50E-06	2.18	0.21	3.66	0.58	0.039
46008	CH ₃ OCH ₃ (3 _{2,1} -3 _{1,2} EE)	84634.90	11.09	2.18E-06	2.58	0.12	2.75	0.32	0.032
46008	CH ₃ OCH ₃ (1 _{5,2,13} -1 _{5,1,14} AA)	88709.07	116.86	4.09E-06	2.02	0.26	2.99	0.75	0.024
46008	CH ₃ OCH ₃ (3 _{2,2} -3 _{1,3} EE)	91476.53	11.08	2.45E-06	1.86	0.28	2.23	0.64	0.020
46008	CH ₃ OCH ₃ (1 _{2,1,11} -1 _{2,0,12} EE)	93666.43	74.02	2.84E-06	2.50	0.39	2.23	0.95	0.046
46008	CH ₃ OCH ₃ (1 _{2,1,11} -1 _{2,0,12} AA)	93668.35	74.02	2.84E-06	2.16	0.21	2.36	0.57	0.025
46008	CH ₃ OCH ₃ (1 _{6,2,14} -1 _{6,1,15} EE)	95731.26	131.80	4.88E-06	2.32	0.42	1.12	0.052	0.018

Table 4. Continued.

TAG	Species & Transition	Frequency (MHz)	Eup (K)	Aij s ⁻¹	V _O δ _{v_o} (km s ⁻¹)	FWHM δ _{FWM} (km s ⁻¹)	Int δ _{int} (K)	Flux δ _{Flux} (K km s ⁻¹)	comments
46008	CH ₃ OCH ₃ (5 _{2,4} -5 _{1,5} EE)	96849.85	19.26	3.12E-06	2.13	0.17	4.12	0.48	0.039
46008	CH ₃ OCH ₃ (5 _{2,4} -5 _{1,5} AA)	96852.46	19.26	3.12E-06	3.04	0.20	1.72	0.41	0.021
46008	CH ₃ OCH ₃ (6 _{2,5} -6 _{1,6} EE)	100463.04	24.71	3.46E-06	2.50	0.22	3.13	0.54	0.040
46008	CH ₃ OCH ₃ (6 _{2,5} -6 _{1,6} AA)	100465.70	24.71	3.46E-06	3.06	0.23	2.22	0.57	0.035
46008	CH ₃ OCH ₃ (8 _{2,7} -8 _{1,8} AA)	109576.78	38.31	4.27E-06	2.39	0.31	2.35	0.75	0.045
46008	CH ₃ OCH ₃ (18 _{3,15} -18 _{2,16} EE)	111813.67	169.80	8.41E-06	2.13	0.39	2.47	1.05	0.037
46008	CH ₃ OCH ₃ (9 _{2,8} -9 _{1,9} EE)	115074.91	46.46	4.78E-06	2.14	0.30	3.46	0.86	0.049
46008	CH ₃ OCH ₃ (16 _{3,13} -16 _{2,14} EE)	115293.58	137.33	8.58E-06	2.53	0.07	2.77	0.20	0.059
46008	CH ₃ OCH ₃ (16 _{3,13} -16 _{2,14} AA)	115295.58	137.33	8.58E-06	2.31	0.14	2.45	0.42	0.027
46008	CH ₃ OCH ₃ (12 _{3,9} -12 _{2,10} EE)	129558.98	83.88	1.00E-05	2.53	0.24	2.85	0.63	0.062
46008	CH ₃ OCH ₃ (12 _{3,9} -12 _{2,10} AA)	129561.82	83.88	1.00E-05	2.76	0.28	2.54	0.67	0.038
46008	CH ₃ OCH ₃ (15 _{1,14} -15 _{0,15} AA)	131912.06	112.60	6.02E-06	1.84	0.13	3.01	0.38	0.039
46008	CH ₃ OCH ₃ (11 _{3,8} -11 _{2,9} EE)	133268.32	72.88	1.04E-05	2.74	0.20	3.08	0.68	0.051
46008	CH ₃ OCH ₃ (11 _{3,8} -11 _{2,9} AA)	133271.31	72.88	1.04E-05	2.29	0.34	2.07	0.95	0.054
46008	CH ₃ OCH ₃ (9 _{3,6} -9 _{2,7} EE)	139503.68	53.67	1.10E-05	2.34	0.12	3.05	0.31	0.090
46008	CH ₃ OCH ₃ (8 _{3,5} -8 _{2,6} EE)	141832.26	45.45	1.11E-05	2.34	0.14	2.94	0.42	0.076
46008	CH ₃ OCH ₃ (13 _{2,12} -13 _{1,13} EE)	143162.99	88.00	7.75E-06	2.55	0.39	3.13	1.10	0.095
46008	CH ₃ OCH ₃ (13 _{2,12} -13 _{1,13} AA)	143166.02	88.00	7.74E-06	2.65	0.14	2.10	0.45	0.072
46008	CH ₃ OCH ₃ (7 _{3,4} -7 _{2,5} EE)	143602.99	38.15	1.10E-05	2.50	0.15	2.39	0.40	0.093
46008	CH ₃ OCH ₃ (6 _{3,3} -6 _{2,4} EE)	144858.98	31.77	1.06E-05	2.51	0.28	3.09	0.90	0.071
46008	CH ₃ OCH ₃ (6 _{3,3} -6 _{2,4} AA)	144862.02	31.77	1.07E-05	2.60	0.06	2.24	0.16	0.063
46008	CH ₃ OCH ₃ (5 _{3,2} -5 _{2,3} AA)	145682.64	26.31	1.01E-05	3.16	0.29	2.32	0.52	0.056
46008	CH ₃ OCH ₃ (3 _{3,1} -3 _{2,1} EE)	146405.19	18.12	2.79E-06	2.98	0.09	1.11	0.29	0.040
46008	CH ₃ OCH ₃ (3 _{2,1} -2 _{1,2} EE)	146704.72	11.09	1.10E-05	2.55	0.09	2.56	0.24	0.196
46008	CH ₃ OCH ₃ (3 _{2,1} -2 _{1,2} AA)	146707.17	11.09	1.10E-05	2.54	0.17	2.18	0.42	0.079
46008	CH ₃ OCH ₃ (5 _{3,3} -5 _{2,4} EA)	146865.98	26.31	8.65E-06	2.73	0.15	1.40	0.38	0.053
46008	CH ₃ OCH ₃ (6 _{3,2} -5 _{2,3} AA)	146872.55	26.31	9.66E-06	2.45	0.28	2.37	0.70	0.086
46008	CH ₃ OCH ₃ (3 _{3,1} -3 _{2,1} AA)	146877.31	26.31	1.03E-05	2.32	0.38	3.00	1.05	0.030
46008	CH ₃ OCH ₃ (5 _{3,3} -5 _{2,4} AA)	147202.09	31.77	1.08E-05	3.01	0.09	2.03	0.24	0.067
46008	CH ₃ OCH ₃ (6 _{3,4} -6 _{2,5} EA)	147203.76	31.77	1.11E-05	2.84	0.20	1.41	0.51	0.081
46008	CH ₃ OCH ₃ (6 _{3,4} -6 _{2,5} AE)	148503.83	45.44	1.24E-05	2.82	0.30	3.27	0.63	0.051
46008	CH ₃ OCH ₃ (6 _{3,4} -6 _{2,5} EE)	149569.78	53.64	1.29E-05	2.51	0.17	2.43	0.40	0.084
46008	CH ₃ OCH ₃ (7 _{3,4} -7 _{2,5} AA)	149573.12	53.64	1.29E-05	2.47	0.22	3.02	0.58	0.047
46008	CH ₃ OCH ₃ (8 _{3,6} -8 _{2,7} EE)	149595.39	62.75	1.35E-05	2.47	0.15	2.53	0.40	0.095
46008	CH ₃ OCH ₃ (10 _{3,8} -10 _{2,9} AA)	149598.65	62.75	1.35E-05	2.28	0.16	2.08	0.39	0.080
46008	CH ₃ OCH ₃ (10 _{3,8} -10 _{2,9} AA)	151593.92	100.61	8.77E-06	2.35	0.11	1.36	0.25	0.051
46008	CH ₃ OCH ₃ (14 _{2,13} -14 _{1,14} EE)	151595.08	62.92	8.02E-06	2.53	0.17	2.34	0.54	0.078
46008	CH ₃ OCH ₃ (11 _{3,9} -11 _{2,10} EE)	152831.37	72.78	1.41E-05	2.78	0.19	2.84	0.66	0.049
46008	CH ₃ OCH ₃ (11 _{3,9} -11 _{2,10} AA)	152834.55	72.78	1.41E-05	2.80	0.34	2.60	0.90	0.039
46008	CH ₃ OCH ₃ (11 _{1,10} -10 _{2,9} AA)	154453.66	62.92	8.02E-06	2.37	0.12	1.32	0.30	0.057
46008	CH ₃ OCH ₃ (11 _{1,10} -10 _{2,9} EE)	154455.08	62.92	8.02E-06	2.53	0.17	2.34	0.54	0.078
46008	CH ₃ OCH ₃ (12 _{3,10} -12 _{2,11} EE)	155128.43	83.73	1.48E-05	2.40	0.07	2.84	0.19	0.097
46008	CH ₃ OCH ₃ (12 _{3,10} -12 _{2,11} AA)	155131.54	83.73	1.48E-05	2.49	0.20	2.39	0.55	0.080
46008	CH ₃ OCH ₃ (13 _{3,11} -13 _{2,12} EE)	157932.36	95.58	1.56E-05	2.42	0.24	2.38	0.60	0.108
46008	CH ₃ OCH ₃ (17 _{1,16} -17 _{0,17} EE)	159320.27	142.66	9.18E-06	2.49	0.08	1.30	0.20	0.089
46008	CH ₃ OCH ₃ (17 _{1,16} -17 _{0,17} AA)	159323.26	142.66	9.18E-06	2.62	0.05	1.17	0.10	0.040

Table 4. Continued.

TAG	Species & Transition	Frequency (MHz)	Eup (K)	A _{ij} s ⁻¹	V _O δ _{ν_o} (km s ⁻¹)	FWHM δ _{FWM} (km s ⁻¹)	Int δ _{Int} (K)	Flux δ _{Flux} (K km s ⁻¹)	comments
46008	CH ₃ OCH ₃ (4 _{2,3} -3 _{1,2} EE)	160204.08	14.72	1.34E-05	2.60	0.17	2.05	0.42	0.089
46008	CH ₃ OCH ₃ (4 _{2,3} -3 _{1,2} AA)	160206.57	14.72	1.35E-05	2.57	0.12	1.18	0.31	0.076
46008	CH ₃ OCH ₃ (1 _{5,14} -1 _{5,15} EE)	160521.55	114.10	9.92E-06	2.19	0.30	2.42	0.77	0.053
46008	CH ₃ OCH ₃ (1 _{4,12} -1 _{4,13} EE)	161282.72	108.35	1.65E-05	2.86	0.21	2.55	0.73	0.086
46008	CH ₃ OCH ₃ (1 _{4,12} -1 _{4,13} AA)	161285.67	108.35	1.65E-05	2.68	0.14	2.14	0.34	0.070
46008	CH ₃ OCH ₃ (1 _{8,15} -1 _{7,14} AA)	162277.21	169.80	5.05E-06	2.40	0.17	1.81	0.44	0.035
46008	CH ₃ OCH ₃ (1 _{8,15} -1 _{7,14} EE)	162279.58	169.80	5.05E-06	2.38	0.19	1.28	0.44	0.057
46008	CH ₃ OCH ₃ (4 _{2,2} -3 _{1,3} EE)	167743.99	14.74	1.36E-05	2.86	0.25	2.12	0.91	0.078
46008	CH ₃ OCH ₃ (4 _{2,2} -3 _{1,3} AA)	167746.53	14.74	1.36E-05	2.55	0.07	1.16	0.16	0.083
46008	CH ₃ OCH ₃ (1 _{6,14} -1 _{6,15} EE)	169743.49	136.61	1.88E-05	2.37	0.17	2.33	0.52	0.087
46008	CH ₃ OCH ₃ (1 _{6,2,15} -1 _{6,1,16} AA)	169907.05	128.46	1.12E-05	2.94	0.16	1.77	0.40	0.061
46008	CH ₃ OCH ₃ (1 _{8,1,17} -1 _{8,0,18} EE)	173084.04	158.96	1.11E-05	3.27	0.20	2.37	0.55	0.070
46008	CH ₃ OCH ₃ (1 _{7,3,15} -1 _{7,2,16} AA)	174896.05	152.09	2.02E-05	3.05	0.21	1.71	0.56	0.064
46008	CH ₃ OCH ₃ (5 _{2,4} -4 _{1,3} EE)	176801.27	19.26	1.67E-05	2.61	0.08	1.96	0.25	0.092
46008	CH ₃ OCH ₃ (9 _{4,6} -9 _{3,7} EE)	204736.58	63.46	7.78E-05	2.33	0.12	2.96	0.30	0.086
46008	CH ₃ OCH ₃ (8 _{4,5} -8 _{3,6} EA)	204832.63	55.27	1.92E-05	2.48	0.17	2.58	0.36	0.037
46008	CH ₃ OCH ₃ (10 _{3,8} -9 _{2,7} EE)	322885.65	62.75	9.35E-05	2.43	0.25	2.08	0.69	0.155
46008	CH ₃ OCH ₃ (10 _{3,8} -9 _{2,7} AA)	322885.97	62.75	9.35E-05	2.69	0.06	1.35	0.16	0.151
46008	CH ₃ OCH ₃ (10 _{3,7} -9 _{2,8} EE)	340612.58	62.81	9.76E-05	2.58	0.03	1.87	0.08	0.159
46008	CH ₃ OCH ₃ (10 _{3,7} -9 _{2,8} AA)	340615.91	62.81	9.76E-05	2.72	0.14	1.18	0.35	0.136
46008	CH ₃ OCH ₃ (11 _{2,9} -10 _{1,10} EE)	349806.09	66.48	3.30E-05	2.49	0.05	1.14	0.11	0.093
46008	CH ₃ OCH ₃ (11 _{2,9} -10 _{1,10} AA)	349809.18	66.48	3.30E-05	2.42	0.05	1.32	0.13	0.077
46008	CH ₃ OCH ₃ (12 _{3,10} -11 _{2,9} EE)	359384.62	83.73	1.13E-04	2.57	0.05	1.26	0.12	0.225
46008	CH ₃ OCH ₃ (12 _{3,10} -11 _{2,9} AA)	359387.66	83.73	1.13E-04	2.79	0.17	1.46	0.42	0.145
46008	CH ₃ OCH ₃ (11 _{3,8} -10 _{2,9} EE)	361874.42	72.88	1.08E-04	2.68	0.18	1.28	0.49	0.196
40502	CH ₃ CCH (5 ₂ -4 ₂)	85450.77	41.21	1.70E-06	3.63	0.10	2.90	0.23	0.049
40502	CH ₃ CCH (5 ₁ -4 ₁)	85455.67	19.53	1.95E-06	3.67	0.04	2.29	0.10	0.140
40502	CH ₃ CCH (5 ₀ -4 ₀)	85457.30	12.30	2.03E-06	3.73	0.04	2.20	0.09	0.181
40502	CH ₃ CCH (6 ₂ -5 ₂)	102540.15	46.13	3.16E-06	3.96	0.05	2.62	0.11	0.087
40502	CH ₃ CCH (6 ₁ -5 ₁)	102546.02	24.45	3.46E-06	3.84	0.02	2.46	0.04	0.198
40502	CH ₃ CCH (6 ₀ -5 ₀)	102547.98	17.23	3.56E-06	3.93	0.04	2.41	0.08	0.235
40502	CH ₃ CCH (8 ₃ -7 ₃)	136704.50	94.56	7.39E-06	3.77	0.12	3.66	0.31	0.085
40502	CH ₃ CCH (8 ₂ -7 ₂)	136717.56	58.43	8.06E-06	3.93	0.16	3.70	0.45	0.100
40502	CH ₃ CCH (8 ₁ -7 ₁)	136725.40	36.76	8.47E-06	3.78	0.04	2.77	0.09	0.226
40502	CH ₃ CCH (8 ₀ -7 ₀)	136728.01	29.53	8.60E-06	3.78	0.15	2.46	0.36	0.287
40502	CH ₃ CCH (9 ₃ -8 ₃)	153790.77	101.94	1.10E-05	3.80	0.08	2.53	0.21	0.081
40502	CH ₃ CCH (9 ₂ -8 ₂)	153805.46	65.82	1.17E-05	3.53	0.10	2.27	0.25	0.110
40502	CH ₃ CCH (9 ₁ -8 ₁)	153814.28	44.14	1.22E-05	3.71	0.03	2.77	0.09	0.209
40502	CH ₃ CCH (9 ₀ -8 ₀)	153817.21	36.91	1.23E-05	3.67	0.10	2.51	0.24	0.276
40502	CH ₃ CCH (10 ₂ -9 ₂)	170892.73	74.02	1.63E-05	3.96	0.22	3.50	0.57	0.123
40502	CH ₃ CCH (10 ₁ -9 ₁)	170902.52	52.34	1.68E-05	3.73	0.10	3.01	0.26	0.247
40502	CH ₃ CCH (10 ₀ -9 ₀)	170905.78	45.11	1.70E-05	3.94	0.05	3.23	0.12	0.301
40502	CH ₃ CCH (12 ₁ -11 ₁)	205076.82	71.20	2.94E-05	3.59	0.29	3.94	0.71	0.149
40502	CH ₃ CCH (13 ₃ -12 ₃)	222128.82	139.66	3.57E-05	3.37	0.24	4.06	0.61	0.085
40502	CH ₃ CCH (13 ₂ -12 ₂)	222150.01	103.54	3.69E-05	3.49	0.19	3.46	0.45	0.096
40502	CH ₃ CCH (13 ₁ -12 ₁)	222162.73	81.87	3.75E-05	3.20	0.23	3.31	0.59	0.121
40502	CH ₃ CCH (13 ₀ -12 ₀)	222166.97	74.64	3.78E-05	3.25	0.13	3.22	0.33	0.012

Table 4. Continued.

TAG	Species & Transition	Frequency (MHz)	Eup (K)	Aij s ⁻¹	V _O (km s ⁻¹)	δ_{V_O} (km s ⁻¹)	FWHM (km s ⁻¹)	δ_{FWHM} (km s ⁻¹)	Int δ_{Int} (K)	Flux (K km s ⁻¹)	δ_{Flux} (K km s ⁻¹)	comments
40502	CH ₃ CCH (14 ₁ -13 ₁)	239247.73	93.35	4.71E-05	3.18	0.15	3.69	0.38	0.088	0.007	0.61	0.11
40502	CH ₃ CCH (14 ₀ -13 ₀)	239252.29	86.12	4.73E-05	2.84	0.21	2.64	0.79	0.100	0.015	0.50	0.09
40502	CH ₃ CCH (16 ₃ -15 ₃)	273372.99	176.56	6.84E-05	3.97	0.28	3.87	0.72	0.081	0.012	0.69	0.13
40502	CH ₃ CCH (16 ₂ -15 ₂)	273399.05	140.45	6.98E-05	2.90	0.09	3.36	0.24	0.059	0.003	0.43	0.09
41502	CH ₂ DCCH (6 _{1,6} -5 _{1,5})	96691.59	21.70	2.90E-06	4.32	0.19	1.49	0.33	0.023	0.005	0.04	0.01
41502	CH ₂ DCCH (6 _{5,5} -5 _{2,4})	97077.80	38.14	2.69E-06	4.68	0.26	2.38	0.68	0.023	0.005	0.07	0.02
41502	CH ₂ DCCH (6 _{0,6} -5 _{0,5})	97080.73	16.31	3.02E-06	4.41	0.24	2.14	0.57	0.023	0.005	0.06	0.02
41502	CH ₂ DCCH (6 _{1,5} -5 _{1,4})	97472.74	21.83	2.97E-06	3.93	0.14	1.72	0.29	0.025	0.004	0.06	0.02
25501	CCH (1 3/2 1 - 0 1/2 1)	87284.16	4.19	2.59E-07	4.00	0.04	1.83	0.11	0.168	0.008	0.40	0.05
25501	CCH (1 3/2 2 - 0 1/2 1)	87316.93	4.19	1.53E-06	3.82	0.03	2.16	0.07	0.598	0.016	1.67	0.18
25501	CCH (1 3/2 1 - 0 1/2 0)	87328.62	4.19	1.27E-06	3.88	0.04	1.99	0.09	0.438	0.017	1.13	0.12
25501	CCH (1 1/2 1 - 0 1/2 1)	87402.00	4.20	1.27E-06	3.83	0.03	2.06	0.07	0.464	0.015	1.24	0.14
25501	CCH (1 1/2 0 - 0 1/2 1)	87407.17	4.20	1.53E-06	3.80	0.01	1.82	0.04	0.287	0.005	0.68	0.08
25501	CCH (1 1/2 1 - 0 1/2 0)	87446.51	4.20	2.61E-07	3.90	0.06	1.79	0.17	0.160	0.012	0.37	0.04
25501	CCH (2 5/2 2 - 1 3/2 2)	174634.91	12.57	1.00E-06	3.95	0.08	2.08	0.19	0.125	0.010	0.40	0.07
25501	CCH (2 5/2 3 - 1 3/2 2)	174663.22	12.58	1.47E-05	3.83	0.15	2.45	0.35	0.823	0.102	3.10	0.53
25501	CCH (2 5/2 2 - 1 3/2 1)	174667.68	12.57	1.36E-05	3.82	0.11	2.20	0.25	0.620	0.062	2.11	0.36
25501	CCH (2 3/2 2 - 1 1/2 1)	174721.78	12.58	1.16E-05	3.79	0.11	2.24	0.25	0.523	0.051	1.81	0.31
25501	CCH (2 3/2 1 - 1 1/2 0)	174728.07	12.58	8.16E-06	3.73	0.11	2.30	0.25	0.252	0.024	0.89	0.15
25501	CCH (2 3/2 2 - 1 3/2 2)	174806.88	12.58	2.67E-06	3.67	0.05	1.94	0.13	0.232	0.013	0.69	0.12
25501	CCH (3 5/2 2 - 2 3/2 2)	262078.93	25.16	6.00E-06	3.73	0.11	2.12	0.19	0.520	0.040	2.30	0.60
26501	CCD (2 5/2 3/2 - 1 3/2 3/2)	144239.71	10.38	1.91E-06	4.98	0.29	3.18	0.77	0.027	0.004	0.12	0.03
26501	CCD (2 3/2 5/2 - 1 1/2 3/2)	144296.72	10.39	6.73E-06	3.87	0.15	2.95	0.38	0.097	0.010	0.41	0.07
26501	CCD (2 3/2 5/2 - 1 3/2 5/2)	144376.68	10.39	1.26E-06	4.48	0.27	2.76	0.89	0.038	0.007	0.15	0.03
26501	CCD (2 3/2 3/2 - 1 3/2 3/2)	144385.44	10.39	6.21E-07	3.93	0.17	1.28	0.44	0.042	0.011	0.08	0.02
26504	CN (1 1/2 3/2 - 0 1/2 1/2)	113170.49	5.43	5.14E-06	4.44	0.14	1.88	0.36	0.473	0.072	1.20	0.13
26504	CN (1 1/2 3/2 - 0 1/2 3/2)	113191.28	5.43	6.68E-06	4.52	0.11	1.76	0.27	0.515	0.066	1.23	0.14
26504	CN (1 3/2 3/2 - 0 1/2 1/2)	113488.12	5.45	6.74E-06	4.43	0.13	1.84	0.32	0.506	0.073	1.26	0.14
26504	CN (1 3/2 5/2 - 0 1/2 3/2)	113490.97	5.45	1.19E-05	4.59	0.16	1.87	0.41	0.880	0.157	2.22	0.24
26504	CN (1 3/2 1/2 - 0 1/2 1/2)	113499.64	5.45	1.06E-05	4.46	0.16	1.97	0.40	0.405	0.066	1.08	0.12
26504	CN (1 3/2 3/2 - 0 1/2 3/2)	113508.91	5.45	5.19E-06	4.48	0.12	1.92	0.27	0.427	0.052	1.11	0.12
26504	CN (1 3/2 1/2 - 0 1/2 3/2)	113520.43	5.45	1.30E-06	4.25	0.01	1.50	0.03	0.191	0.003	0.39	0.04
45506	HCS ⁺ (2-1)	85347.89	6.14	1.11E-05	4.02	0.06	2.49	0.13	0.059	0.003	0.19	0.03
45506	HCS ⁺ (4-3)	170691.60	20.48	9.86E-05	3.60	0.10	2.79	0.23	0.170	0.012	0.72	0.13
45506	HCS ⁺ (5-4)	213360.65	30.72	1.97E-04	3.52	0.09	4.20	0.22	0.177	0.008	1.28	0.22
45506	HCS ⁺ (6-5)	256027.10	43.01	3.46E-04	3.84	0.04	3.81	0.09	0.188	0.004	1.44	0.25
45506	HCS ⁺ (8-7)	341350.23	73.73	8.35E-04	3.63	0.12	3.32	0.29	0.233	0.017	1.48	0.27
42501	H ₂ CCO (4 _{1,4} -3 _{1,3})	80076.65	22.66	5.04E-06	3.25	0.23	2.34	0.53	0.045	0.009	0.14	0.03
42501	H ₂ CCO (4 _{0,4} -3 _{0,3})	80832.12	9.70	5.52E-06	2.84	0.16	3.04	0.43	0.037	0.004	0.14	0.03
42501	H ₂ CCO (4 _{1,3} -3 _{1,2})	81586.23	22.84	5.33E-06	3.56	0.22	2.78	0.54	0.057	0.009	0.20	0.03
42501	H ₂ CCO (5 _{1,5} -4 _{1,4})	100094.51	27.46	1.03E-05	3.29	0.05	3.09	0.13	0.076	0.003	0.31	0.04
42501	H ₂ CCO (5 _{0,5} -4 _{0,4})	101036.63	14.55	1.10E-05	2.92	0.08	2.11	0.19	0.050	0.004	0.14	0.02
42501	H ₂ CCO (5 _{1,4} -4 _{1,3})	101981.43	27.74	1.09E-05	2.96	0.20	2.99	0.50	0.076	0.010	0.30	0.04
42501	H ₂ CCO (7 _{1,7} -6 _{1,6})	140127.47	39.95	2.96E-05	3.13	0.16	3.08	0.38	0.128	0.014	0.56	0.10
42501	H ₂ CCO (7 _{0,7} -6 _{0,6})	141438.07	27.15	3.11E-05	2.63	0.11	2.07	0.32	0.120	0.012	0.36	0.06
42501	H ₂ CCO (7 _{1,6} -6 _{1,5})	142768.95	40.46	3.13E-05	3.15	0.16	2.95	0.40	0.143	0.016	0.61	0.11

Table 4. Continued.

TAG	Species & Transition	Frequency (MHz)	Eup (K)	A _{ij} s ⁻¹	V _O δ _{v_o} (km s ⁻¹)	FWHM δ _{FWM} (km s ⁻¹)	Int δ _{int} (K)	Flux δ _{flux} (K km s ⁻¹)	comments			
42501	H ₂ CCO (8 _{1,8} -7 _{1,7})	160142.24	47.64	4.48E-05	2.81	0.19	2.19	0.44	0.159	0.028	0.52	0.09
42501	H ₂ CCO (8 _{0,8} -7 _{0,7})	161634.07	34.91	4.68E-05	2.83	0.18	2.04	0.42	0.133	0.024	0.41	0.07
42501	H ₂ CCO (8 _{1,7} -7 _{1,6})	163160.88	48.29	4.74E-05	2.90	0.13	2.06	0.31	0.167	0.022	0.51	0.09
42501	H ₂ CCO (10 _{1,9} -9 _{1,8})	203940.23	66.89	9.41E-05	2.76	0.31	2.78	0.83	0.137	0.034	0.63	0.11
30008	NO (2Π _{1/2} 3/2 ^e , 5/2 - 1/2 ^e , 3/2)	150176.48	7.21	3.31E-07	4.09	0.13	1.97	0.32	0.153	0.021	0.44	0.08
30008	NO (2Π _{1/2} 3/2 ^e , 3/2 - 1/2 ^e , 1/2)	150198.76	7.21	1.84E-07	3.95	0.10	1.41	0.23	0.092	0.013	0.19	0.04
30008	NO (2Π _{1/2} 3/2 ^e , 3/2 - 1/2 ^e , 3/2)	150218.73	7.21	1.47E-07	3.99	0.06	1.09	0.14	0.072	0.008	0.11	0.02
30008	NO (2Π _{1/2} 3/2 ^e , 1/2 - 1/2 ^e , 1/2)	150225.66	7.21	2.94E-07	3.91	0.08	1.83	0.21	0.073	0.006	0.19	0.04
30008	NO (2Π _{1/2} 3/2 ^f , 1/2 - 1/2 ^f , 1/2)	150580.56	7.24	2.96E-07	4.26	0.04	1.10	0.11	0.065	0.005	0.10	0.02
30008	NO (2Π _{1/2} 7/2 ^f , 9/2 - 5/2 ^f , 7/2)	351043.52	36.13	5.43E-06	3.95	0.37	4.90	1.35	0.152	0.018	1.44	0.26
30008	NO (2Π _{1/2} 7/2 ^f , 7/2 - 5/2 ^f , 5/2)	351051.71	36.13	4.99E-06	3.97	0.21	3.45	0.66	0.190	0.022	1.27	0.23
19002	HDO (2 ₁₁ -2 ₁₂)	241561.55	95.23	1.19E-05	2.87	0.21	6.13	0.58	0.182	0.010	2.11	0.36
56502	CCS(6 ₇ -5 ₆)	81505.17	15.39	2.43E-05	3.86	0.06	1.79	0.10	0.170	0.010	0.44	0.05
56502	CCS(7 ₆ -6 ₅)	86181.39	23.35	2.82E-05	4.31	0.22	2.59	0.57	0.055	0.005	0.18	0.03
56502	CCS(7 ₇ -6 ₆)	90686.38	26.12	3.34E-05	4.13	0.08	1.71	0.27	0.078	0.007	0.16	0.02
56502	CCS(7 ₈ -6 ₇)	93870.11	19.89	3.74E-05	4.08	0.03	1.63	0.10	0.184	0.008	0.39	0.04
56502	CCS(8 ₇ -7 ₆)	99866.52	28.14	4.46E-05	4.08	0.05	1.93	0.11	0.059	0.005	0.16	0.02
56502	CCS(8 ₈ -7 ₇)	103640.76	31.09	5.05E-05	4.02	0.07	1.88	0.18	0.075	0.004	0.18	0.02
56502	CCS(8 ₉ -7 ₈)	106347.73	25.00	5.56E-05	4.32	0.12	2.14	0.34	0.036	0.009	0.10	0.02
56502	CCS(9 ₈ -8 ₇)	113410.19	33.58	6.53E-05	4.24	0.21	3.46	0.49	0.062	0.008	0.29	0.04
56502	CCS(10 ₉ -9 ₈)	129548.45	42.90	9.90E-05	4.35	0.21	1.45	0.46	0.058	0.016	0.12	0.02
56502	CCS(10 ₁₁ -9 ₁₀)	131551.97	37.02	1.06E-04	4.50	0.18	2.58	0.47	0.073	0.007	0.25	0.04
56502	CCS(11 ₁₁ -10 ₁₀)	142501.70	49.74	1.33E-04	3.86	0.21	2.60	0.49	0.058	0.010	0.22	0.04
56502	CCS(12 ₁₁ -11 ₁₀)	153449.77	53.76	1.66E-04	4.00	0.44	3.10	1.04	0.050	0.015	0.23	0.04
37003	c-C ₃ H (2 _{1,2} 5/2 3 - 1 ₁ , 3/2 2)	91494.35	4.39	1.59E-05	4.16	0.07	1.81	0.14	0.038	0.003	0.09	0.01
37003	c-C ₃ H (2 _{1,2} 5/2 2 - 1 ₁ , 3/2 1)	91497.61	4.39	1.38E-05	4.54	0.32	1.88	0.66	0.025	0.008	0.06	0.01
37003	c-C ₃ H (3 _{1,3} 5/2 3 - 2 _{1,2} 3/2 2)	133187.72	10.80	5.70E-05	4.55	0.18	1.69	0.46	0.044	0.010	0.11	0.03
49503	C ₄ H (9 ₉ -8 ₈)	85634.00	20.55	2.60E-06	3.94	0.16	1.75	0.39	0.062	0.012	0.14	0.02
49503	C ₄ H (9 ₈ -7 ₇)	85672.58	20.56	2.59E-06	3.95	0.06	1.98	0.14	0.056	0.003	0.14	0.02
49503	C ₄ H (10 ₁₀ -9 ₉)	95150.39	25.11	3.60E-06	3.95	0.08	1.32	0.62	0.057	0.022	0.10	0.01
49503	C ₄ H (10 ₉ -9 ₈)	95188.95	25.13	3.58E-06	4.11	0.20	1.26	0.53	0.061	0.021	0.10	0.01
49503	C ₄ H (11 ₁₁ -10 ₁₀)	104666.57	30.14	4.81E-06	4.09	0.11	1.47	0.30	0.044	0.007	0.09	0.02
49503	C ₄ H (11 ₁₀ -10 ₉)	104705.11	30.16	4.79E-06	3.96	0.06	1.70	0.13	0.041	0.003	0.09	0.02

All lines have been identified with the line identification package CASSIS (<http://cassis.cea.fr>), except the deuterated forms of methanol. For these latter species, not yet included in the JCMT and CDMS databases, the molecular data come from Parise et al. (2002, 2004) and we derived the line parameters with the GILDAS-CLASS package (<http://www.iram.fr/IRAMFR/GILDAS>).^{*} The deuterated forms of methanol, not being included in the CDMS or JPL spectroscopic databases, do not have TAG and A_{ij}. CASSIS ingest the CDMS and JPL spectroscopic databases, and the TAGs are those given by these databases to identify the molecules. CASSIS also ingest the VASTEL spectroscopic database (<http://www.astro.caltech.edu/~vastel/CHIPPENDALEs>), in which the separation of the ortho and para forms has been performed for some molecules listed in CDMS and JPL. For this database, the TAG are adapted from those of the molecules in the original database. The columns δ_{int} and δ_{FWM} only give respectively the statistical errors on the peak intensity and FWHM computed during the fit. The column δ_{flux} gives the quadratic error on the total flux in the line, taking into account the calibration error given in the Section 3 Calibration. It is computed as: δ_{flux} = √(Cal × Flux)² + (rms² × 2 × FWHM × dv), where, respectively, Cal is the calibration error, Flux is the line flux, rms is the observed rms, FWHM is the full width half maximum of the line, and dv the velocity resolution, at the given line frequency.